



# ISAS - INTERNATIONAL SCHOOL FOR ADVANCED STUDIES

## Membrane IgE Isoforms : Molecular, Biochemical and Functional Characterization

Thesis submitted for the Degree of  
*Doctor Philosophiae*

Candidate:  
Shubha Anand

Supervisor:  
Dr. Oscar Burrone

Academic Year 1997/1998

## Acknowledgements

This work was carried out in the Molecular Immunology Group at the International Centre for Genetic Engineering and Biotechnology.

Working under the supervision of Dr. Oscar Burrone has been an immensely fulfilling experience. I will always appreciate his friendly and stimulating guidance and his constant availability and encouragement.

I am indebted to Dr. Facundo Batista, with whom I began to work in a close and ardent collaboration. Without his help, (which was rendered selflessly, at all times), his unending patience, keen interest and valuable suggestions, this work would not have been possible.

My heartfelt gratitude also to Dr. Dimitar Efremov, whose counsel and critical supervision and astute questioning intellect, helped me to refine my facts. I will always treasure his advice and his friendship.

Special thanks to Dr. Roberto Lorenzi for his critical assessment of my thesis and manuscript. A very special thanks also to Lorenza Cianl and Jorge Sepulveda for their invaluable help with the figures of my thesis.

I would like to thank all my Professors of the PhD course, who kept the course very informal and relaxed, and instigated us to write projects and participate in journal clubs.

I was very fortunate to have very supportive, friendly and helpful laboratory members, and it was a pleasure to work with them. I will always remember the cordiality of Drs. Sun Maosheng, Martin Ivanovski, Sabrina Mancardi, Marco Bestagno, Federica Benvenuti and Elsa Fabbretti.

My heartfelt thanks go to my close friends Cecilia Miozzo, Iva Afrikanova, Michael Gromiha and Daniela Gardiol who were an invaluable source of strength and inspiration and who stood by me in the most difficult periods. My deep appreciation goes to Mikhail Lomonosov, for his thoughtfulness and for his unique way of taking care. I would like to express my immense obeisance to my parents for their continuous motivation and their trust in me during my studies and career. Finally, I would like to thank my sisters Vibha and Anupama who made me feel wanted even from far away.

# CONTENTS

## List of abbreviations

## CHAPTER 1

### INTRODUCTION

1.1	Immunoglobulin Structure and Function	1
1.2	Genetics of Immunoglobulin Genes	3
1.2a	Heavy Chain Genes	3
1.2b	Light Chain Genes	9
1.3	Regulation of Ig Gene Expression	11
1.3a	Heavy Chain Gene Expression	11
1.3b	Light Chain Gene Expression	13
1.4	Differentiation of B Lymphocytes	14
1.5	The B Cell Antigen Receptor Complex	17
1.5a	Signal Transduction from the BCR	20
1.5b	Internalization of the BCR	21
1.6	Generation of the Antibody Repertoire	23
1.6a	Primary Diversification Mechanisms	23
1.6b	Secondary Antibody Repertoire	24
1.7	Class Switching	27
1.7a	Switching to IgE	31
1.8	IgE and Allergy	33
1.8a	Alternative Spliced Forms of Human IgE	36

## CHAPTER 2

### MATERIALS AND METHODS

2.1	RNA and DNA samples	41
2.2	3'-End Amplification of $\epsilon$ cDNA	41
2.3	Cloning and Sequencing	42
2.4	PCR amplification of unknown 3' flanking DNA	42
2.5	Northern Blot Hybridizations	43
2.6	RT-PCR analysis of $\epsilon$ transcripts	43

2.7	Cell lines and transfections	44
2.8	Construction of chimeric mouse/human $\epsilon$ chains	45
2.9	Flow cytometric analysis	46
2.10	Immunoprecipitations	46
2.11	Surface biotinylation and immunoprecipitation of IgE and IgM BCRs	47
2.12	In vitro kinase assay	48
2.13	Detection of tyrosine phosphorylated proteins by western blotting	48
2.14	Cellular proliferation assay	49
2.15	Apoptosis assay	49
2.16	Internalization assay	49

## CHAPTER 3

### RESULTS

#### Section 1

#### **3.1.0 Identification and characterization of murine immunoglobulin $\epsilon$ mRNAs and their polyadenylation sites**

3.1.1	Introduction	51
3.1.2	Characterization of the two murine membrane $\epsilon$ mRNA polyadenylation sites	52
3.1.3	Both poly (A) signals are used by the membrane $\epsilon$ transcripts	56
3.1.4	Alternatively spliced membrane exon transcripts are produced by I29 $\epsilon^+$ cells and mouse splenocytes	58

#### Section 2

#### **3.2.0 Characterization, expression and functional analysis of the two membrane isoforms of human IgE**

3.2.1	Introduction	62
3.2.2	Investigation of the expression of the two membrane $\epsilon$ species in PBLs	64
3.2.3	Expression of m $\varsigma$ IgE and m $\mu$ IgE	64
3.2.4	Assembly and transport of m $\varsigma$ IgE and m $\mu$ IgE	67
3.2.5a	Characterization of IgE-BCR components	70
3.2.5b	Detection of two new proteins associated with IgE-BCRs	73



3.2.5c	Two-dimensional analysis of the IgE-BCR components	73
3.2.6	In vitro phosphorylation of IgE-BCR associated proteins	75
3.2.7	Protein tyrosine phosphorylation upon crosslinking of the IgE-BCRs	77
3.2.8	Cellular responses induced by crosslinking of m <sub>S</sub> IgE and m <sub>L</sub> IgE-BCR	81
3.2.8b	Apoptosis assay for monitoring cell death	82
3.2.9	Internalization of the two IgE-BCRs	84

### Section 3

#### 3.3.0 Characterization of the two IgE-BCRs in mature B cells

3.3.1	Expression of the two IgE isoforms in A20 cells	86
3.3.2	Characterization of the IgE-BCR components on A20 cells	87
3.3.3	Protein tyrosine phosphorylation upon crosslinking of the IgE-BCRs on A20 cells	89

## CHAPTER 4

### DISCUSSION

4.1	Characterization of the two murine membrane $\epsilon$ mRNA - polyadenylation sites	92
4.2	Alternatively spliced forms of $\epsilon$ mRNA are expressed in a mouse IgE producing lymphoma and in normal B cells	94
4.3	A tale of two receptors	98
4.4	The association of BCR associated proteins ( $\epsilon$ BAPs) with IgE	99
4.5	Functional differences between the two IgE-BCRs	101

<b>CONCLUSIONS</b>	103
--------------------	-----

<b>BIBLIOGRAPHY</b>	105
---------------------	-----

## List of abbreviations

BAP	B cell antigen receptor associated protein
BCR	B cell antigen receptor
BSAP	B cell lineage specific activator protein
C	constant region of immunoglobulin
CDR	complementarity determining region
D	diversity region of immunoglobulin
EBV	Epstein-Barr Virus
ER	endoplasmic reticulum
FACS	fluorescence activated cell sorter
FDC	follicular dendritic cells
FITC	fluorescein isothiocyanate
H	heavy chain of immunoglobulin
IFN	interferon
Ig	immunoglobulin
IL	interleukin
ITAM	immunoreceptor tyrosine-based activation motif
J	joining region of immunoglobulin
L	light chain of immunoglobulin
LPS	lipopolysaccharide
MHC	major histocompatibility complex
nt	nucleotide
PBL	peripheral blood lymphocyte
PS	phosphatidylserine
PTK	protein tyrosine kinase
RACE	rapid amplification of cDNA ends
RAG	recombinase activating gene
S	switch region
STAT	signal transducer and activators of transcription
TGF	transforming growth factor
V	variable region of immunoglobulin

## CHAPTER 1

## INTRODUCTION

### 1.1 Immunoglobulin Structure and Function

The human immune system is capable of specifically recognizing and responding to an enormous number of antigens. The interaction of antigens with the cells involved in the immune response is mediated by two distinct antigen specific receptor molecules, the immunoglobulins and the T-cell receptor, expressed on the surface of B and T lymphocytes, respectively.

A monomeric immunoglobulin molecule is composed of two identical heavy (H) and two identical light (L) chains that are linked together by disulfide bonds (Fig. 1.1). Both H and L chains are organized into domains that are defined by homology and that are approximately 110 amino acids in length. Each domain forms a conserved structure known as the "antibody fold", which is stabilized by an internal disulfide linkage that forms a loop of about 65 amino acids. The amino terminal domain of H and L chains comprises the variable region, which varies from 112 to 136 amino acids in length. Within the variable region are three areas of greatest sequence variability (hypervariable regions) that are separated by regions of relatively constant amino acid sequence (framework regions) (1). H and L chain hypervariable regions together form the potential antigen-binding site, and are therefore referred to as complementarity-determining regions (CDRs) (2).

Amino acid sequences within the remainder of H and L chains (Fig. 1.1) are relatively invariable, but deviate among different constant (C) region types (isotypes) that were originally classified according to reactivity to specific antisera (1). Heavy chain C region isotypes define the classes and subclasses of mammalian Igs. Five types of H-chain exist which define the corresponding immunoglobulin classes IgM, IgD, IgG, IgE and IgA and which are designated by their respective Greek letters ( $\mu$ ,  $\delta$ ,  $\gamma$ ,  $\epsilon$ , and  $\alpha$ ).

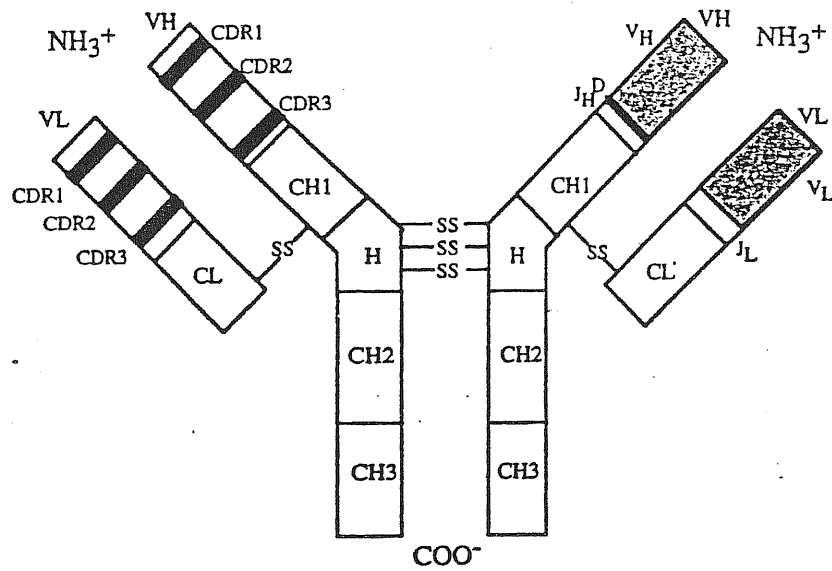


**Figure 1.1:** Structure of an IgG molecule. The typical antibody molecule consists of two identical H chains and two identical L chains linked to each other by disulfide bonds (ss). The V<sub>H</sub>, C<sub>H</sub>, V<sub>L</sub> and C<sub>L</sub> homology domains are shown in boxes and the hinge region is denoted H. The approximate boundaries of CDR regions and of sequences encoded by V<sub>H</sub>, D, J<sub>H</sub>, V<sub>L</sub>, and J<sub>L</sub> segments are indicated by different shadings.

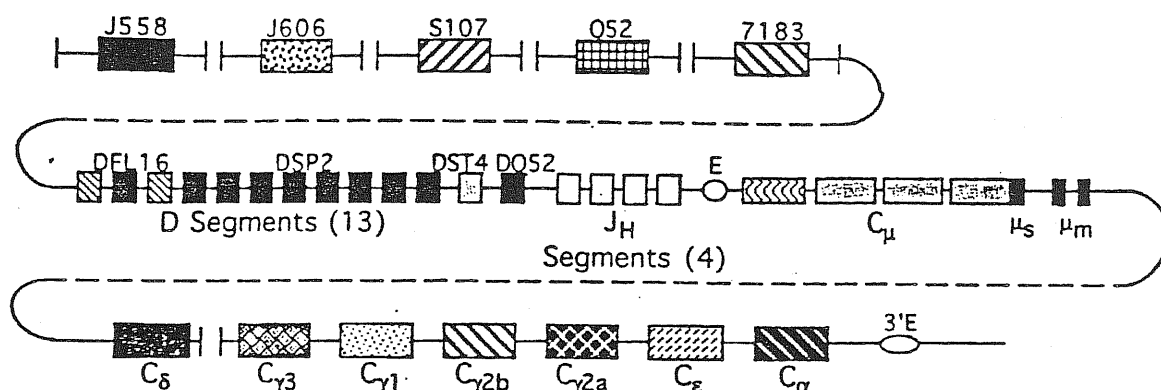
The IgG and IgA classes are further divided into subclasses defined by distinct CH region amino acid sequences. In humans the IgG class is divided into subclasses 1, 2, 3, and 4, whereas in the mouse these subclasses are defined as IgG1, IgG2a, IgG2b, and IgG3. The C regions mediate immunologic effector functions, such as complement fixation, placental transfer, and binding to cell surface Fc receptors, that are specific to particular isotypes (3). Functional differences have not been identified for the two isotypes of mammalian L chains, kappa ( $\kappa$ ) and lambda ( $\lambda$ ). There is a single subtype of  $\kappa$  and at least four subtypes of  $\lambda$ . H chain C regions contain between two and four domains that are distinctly homologous to each other and to each L chain C region domain. Certain H chain isotypes also contain a hinge region between the CH1 and CH2 domains, that may facilitate antigen binding by increasing H chain flexibility. The Ig molecule is expressed on the cell surface as a monomer, but Ig molecules can be secreted as monomers (IgG and IgE) or, in conjunction with the J chain protein, as dimers (IgA), or as pentamers (IgM) (4).

## 1.2 Genetics of Immunoglobulin Genes

### 1.2a Heavy Chain Genes

The expression of a complete immunoglobulin molecule is a consequence of a DNA recombination event that takes place independently in each lymphocyte precursor and leads to the assembly of specific DNA segments in both the H and the L-chain loci. The V region is encoded by a newly formed exon assembled upstream of the C region as a consequence of the recombination process that joins three different gene segments: a variable ( $V_H$ ), a diversity (D) and a joining ( $J_H$ ) segment (5) (Fig. 1.2). Each  $V_H$  gene segment contains two exons: the first encodes a hydrophobic leader sequence that facilitates vectorial translocation of the molecule to the endoplasmic reticulum; while the

A. Heavy Chain Genes:



B.  $\kappa$  Light Chain Gene Organization:



C.  $\lambda$  Light Chain Gene Organization:

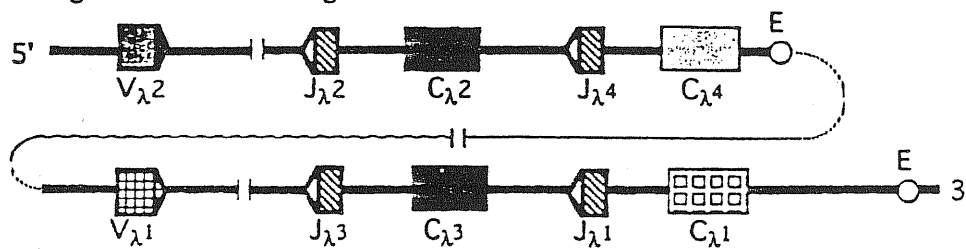


**Figure 1.2:** Ig gene organization. (A) Organization of mouse IgH genes. Shaded boxes indicate the chromosomal locations of five of the V<sub>H</sub> segment families. The D segment families and the J<sub>H</sub> segments are shaded differently and the intronic enhancer (E) is shown just 5' of C<sub>μ</sub>. Separate H chain C region exons are shown for the C<sub>μ</sub> sequences only. The C<sub>H</sub> genes are shown in their proper order along with the 3' IgH enhancer (3'E). (B) Organization of the mouse  $\kappa$  light chain locus. V <sub>$\kappa$</sub>  segments are shaded differently to indicate that there are separate V <sub>$\kappa$</sub>  families. The C <sub>$\kappa$</sub>  region is flanked by the intronic  $\kappa$  enhancer and the 3'  $\kappa$  enhancer elements (3'E). (C) Organization of the mouse  $\lambda$  light chain. The four  $\lambda$  gene families are shown in their proper order along with their corresponding enhancer elements (E).

second encodes the FW1, CDR1, FW2, CDR2 and FW3 amino acids of the V region H-chain. CDR3 is encoded by the D segment (3-27 amino acids) and by sequences at the  $V_H$ -D and D- $J_H$  junctions, and a part of  $J_H$ . The remainder of a  $J_H$  segment encodes the fourth framework region, which consists of 11 amino acids. The variable region of each L chain isotype is encoded by an upstream exon that is assembled from analogous  $V_L$  and  $J_L$  segments which are joined directly to each other; there are no L chain D segments (Fig. 1.2) (5). The basic V-(D)-J structure of these segments has been conserved among species, but their number and organization varies widely. In mice and humans, the V, D, and J segments are present as clusters with multiple members (Fig. 1.2).

### *The murine IgH locus*

The murine IgH locus lies on chromosome 12. There are four  $J_H$  segments which are located approximately 8kb upstream of the  $C\mu$  constant region gene. There are 13 known D segments and these are located from approximately 1 to 80 kb 5' of the  $J_H$  cluster (5). The D segments can be divided into four families based on flanking sequence homology: the single Q52 type D segment (DQ52) is located about 750 bp 5' of  $J_H1$ , the nine SP2-type D segments lie between 10 and 80 kb upstream of DQ52, and the two known FL16-type D segments are located on either side of the most 5' DSP2 segment (5). The  $V_H$  segments are located an unknown distance 5' of the D cluster, probably within 100-200kb of the  $J_H$  locus. The number of individual  $V_H$  segments vary with the strain of mouse and range from 100 to as many as several thousand (6). All characterized murine  $V_H$  segments are members of one of 14 families that are defined by nucleotide sequence homology within the coding region (6-8). These families have been placed into three general groups on the basis of nucleotide and amino acid sequence similarities. Most murine  $V_H$  families are extremely polymorphic in different inbred strains of mice both in terms of restriction fragment lengths (RFLP) as well as in the numbers of cross-hybridizing sequences. Since the majority of murine  $V_H$  gene segments appear to be in



the same transcriptional orientation as the  $J_H$  segments,  $V_H$  to  $DJ_H$  joining most often results in deletion of intervening DNA. The loss of this intervening DNA in  $V_H(D)J_H$  rearrangements in myelomas, B lymphomas, B cell hybridomas, and A-MuLV transformed pre-B lines has been used to 'deletion map' the order of the 14  $V_H$  families (7, 9, 10).

### *The human IgH locus*

The IgH locus in humans is located on chromosome 14 at band 14q32.33 (11). As in the mouse, the  $J_H$  and  $D_H$  regions are clustered. In humans, a DQ52-related D segment is located about 100 bp 5' of six functional  $J_H$  segments. Approximately 30  $D_H$  gene segments that fall into seven unrelated families (including DQ52) occupy about 50 kb of chromosomal sequence just 5' of the  $J_H$  (12, 13). The  $J_H$  proximal  $D_H$  families are organized into four 9 kb repeated units each of which generally contains 5-6  $D_H$  gene segments from different families. These repetitive units have been ordered as D4-D1-D2-D3-DQ52- $J_H$  with the D3 unit being approximately 25 kb upstream of DQ52 (12, 13). In contrast to the mouse in which a single  $D_H$  reading frame is predominantly utilized, human  $D_H$  segments are used equally in all three reading frames (12). Thus, it appears that the human Ig H chain CDR3 region may have more diversity contributed from the germline D locus than that of mouse as a result of an increased number and diversity of germline  $D_H$  gene segments, greater plasticity with respect to joining events, and similar usage of all three potential reading frames. Between 50 and 150 human  $V_H$  segments, up to 50% of which are pseudogenes, can be divided into six distinct homology based families ( $V_{H1}$ - $V_{H6}$ ) (14). A seventh 'family' closely related (about 80%) to  $V_{H1}$  has recently been identified (15). The human  $V_H$  complex is thought to occupy 1-3 megabases (14). Although many human  $V_H$  segments are closely related to murine  $V_H$  segment families, others are not (16).

### *Heavy Chain Constant Region Genes*

The heavy chain constant region genes are organized in 200kb of DNA. Each C region is encoded by a separate exon cluster, that also encodes the hinge region and alternate carboxy-terminal sequences (5). In mice and humans, the  $\mu$  constant region ( $C\mu$ ) is located closest to the  $J_H$  segments, and is followed approximately 2.5kb downstream by the  $C\delta$  gene and much further downstream, (50-150 kb from  $C\delta$ ) by the exon clusters encoding the other H chain isotypes (Fig. 1.2) (16-18). B lymphocytes express  $\mu$  H chains first during differentiation (18). Differential splicing of primary RNA transcripts joins V and C region exons, thereby permitting the simultaneous expression of  $\mu$  and  $\delta$  H chains that contain the same variable region (Fig. 1.3) (5, 19, 20). Most virgin B lymphocytes express both IgM and IgD (20, 21) on their surface. The function of IgD remains unclear; it might be a particularly effective antigen receptor because it contains an unusually large hinge region (20). However, mice engineered to lack the functional  $C\delta$  gene show no major impairment in B-cell development or immune responsiveness (22, 23), although they may show a delay in affinity maturation during the early primary T cell dependent immune response (24). During an immune response, a B lymphocyte can express a different H chain isotype (i.e.  $C\gamma_1$  or  $C\epsilon$ ), by replacing the  $C\mu$  coding sequences with those of a different C region by a DNA recombination mechanism (class switching) that is distinct from the mechanism involved in assembly of the variable region exons (25). This process allows the progeny of a given B lymphocyte to produce antibodies that retain their original specificity but can perform different effector functions (25, 26).

The human  $C_H$  genes are similar to the mouse counterparts. However, a large duplication exists in humans at the 3' end of the H chain gene locus, with two copies of a  $\gamma$ - $\gamma$ - $\epsilon$ - $\alpha$  unit (27). One of the duplicated  $\epsilon$  sequences is a pseudogene in which the CH1 and CH2 domains have been deleted.

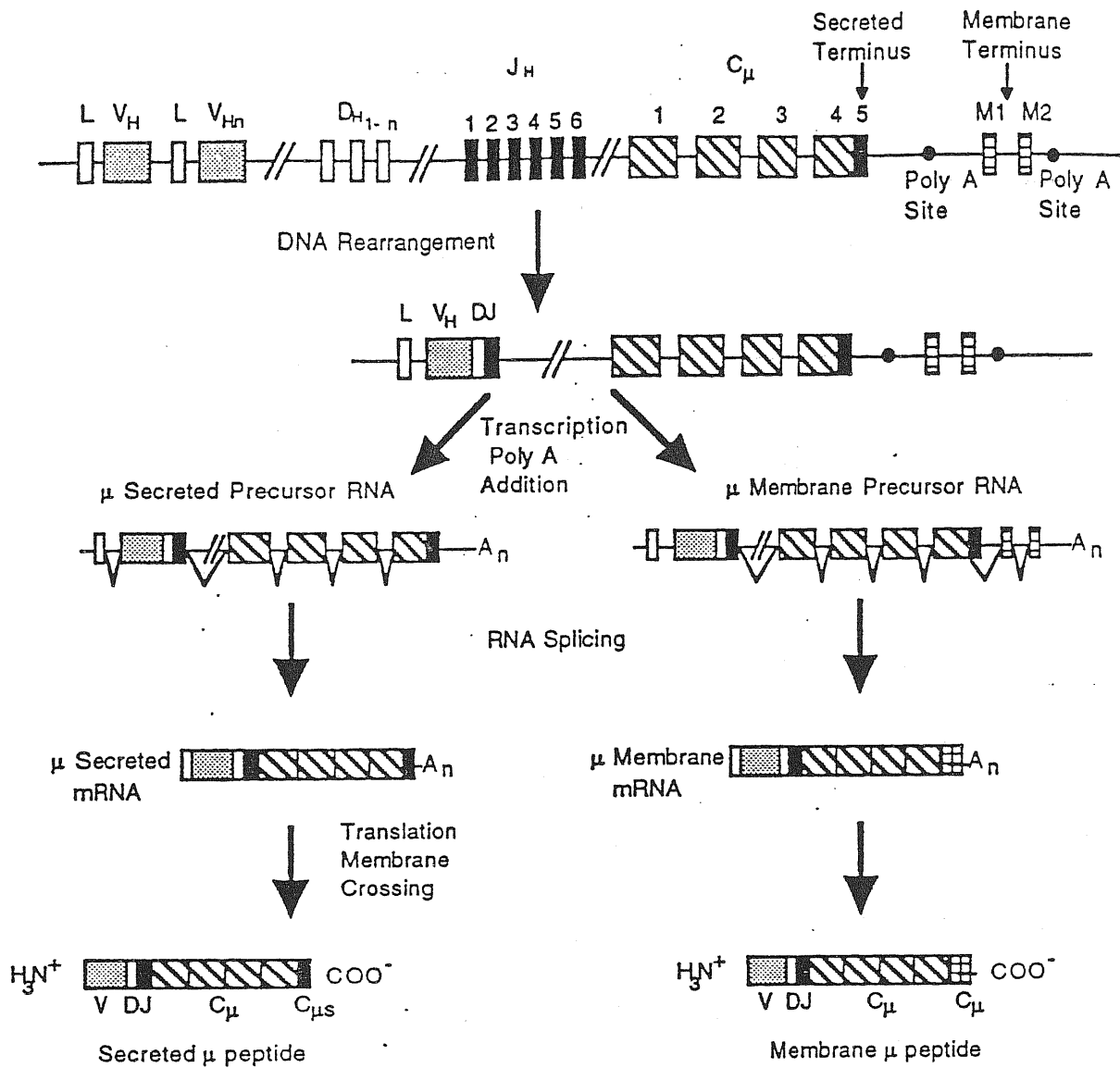


**Figure 1.3:** Schematic model of the organization of the human  $\mu$  heavy chain gene. There are multiple  $V_H$  regions, each with a leader sequence, families of diversity (D) segments, six functional joining ( $J_H$ ) and a single constant ( $C_\mu$ )  $\mu$  gene that is made up of a number of domains. Single  $V_H$ , D and  $J_H$  are joined at the DNA level. Both secreted and membrane form of IgM are derived from a single constant  $\mu$  region locus. Alternative sites of poly A addition and RNA splicing result in the different mRNAs containing either the secreted ( $C_{\mu s}$ ) or the hydrophobic membrane ( $C_{\mu m}$ ) terminus.

## 1.2b Light Chain Genes

### *The murine $\kappa$ and $\lambda$ light chain locus*

The murine  $\kappa$  locus is located on chromosome 6. There are five murine  $J_{\kappa}$  segments ( $J_{\kappa}$  1-5), which are located approximately 2.5 kb upstream of a single  $C_{\kappa}$  gene. At least 200  $V_{\kappa}$  segments, which are grouped into 19 homology based families, lie at an unknown distance 5' of the  $J_{\kappa}$  segments (8). Lambda light chains account for only about 5% of the serum light chains in the mouse. In BALB/c mice, three  $V_{\lambda}$  segments and four  $C_{\lambda}$  region exons (each C region having a  $J_{\lambda}$  gene segment in close proximity to it) have been identified (28) (Fig. 1.2). The  $\lambda$  C region exons have been amplified to different copy numbers in separate populations of feral mice, suggesting that expansion and contraction events in this locus can also occur relatively rapidly.

### *The human $\kappa$ and $\lambda$ light chain locus*

In humans, kappa light chains comprise approximately 60% of the human light chain protein. The genes of this locus are located on chromosome 2 at band 2p13 (29). The V protein domain is the consequence of a DNA rearrangement event which joins the  $V_{\kappa}$  and J gene segments. The first 95 aminoacids of the V region protein are encoded by one of the multiple V gene segments (the total number is estimated to be around 75-80), divided in four families based on sequence homology. Similar to the  $V_H$  genes, each of these  $V_{\kappa}$  segments has two exons separated by an intron. The 5' exon codes for a major portion (residues -19 to -4) of the leader sequence, while the 3'  $V_{\kappa}$  exon codes for the remaining portion of the leader sequence and most of the V region (residues -3 to 95). The rest of the  $V_{\kappa}$  region chain is encoded by one of the five functional  $J_{\kappa}$  gene segments which are separated by 250-300 bp of non coding sequences (Fig. 1.4). The human  $\lambda$  light chain locus is on chromosome 22 at band 22q11.2 region (29). The  $C_{\lambda}$  complex spans about

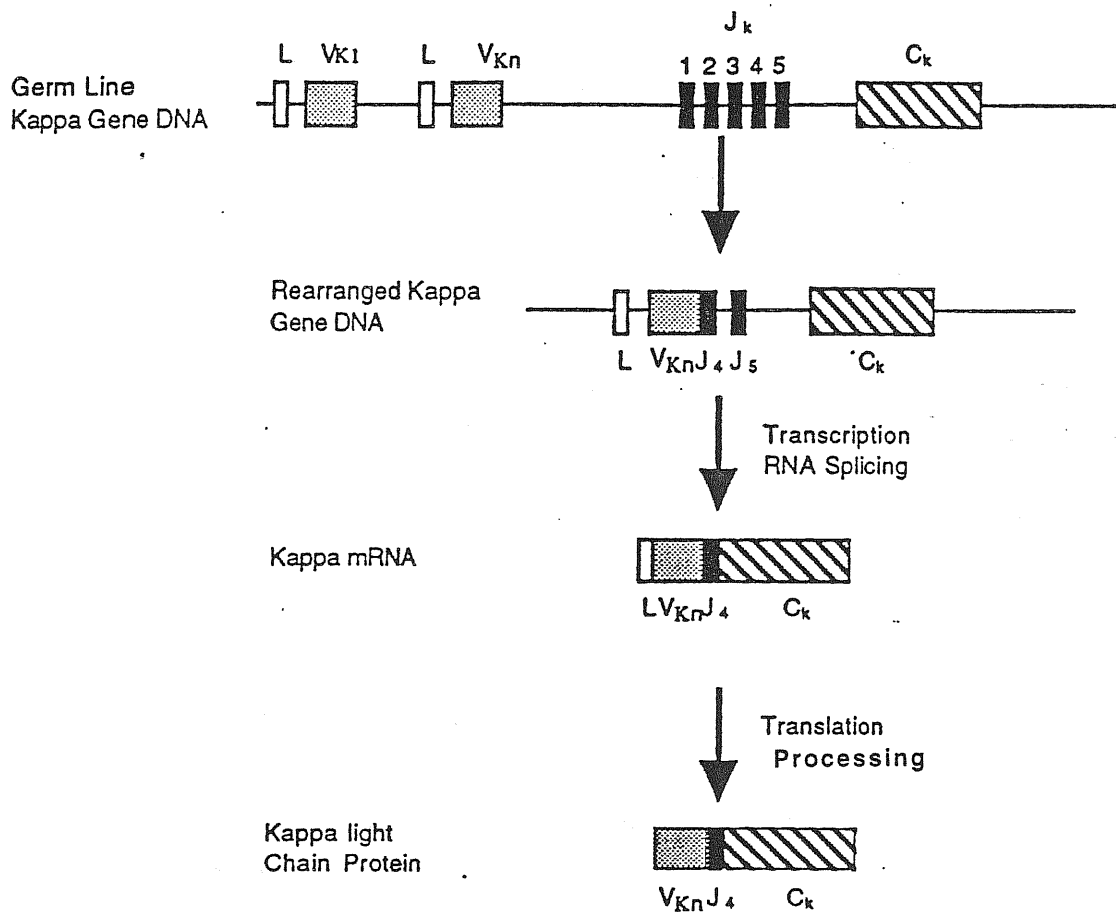


**Figure 1.4:** Arrangement of the human  $\kappa$  gene locus. Multiple variable ( $V_{\kappa}$ ) regions each with an associated leader (L) sequence. There are five alternative joining ( $J_{\kappa}$ ) segments encoding the remaining of the variable region. There is a single constant region per chromosome. DNA rearrangements lead to the junction of a single  $V_{\kappa}$  with one of the five  $J_{\kappa}$  segments. When the gene is activated, RNA is transcribed and the intervening sequences are removed by RNA splicing.

34 kb and contains seven  $C_\lambda$  genes, each associated with a 5'  $J_\lambda$  gene segment (30). Approximately, 40% of human serum L chains are of the  $\lambda$  type and, correspondingly, the human  $V_\lambda$  locus is more complex than that of the mouse. The human  $V_\lambda$  segments can be divided into at least four homology based subgroups. These  $V_\lambda$  gene segments are organised in an intermingled fashion in the  $V_\lambda$  locus, and in the same transcriptional polarity as the  $C_\lambda$  complex. Six  $V_\lambda$  gene segments, only one of which appears functional, occupy a stretch of approximately 60 kb in length directly upstream of  $C_{\lambda 1}$ .

### **1.3 Regulation of Ig Gene Expression**

#### **1.3a Heavy Chain Gene Expression**

The H-chain locus is the first to be rearranged. This process occurs in two steps. The first event is a D to  $J_H$  rearrangement, which invariably occurs on both H chain alleles. Precursor B cells then undergo  $V_H$  to  $DJ_H$  rearrangement on one or both alleles, generating potentially functional VDJ H-chain genes.  $V_H$  to  $DJ_H$  rearrangement does not occur on alleles that have not first undergone D to  $J_H$  rearrangement (31, 32). Since the  $V_H$  to  $DJ_H$  rearrangements are not precise, many of them generate "non productive" out-of-frame joined segments (VDJ<sup>-</sup> alleles). When productive rearrangement of any one allele occurs, further changes in the second allele are inhibited (allelic exclusion) and the cells proceed to IgL rearrangement. Experimental evidence supports the role of membrane  $\mu$  chain ( $\mu_m$ ) expression in signalling allelic exclusion at the IgH locus. Transgenes encoding an intact  $\mu$  chain (specifically its membrane-bound form) prevent or profoundly impede rearrangements at the endogenous IgH loci. Also, mutants expressing only the secreted form of the  $\mu$  chain ( $\mu_s$ ) from one chromosome generate allelically 'included', double-producing cells (33).

Control of H chain gene transcription involves both the  $V_H$  promoter and a transcriptional enhancer element which is located within the  $J_H$ - $C_\mu$  intron (Fig. 1.2) (34). The IgH chain intronic enhancer ( $E_\mu$ ), functions in *cis*, and can do so in either orientation and at a distance of several kb (34, 35). This enhancer element is active specifically in lymphoid cells, and functions synergistically with the  $V_H$  promoter, which is also tissue specific. An enhancer like element has also been found in the 3' region of the Ig HC locus, approximately 15 kb downstream of the last  $C_H$  gene exons (36). This enhancer is apparently not required for variable region gene assembly or for expression of Ig  $\mu$  heavy chains. More recently, in human IgH locus, arrays of enhancers homologous to those 3' of mouse  $C\alpha$  have been identified (37). These enhancers lie near the 3' ends of the two duplication units in humans, which encompass the  $\gamma 3$ - $\gamma 1$ - $\psi\epsilon$ - $\alpha 1$  and  $\gamma 2$ - $\gamma 4$ - $\epsilon$ - $\alpha 2$  gene clusters.

### ***Membrane vs Secreted Ig***

H chains can be produced in either a membrane-bound or a secreted form, which are distinguished by specific sequences at their carboxy termini (38). These two forms have the same rearranged VDJ segment, but differ in their carboxy terminal amino acids. The two forms are encoded by mRNA species that arise by alternative splicing of transcripts derived from a single H-chain gene (39-41). It has been proposed that differential transcription termination and polyadenylation of the primary RNA transcripts determines which of the two mRNAs is expressed (39-41). Each immunoglobulin H-chain gene contains at least two polyadenylation sites. Usage of the promoter proximal poly A site, located immediately 3' to the stop codon of the last CH domain results in a mRNA encoding a secreted H-chain. If, however, transcriptional termination and polyadenylation occurs at a site located several kilobases to the 3' of the first poly A site, a mRNA containing sequences from two additional exons (M1 and M2) is produced. These exons encode the extracellular membrane proximal, hydrophobic transmembrane and

hydrophilic cytoplasmic carboxyterminal portions of the membrane H-chain. RNA processing events remove the first poly A site from the membrane mRNA by splicing from a conserved donor site in the terminal CH exon (either the CH3 or CH4 exon depending on the H-chain isotype) to the M1 exon. Thus, it appears that in the case of immunoglobulin H-chain gene expression, transcription termination at alternative end sites determines the expression of either the membrane or secreted protein (Fig. 1.3).

### 1.3b Light Chain Gene Expression

The assembly of L-chain genes follows H-chain gene rearrangement, usually after the production of a H-chain polypeptide. This DNA recombination event joins one of the many germline V regions with a particular joining ( $J_{\kappa}$ ) region. If a  $V_{\kappa}$  and a  $J_{\kappa}$  gene segment are effectively joined in a cell already possessing an effective H-chain VDJ recombination, a  $\mu$ ,  $\kappa$  surface immunoglobulin B cell results. Frequently, however, both the maternal and paternal set of  $\kappa$  alleles rearrange aberrantly, or are deleted. If this occurs,  $\lambda$  gene rearrangements are initiated and, if effective, they result in a  $\mu$ ,  $\lambda$  bearing B cell. L chain gene expression appears to be regulated by mechanisms that are analogous to those that control H chain gene expression.  $V_{\kappa}$  and  $V_{\lambda}$  promoters are structurally similar to  $V_H$  promoters, and are most active in lymphoid cells. Activity of the promoter of a rearranged  $V_{\kappa}$  segment depends on a tissue specific enhancer located within the  $J_{\kappa}$ - $C_{\kappa}$  intron, which seems to act synergistically with the  $V_{\kappa}$  promoter. There is an additional, quite strong, enhancer element located approximately 5 kb downstream of the  $C_{\kappa}$  gene; the role of this 3' $\kappa$  enhancer is not totally clear (42). Recent studies have however implicated the activity of both the intronic and 3' $\kappa$  enhancer as being important for the somatic hypermutation of associated  $\kappa$  transgenes (43, 44).



## 1.4 Differentiation of B Lymphocytes

B lymphocytes develop from hematopoietic stem cells in specialized microenvironments provided by the fetal liver and adult bone marrow of mammals, in an ordered process that is marked by sequential rearrangements of the immunoglobulin genes (45, 46). The development of B lymphocytes can be broadly divided into two major phases. In the first, antigen independent phase, a programmed sequence of immunoglobulin V-(D)-J gene rearrangements yields a population of lymphocytes, each of which makes its own characteristic immunoglobulin molecule. In the second phase, encounter with foreign antigen leads to a selective expansion of those B cells that make a cognate antibody: they differentiate into either antibody-secreting plasma cells or memory B cells.

Progression along the B cell differentiation pathway can be monitored by the expression of developmentally regulated genes. One of the earliest expressed surface marker of B lineage cells is the Ig gene superfamily member, CD19, a signal transduction molecule which is expressed throughout B cell development, except on plasma cells (Fig. 1.5), in both humans and mice. Other cell surface molecules defining early developmental stages of B cells and their progenitors include CD34, CD22 and CD10 in humans, B220, CD43, CD24 and BP-1 in mice, and intracytoplasmic and surface Ig in both species.

B lymphocytes undergo genotypic changes by rearranging V, D and J gene segments to encode functional antigen receptors, making the rearrangement status of the immunoglobulin  $V_H$  and  $V_L$  ( $\kappa$  and  $\lambda$ ) genes useful developmental markers. The  $V_H$  gene rearrangement process is initiated (D- $J_H$ ) in pro-B cells, which remain incapable of Ig production except in mice, in which transcripts of  $DJ_H$  rearrangements in reading frame (RF) 2 are translated into truncated  $D\mu$  protein. There is powerful selection against cells using RF2 because of the defective receptor role for the  $D\mu$  protein (47). The  $Ig\alpha$  and  $Ig\beta$  chain components of the antigen receptor are expressed within pro-B cells, as are surrogate light chain ( $\psi LC$ ) proteins encoded by the  $VpreB$  and  $\lambda 5$  (mouse) or 14.1

(human) genes (48). VpreB and  $\lambda 5$  genes are exclusively expressed in pre-B cells and have single Ig like domains, the former resembling variable regions and the latter resembling  $\lambda$  constant regions. Unlike the classical light chain genes, the  $\lambda 5$  and VpreB genes do not undergo rearrangement. Completion of a productive  $V_H$  rearrangement ( $V-DJ_H$ ) results in pre-B cell expression of  $\mu$  heavy chains, most of which are retained in the endoplasmic reticulum (ER) and some of which associate with  $Ig\alpha$ ,  $Ig\beta$  and  $\psi LC$  to reach the cell surface as the pre-B cell receptor (BCR) (47, 48).  $Ig\alpha/Ig\beta$  heterodimers are essential components of the pre-BCR. Ig molecules fail to reach the cell surface in the absence of these signal transducing units, leading to severe pre-B cell deficiency in gene knockout models (49).

The pre-BCR is involved in the selection and amplification of pre-B cells by signalling the proliferative expansion of those pre-B cells that have succeeded in a functional  $V_H(D)J_H$  rearrangement. In the pro-B cell stage, where the rearrangement of the IgH locus is initiated, only 15% of the cells are in the S or G2/M phase of cell cycle. Productive IgM rearrangement and appearance of pre-BCR expression coincides with the transition to large, rapidly cycling pre-B-II stage in which 70% of the cells are in S or G2/M. These large pre-B-II cells subsequently give rise to a resting population (small pre-B-II), in which fewer than 5% of the cells are in S and G2/M phases; this population is the principal site of IgL-chain rearrangement. In mice which are deficient in the recombinase activating genes (RAGs) that are required for Ig gene assembly, the pro/pre-B-I to large pre-B-II transition is blocked and the total number of B-cell progenitors is reduced. Expression of a  $\mu$  transgene in RAG-deficient mice overcomes this block, restoring the B-cell progenitor pool to its normal size and resulting in the accumulation of cells at the small pre-B-II stage. In addition to this role, pre-BCR also signals for allelic exclusion at the IgH locus by turning off  $V_H$  to  $DJ_H$  rearrangements at the second IgH allele. Recently performed domain swapping experiments indicate that the cytoplasmic domains of  $Ig\alpha$  and  $Ig\beta$  are interchangeable in signalling B cell development and allelic

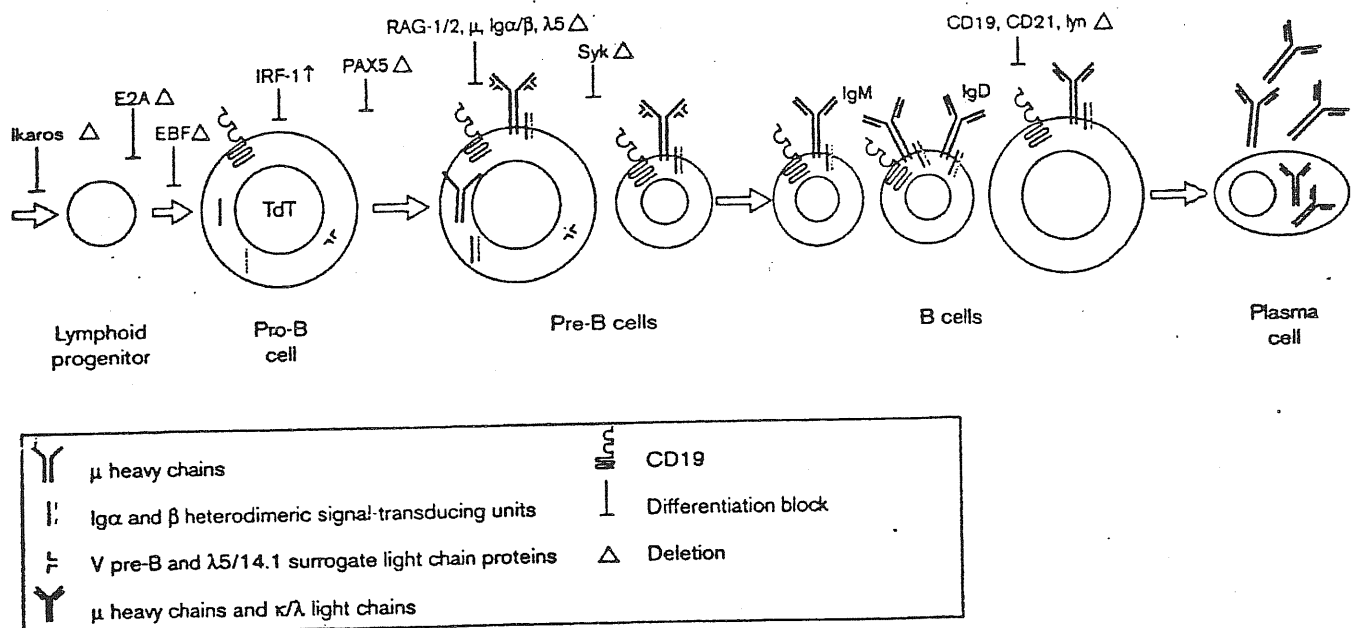


**Figure 1.5:** Scheme of the B cell differentiation pathway, beginning with the lymphoid progenitor offspring of multipotent hemopoietic stem cells (not shown) and ending with Ig-secreting plasma cells. This model depicts one view of the stage-specific expression of pre-B cell receptors, which are composed of  $\mu$  HCs, Ig $\alpha$  and Ig $\beta$  heterodimeric signal-transducing units and V pre-B and  $\lambda 5/14.1$  surrogate light chain proteins, and B cell receptors, which utilize conventional light chains, either  $\kappa$  or  $\lambda$ . The CD19 molecule serves as an important lineage marker and coreceptor for both the pre-B and the B cell receptors. TdT in pro-B cells adds nontemplated (N) sequences in the receptor V(D)J joints. The inverted T symbols indicate the stages in the pathway in which differentiation blocks result from deletion of murine genes encoding essential transcription factors (Ikaros, E2A, EBF, Pax5), proteins necessary for receptor gene recombination (RAG-1/2), or signaling elements (Syk, lyn).

exclusion since, deletion of almost the entire Ig $\alpha$  cytoplasmic domain had only a minor effect on B cell development, because receptor expression and Ig $\beta$  signalling remains intact (50). Nevertheless, the generation of the peripheral B cell pool was severely impaired in these mice, suggesting that an Ig $\alpha$  mediated developmental checkpoint screens for functionally intact BCRs.

The pre-BCR may also be involved in repertoire selection, since pre-B cells expressing certain V<sub>H</sub> genes are selected for contribution to the B-cell repertoire (51). Subsequent rearrangement of a  $\kappa$  or  $\lambda$  LC V gene (V<sub>L</sub>-J<sub>L</sub>) permits cell surface expression of conventional sIgM receptors on the immature B cell which exits the bone marrow and migrates to the periphery. Mature B cells in spleen and secondary lymphoid organs express both IgM and IgD receptors and in response to cognate antigen and T cells undergo proliferation and differentiation into either memory B cells or Ig-secreting plasma cells. Memory B cells are relatively long lived and are more easily triggered than virgin B cells on subsequent encounters with the same antigen. The differentiation of the mature B cell to plasma cell is accompanied by the loss of surface immunoglobulin expression as a consequence of conversion from the synthesis of membrane to secretory immunoglobulin molecules. Mature plasma cells are short lived and produce large amounts of secreted immunoglobulins.

### 1.5 The B Cell Antigen Receptor Complex

B cell antigen receptor (BCR) complexes of all Ig classes consist of a membrane bound Ig (mIg) molecule and an Ig- $\alpha$ /Ig- $\beta$  heterodimer. Ig- $\alpha$  and Ig- $\beta$  are transmembrane proteins comprising an extracellular Ig domain and a cytoplasmic sequence of 61 and 48 amino acids respectively. These proteins are encoded by the B-cell specific genes mb-1 and B29, respectively. The association of the Ig- $\alpha$ /Ig- $\beta$  heterodimer with mIg is usually required for surface expression and is always necessary for the signalling function of the

BCR complex. The human and mouse Ig- $\alpha$  and Ig- $\beta$  proteins display a sequence homology of more than 70% and 75% respectively (52-54). The conservation is particularly strong in the transmembrane and cytoplasmic part of these proteins. In the latter sequence both Ig- $\alpha$  and Ig- $\beta$  carry the TyrXXLeuXXXXXXXXXXTyrXXIle motif (where X= any amino acid) (55, 56) which is called the immunoreceptor tyrosine-based activation motif (ITAM) (Fig. 1.6).

The B cell antigen receptor (BCR) regulates three central features of immune system function. First, it acts as a checkpoint regulator in B-cell development, controlling both allelic exclusion and early cellular transitions, thus signalling the fate of a B cell even before it encounters antigen. Second, as predicted by the clonal selection theory, crosslinking of the B-cell receptor with antigen can lead to clonal expansion and the production of specific antibodies. The third function of membrane-bound immunoglobulin is as a receptor for antigen capture and presentation. More recently, a fourth function for the BCR has been elucidated (57). Lam et al. have shown that the persistence of mature B lymphocytes depends on the continued presence of BCR, even without encountering the foreign antigen. This means that mature B cells need continual signalling from BCR in order to stay alive. This persistence signal does not lead to the entry of B cells into cell cycle or an upregulation of the costimulatory molecules for T cell interaction- changes which rapidly ensue when the BCR on the same cells is intentionally crosslinked with high affinity antigen or anti-immunoglobulin antibodies. Thus, on a single cell, BCR can deliver quite different signals: one that leads to persistence and another leading to activation. The distinction may lie in the nature and extent of BCR crosslinking.

## The antigen B-cell receptor

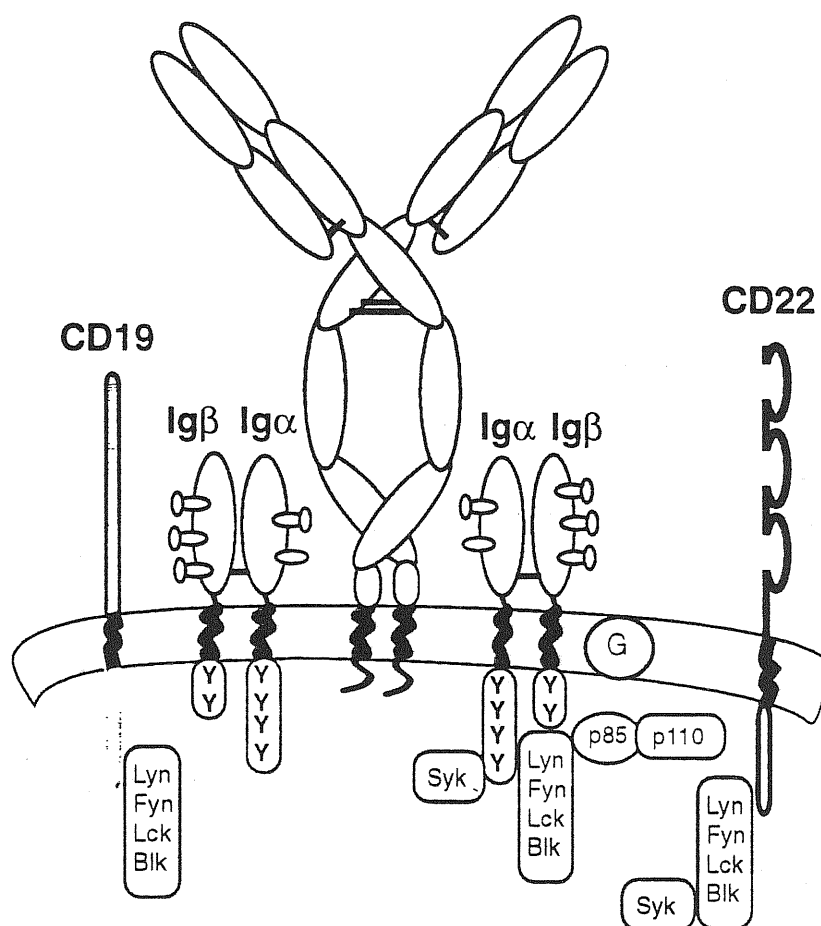


**Figure 1.6:** Structural model of the B-cell antigen receptor complex (BCR). The antigen receptor consists of membrane Ig, with its two transmembrane heavy chains and two light chains, bound in a complex with one or more disulfide-linked heterodimers of Ig- $\alpha$  and Ig- $\beta$ . Upon crosslinking of the BCR, src-family kinases are activated, tyrosine residues (Y) in the immunoreceptor tyrosine-based activation motif (ITAM) are phosphorylated and the spleen tyrosine kinase Syk is recruited to the activated receptors. These events induce activation of phospholipase C $\gamma$  (PLC $\gamma$ ), production of inositol (1,4,5)-triphosphate [Ins(1,4,5)P $_3$ ] and Ca $^{2+}$  release.

### 1.5a Signal transduction from the BCR

Crosslinking of the BCR results in the activation of several protein tyrosine kinases (PTKs), leading to tyrosine phosphorylation of substrates and activation of multiple biochemical pathways. The ITAM motif plays an important role in the communication between the BCR and two types of PTKs: the src- family kinases (Lyn, Blk, Fyn and Lck) and the spleen tyrosine kinase Syk. The N- terminus of Lyn or Fyn binds unphosphorylated Ig- $\alpha$ , and amino acids close to the second ITAM tyrosine residue of Ig- $\alpha$  were shown to influence binding to Fyn (58). A functional analysis of Ig- $\alpha$  mutations in an Ig- $\alpha$ -deficient B-cell line showed that a double mutation of the two ITAM tyrosine residues prevents PTK activation via the BCR (59). Phosphorylation of these residues results in increased binding of proteins with src-homology 2 (SH2) domains such as the src-family kinases or the SH2-domain containing adapter protein Shc (60). The stoichiometry of this association, however, is low (1-3%). Depending on the developmental stage of the B cell or the presence of co-stimulatory signals, signal transduction via the BCR can result in either cell activation or cell death by apoptosis. The src-related PTKs may play a role in the latter response as antisense oligonucleotides to blk can prevent apoptosis in activated CH33 B lymphoma cells (61). The two tandem SH2 domains of Syk also bind to the double-tyrosine phosphorylated ITAMs of the BCR. Deletion of both alleles of the gene encoding Syk from the genome of a chicken B-cell line demonstrated that Syk controls the signalling pathway between the BCR and phospholipase C $\gamma$  (PLC $\gamma$ ) (62). The surface proteins CD22 and CD19 as well as cytoplasmic proteins HS1, PLC $\gamma$ 2 and Vav have been identified as PTK substrates in BCR-dependent signal cascades (63, 64). HS1 carries an SH3 domain and seems to play a critical role in the induction of apoptosis in activated B cells.

### 1.5b Internalization of the BCR

Crosslinking of the BCR results in internalization of the receptor with the bound antigen (65, 66). This internalization is thought to occur by a clathrin-independent pathway involving capping and invagination of the lymphocyte plasma membrane. The BCR-antigen complex is processed in lysosomal compartments and antigen is presented in the form of major histocompatibility complex (MHC)-bound peptides on the surface of the B cell. Signalling and internalization of the BCR are regulated differently. Internalization does not require PTK activation nor the presence of a functional ITAM in the cytoplasmic tail of Ig- $\alpha$  or Ig- $\beta$ . However, a functional analysis of IgM-Ig- $\beta$  chimeric molecules has shown that the cytoplasmic tail of Ig- $\beta$  promotes internalization (65). On the other hand, internalization seems also to occur independently of the Ig- $\alpha$ /Ig- $\beta$  heterodimer in COS and L cells, which do not produce these proteins. A  $\mu$ m chain with a deletion of the first constant domain (CH1) can be expressed as a transmembrane protein on these cells and is also internalized after cross-linking (67). However, because of the absence of a time course experiment and of a parallel study of Ig- $\alpha$ /Ig- $\beta$ -associated mIgM molecules on COS cells, it is unclear whether the internalization of the truncated  $\mu$ m chain is as efficient as that of the complete BCR complex. In a mutation analysis of the  $\mu$ m transmembrane segment it has been shown previously that a Tyr to Phe mutation at position 14 of the  $\mu$ m sequence can abolish antigen presentation but not signal transduction (68). A similar result was obtained in a domain shuffling experiment, a chimeric mIgM/I-A $\alpha$  molecule, in which the first 8 amino acids of the  $\mu$ m sequence are replaced by the transmembrane sequence of the MHC class II I-A $\alpha$  protein, is competent for signalling but deficient in antigen presentation (69). These data suggest that the BCR can interact in multiple ways with the internalization machinery, either via the  $\mu$ m transmembrane part and/or via the cytoplasmic sequence of Ig- $\alpha$  and Ig- $\beta$ .



Antigen capture and presentation by B cells is thought to be particularly important in secondary immune responses. The pool of antigen-specific B cells that participate in memory responses are selected and clonally expanded during the primary response. Thus, there are more B cells with high affinity receptors for specific antigen available for antigen capture during secondary responses, and these memory B cells appear to be particularly efficient at presenting antigens. Memory B cells frequently carry somatic mutations in their immunoglobulin genes, these mutations are produced by an unknown mechanism during clonal expansion in response to antigen in germinal centers. Memory B cells also express secondary heavy chain isotypes, such as  $\gamma$ ,  $\alpha$  and  $\epsilon$ . Experiments were done to determine whether the conserved cytoplasmic domains of the membrane IgG and IgE are essential for memory B cells to respond to antigen. Mouse and human IgM and IgD have a three amino acid cytoplasmic tail (Lys-Val-Lys), that of IgA has 14 amino acids, and those of IgGs and IgE are extended by 25 and 28 amino acids respectively (70). Knight et al. analyzed the cytoplasmic tail of human IgG1 and found that the sequence mediated both internalization and targeting to the endosomal compartment for antigen processing and subsequent presentation (71). By comparing the reconstituted IgG1 in cell lines either expressing or lacking Ig- $\alpha/\beta$ , they found no difference in antigen presentation as long as the cytoplasmic tail was intact. A complete IgG1 presented antigen equally efficiently in the presence or absence of Ig- $\alpha/\beta$ . An IgG1 lacking a cytoplasmic tail, however, presented antigen ten fold less efficiently in the absence of Ig- $\alpha/\beta$ , a drop that was not apparent when Ig- $\alpha/\beta$  was present. Kaisho et al. and Achatz et al. used gene targeting to generate mice homozygous for alterations to the cytoplasmic tails of IgG1 and IgE (72, 73). Truncation mutations were done such that the cytoplasmic tails of the memory isotype became identical to that of IgM, or both the cytoplasmic and transmembrane regions were deleted. Deletion of the cytoplasmic domains of  $\gamma 1$  or  $\epsilon$  heavy chains resulted in a substantial reduction in the number of B cells expressing surface immunoglobulin G1 or E, and a marked decrease in serum

immunoglobulin G1 or E. With the  $\gamma 1$  tail deletion, primary IgG1 responses were one order of magnitude below the control level and with the  $\epsilon$  tail deletion, IgE responses were 50% of the control level. In addition, there was a failure of affinity maturation of the antibody response with the  $\gamma 1$  tail deletion. Thus, the conserved cytoplasmic tails of the  $\gamma$  and  $\epsilon$  heavy chains are essential for normal immune responses and for expansion and maintenance of IgG1 or IgE bearing memory cells. The above experimental data suggest that the structural requirements for internalization and subsequently antigen presentation differ from and are more stringent than those for signalling.

## **1.6 Generation of the antibody repertoire**

### **1.6a Primary diversification mechanisms**

Newly - generated virgin B lymphocytes express a 'primary' repertoire of antigen binding specificities which has not been influenced by contact with antigens or other selective forces. The wide range in specificities of this primary Ig repertoire in mouse and humans derives from the somatic V(D)J assembly process (4). The reservoir of hundreds of germline  $V_H$  and  $V_L$  gene segments provides a primary source of diversity in CDR1 and CDR2. The assortment of different  $V_H$ , D and  $J_H$  sequences or  $V_L$  and  $J_L$  sequences provides an even greater source of diversity in CDR3. Mechanisms also exist to promote heterogeneity in the junctions of coding segments (junctional diversity) leading to great variations in the amino acid sequence of CDR3, even among variable region genes generated from the same V, (D), and J segments (74, 75). The pairing of different combinations of H and L chains further diversifies the primary antibody repertoire, which is estimated to be about  $10^{11}$  different antibodies or greater (76).

### *Selection of the primary antibody repertoire*

The mechanisms shaping the primary antibody repertoire (that is, the repertoire expressed by the cells joining the peripheral pool of  $IgM^+ IgD^+$  cells) fall in two categories. First, the mechanisms of antibody diversifications can themselves mediate selection. In the newborn mouse, the repertoire is restricted by the paucity of N-region insertion, together with preferential recombination of V, D and J elements at short sequence homologies. Later, diversity is drastically increased by N-region insertion at the borders of  $D_H$  and in humans, the  $V\kappa$ - $J\kappa$  border (77). Diversity is also restricted by the inability of certain H and L chains to pair properly and by differences in the usage of the various germline V, D and J elements (47). Second, there is ligand-mediated negative selection of cells expressing autoreactive antibodies. Transgenic mice, in which most newly generated B cells express an antibody against an antigen with strong crosslinking capacity that is present in the bone marrow have no such B cells in their peripheral immune system (47). This negative selection is either due to apoptotic death on encountering antigen or by rescue of the autoreactive cells by further immunoglobulin rearrangement. Depending on their affinity for antigen, autoreactive cells may survive in the bone-marrow for long enough to be rescued if their receptor is replaced by an innocent one. This receptor editing is frequently seen at the  $Ig\kappa$  locus, which can undergo successive rearrangements and can be inactivated by RS recombination, facilitating  $Ig\lambda$  rearrangements (47).

Newly generated autoreactive B cells are also negatively selected on encountering soluble antigen, producing inefficient BCR crosslinking. Such cells can leave the bone marrow, but they down-regulate surface  $IgM$  and enter an anergic (antigen-unresponsive) state (78).

### **1.6b Secondary antibody repertoire**

Affinity maturation of antibodies and immunological memory both reflect a process of somatic evolution in which mutants are generated from the primary antibody repertoire.

The antigen not only selects rare antibody mutants on the basis of their affinity, or improved on-rate of binding, but also induces their generation, triggering hypermutation in antigen-activated B cells in a special pathway of differentiation called the germinal centre response (47). When the antibody V-region genes in the germ line were compared to those carried by B cells at various stages of differentiation, it was seen that the antibodies were virtually unmutated early in the response, but point mutations were seen in the V (but not C) regions at increasing frequency as the response progressed (79). Both silent and replacement mutations occurred, and these key mutations increased the affinity of the antibody. The existence of sequences sharing identical, unique  $V_H D_H J_H$  or  $V_L J_L$  rearrangements, but differing by point mutations indicated that somatic mutation occurs stepwise in the course of cell proliferation, corresponding to stepwise affinity maturation.

### *Somatic hypermutation*

The somatic mutation process can occur over the entire assembled variable region gene and hence it can generate diversity in all CDRs. Although the mutations can be scattered over the rearranged V genes, this process is not random, in that intrinsic hot spots can be discerned (80). Replacement mutations are often overrepresented in CDRs and underrepresented in the framework regions, whereas the opposite is true for silent (S) mutations. Little is known about the cis-acting DNA sequences responsible for the hypermutation mechanism. An approach for systematic delineation of such sequences came from the observation that the rearranged V gene of an immunoglobulin L $\kappa$  chain transgene can constitute a target for the hypermutation process (44). Using this approach it was demonstrated that sequences downstream of C $\kappa$  are necessary for somatic mutation of the linked V-transgene (43). Removal of either the 3' enhancer or the intron enhancer resulted in a dramatic fall in the rate of hypermutation. However, the substitution of the V gene promoter and 5' untranslated region with that of the  $\beta$ -globin gene did not affect the

mutation rate to any significant degree suggesting that the V region promoter does not possess factors involved in recruiting the hypermutation mechanism (44).

An additional somatic mechanism, gene conversion, has been implicated as the primary generator of Ig H and L chain diversity in chickens (81). Gene conversion is the process by which a portion of sequences within one gene is replaced by sequences from another gene, while both structures remain intact along the chromosome (82). However, somatic gene conversion is not a general mechanism for repertoire diversification in human or murine B lymphocytes (83).

### *The germinal centre reaction*

Affinity maturation and memory generation take place in the special microenvironment of germinal centres (84). Germinal centres arise inside 'follicles' composed of naive B cells on immunization with T-cell-dependent antigens. They are characterized by the rapid expansion of an oligoclonal population of antigen-activated B cells in a highly organized microenvironment whose main other components are antigen-specific helper T cells and follicular dendritic cells (FDC). The FDC carry on their surface antigen complexed to antibodies and components of the complement system, and this form of antigen presentation, together with signals delivered by the T helper cells, is critical for the selection and maturation of high affinity memory cells (84). Unlike resting, naive and memory B cells, proliferating germinal centre cells express only low levels of Bcl-2 and seem programmed to die unless rescued by signals involving antigen and antigen-specific T cells. Cells expressing high-affinity antibodies are thus positively selected in this microenvironment and competition between mutants for antigen and T-cell help could be an important contributor to efficient selection. Another factor may also be the isotype switch which takes place in the germinal centre and leads to the expression of antibodies of class G, A or E, instead of the original classes M and D (87).

The germinal centre B cells can also be negatively selected by ligands binding to their BCR. They undergo rapid apoptosis on encountering antigen in the absence of T-cell help (85).

After a few weeks, the germinal centres shrink and disappear. Surviving B cells, which have probably undergone several rounds of positive selection in the germinal centre, upregulate bcl-2 and enter a resting state. These cells express a novel repertoire of hypermutated, high affinity antibodies (86).

### 1.7 Class Switching

After antigen activation, surface IgM<sup>+</sup>IgD<sup>+</sup> B cells often switch to expressing a different heavy-chain constant region (C<sub>H</sub>), resulting in a change in the class of antibody synthesized and a change in the effector function of the antibody produced. The expressed V(D)J region and light chain do not change, thus specificity of antigen binding is unaltered. The change in antibody class is effected by a deletional DNA recombination event called switch recombination, which occurs between tandemly located sequences, called switch (S) regions, which are located upstream to each of the C<sub>H</sub> genes (Fig. 1.7). An exception is IgD, which is co-expressed with IgM in mature B cells by alternative RNA processing and termination of transcription (88). Because switch recombination occurs in mature B cells upon exposure to antigen, the heavy chain class chosen is influenced by the antigen. In T-cell dependent (TD) responses, antigen induces switching in conjunction with contact-dependent signals from T cells and signals from cytokines. T-cell independent (TI) responses also induce class switching by signals from surface Ig crosslinking, along with cytokines synthesized by a variety of cell types. Normally, class switching is induced in response to TD antigens by signals from both surface Ig crosslinking and from CD40. Mice that are deficient in CD40 or CD40 ligand (CD40L) respond normally to TI-2 antigens producing abundant antigen specific IgM and IgG3

and normal amounts of IgG1, IgG2b, and IgA. Expression of IgE, however, appears to require CD40 signalling (89, 90). Antibody class switching begins in B-cell foci in the periarteriolar lymphoid sheaths and also in germinal centers, about six days after activation by TD antigens. It occurs approximately simultaneously with, but independently of, somatic mutation (91).

Cytokines e.g [IL-4, transforming growth factor (TGF- $\beta$ ) and interferon (IFN)- $\gamma$ ] regulate the isotype specificity of switching by regulating transcription of unrearranged or germline Ig C<sub>H</sub> genes before class switching.

The germline transcripts originate 5' to the switch regions; the spliced products contain an I exon joined to the C region. The transcription of the germline transcripts terminates at the normal poly(A) sites for secreted or membrane-bound heavy chain mRNAs (88). The I exons generally display multiple stop codons in the three reading frames and therefore are unable to code for any peptide of significant length. After switch recombination, the segment of DNA 5' to the switch region is deleted from the chromosome, and thus germline transcripts cannot be synthesized after class switching; instead mature heavy-chain mRNA is transcribed. Although there is no significant sequence conservation among different germline CH transcripts, their overall structure is conserved, suggesting that the germline transcripts function in the regulation of class switching recombination (92). This has now been confirmed by gene targeted mutation experiments. Replacement of the promoter and I exons of unrearranged  $\gamma$ 2a or  $\gamma$ 1 genes with a neomycin-resistance gene in the reverse orientation relative to the heavy-chain gene results in no switching on that chromosome to that particular CH gene, although the other allele and other CH genes on that chromosome are unaffected (93). If the promoter I $\epsilon$  or I $\gamma$ 1 segments are replaced by heterologous strong promoters, each of which was shown to drive transcription through the S region and CH gene, switching still does not occur to that CH gene, indicating that transcription *per se* is not sufficient to direct switching to that switch region (92, 93). When the DNA segment containing the splice site for the I $\gamma$ 1 exon is

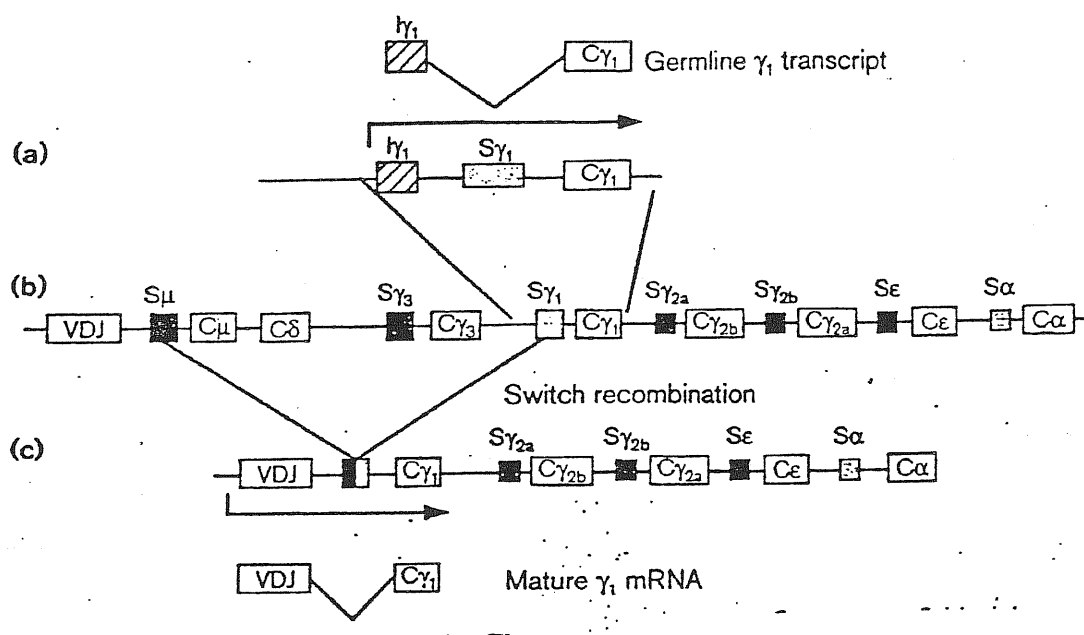


**Figure 1.7:** Diagrams of the Ig heavy-chain locus in a mouse B cell expressing IgM and of the class switch to IgG1. (a) Expanded diagram of a DNA segment containing the unrearranged  $C\gamma_1$  gene, showing the  $I\gamma_1$  exon and primary transcript and a splicing diagram of germline  $\gamma_1$  transcript. As is true for all germline transcripts, the primary transcript is spliced to generate a germline RNA containing an upstream or germline exon (I exon) spliced at the normal splice acceptor for mature heavy-chain mRNA. (b) Ig heavy-chain locus in an IgM<sup>+</sup> B cell and switch recombination to IgG1. (c) Ig heavy-chain locus in an IgG1<sup>+</sup> B cell, showing primary  $\gamma_1$  transcript and mature mRNA.



restored back to its original location and placed immediately 3' to the heterologous promoter, switching is recovered (94). Hence, the correctly spliced transcript, and not just nuclear transcription of the region, is needed for switch recombination.

Switch regions consist of G-rich, simple tandem-repeat sequences of 1-10 kb in length. Switch recombination can occur at many different sites within S regions, and no precise sequence specificity exists for the site of recombination within the S regions, although recombination may occur preferentially near certain sequence motifs within the tandem repeats (95). B cells that have undergone a class switching recombination event usually have deleted all of the  $C_H$  gene segments between the  $S_\mu$  region and the S region of the  $C_H$  gene that is expressed, since extra chromosomal circles generated by S-S mediated deletions and containing intervening DNA have been isolated (96). There is also some evidence that intervening DNA may be deleted as a linear molecule but it is not clear how frequently this occurs. A variety of evidence also indicates that once a B cell has switched to a particular  $C_H$  gene, it can, upon appropriate stimulation, undergo an additional switch to a downstream  $C_H$  gene. The evidence for this came from the findings that some switch recombination sites contained fusions of three separate S regions (e.g the  $S_\mu$  region linked to  $S_\epsilon$  by a segment of  $S_\gamma$  (97, 98). Also, following switch recombination, the germline  $I_\mu$  promoter continues to be actively transcribed in association with the downstream  $C_H$  gene, generating a hybrid germline transcript consisting of the  $I_\mu$  exon spliced to the  $C_H$  exons of the switched  $C_H$  gene (99). Because of the potential involvement of germline transcripts in switch recombination, such a transcript could be important for sequential switch recombination. Sequential switching appears to be a physiologically relevant process, but its precise role has yet to be determined since it is not a required pathway. For example, mice harbouring a deletion of the  $I\gamma_1$  exon and promoter still undergo switching to the  $C_\epsilon$  locus even though they are unable to switch to  $C\gamma_1$  locus first (100).

### 1.7a Switching to IgE

In both mouse and humans, IL-4 is the critical stimulus for isotype switching to IgE. This cytokine stimulates IgE responses by purified mouse mononuclear cell cultures stimulated with either LPS (101) or activated T cells (102), or by purified human B cells cultured with EBV (103), anti-CD40 antibody (104), hydrocortisone (105), mouse EL-4 cells + PMA (106). IL-4 induced IgE production can be blocked with anti-IL4 antibodies, further confirming the role for this cytokine in the IgE class switching. Similarly, IL-4 knock-out mice are unable to synthesize IgE (107). More recently another cytokine, IL-13 has been identified as a switch factor to IgE in humans (108). IL-13 has an approximately 30% homology to IL-4 and shares many of its biological activities. In mice this cytokine does not promote IgE synthesis since murine B cells do not express a receptor for IL-13. Both IL-4 and IL-13 are capable of inducing  $\epsilon$ -germline transcripts in human B cells, and they provide the first signal for the induction of IgE synthesis. The promoter region of the I $\epsilon$  exon contains a binding site for an IL-4 responsive element (109). This site (TCCNNNGAA) is known to bind a family of transcription factors known as signal transducers and activators of transcription (STAT). STAT proteins are found in the cytoplasm; they are activated after tyrosine phosphorylation, translocate into the nucleus, and activate gene transcription through binding of STAT binding sequences (110). IL-4 and IL-13 both induce STAT6, which binds the STAT binding sequence of the I $\epsilon$  promoter and can induce germline transcription (109, 111). STAT6-deficient mice are unable to make IgE, supporting the hypothesis that STAT6 - driven C $\epsilon$  gene transcription is critical for class switching. STAT6 acts in concert with other transcription factors e.g., one or more members of the C/enhancer binding protein (C/EBP) family and nuclear factor- $\kappa$ B (NF $\kappa$ B/Rel) proteins (112). A region in the murine  $\epsilon$  germline promoter 3' to the STAT6 binding site has also been shown to bind another transcription factor, B cell lineage specific activator protein (BSAP) (113). BSAP is encoded by Pax5, which is a

member of the Pax gene family of homeodomain transcription factors (114). Recent studies have investigated the role of BSAP in the transcriptional regulation of the  $\epsilon$  germline promoter in human B cells. The data shows that BSAP binds to the human  $\epsilon$  germline promoter and is essential for both IL-4 dependent induction and CD40 mediated upregulation of human  $\epsilon$  germline transcription (115).

In addition to cytokines, activation of the CD40 molecule on B cells is important for isotype switching. Crosslinking of CD40 on B cells with anti-CD40 antibodies allows for IgE production in the presence of IL-4 or IL-13, and IgA production in the presence of IL-10 and TGF- $\beta$  (116). The natural ligand for CD40 is CD40L, which is expressed on activated T cells and mast cells (117, 118). The critical role of CD40 in B cell function has been illustrated in patients with X-linked hyper-IgM syndrome who lack the expression of functional CD40L due to mutations in its gene (119). B cells from patients with hyper-IgM syndrome do not switch from IgM to other Ig classes and do not form germinal centers in the spleen. Also, some patients have normal expression of CD40L but have defects in the CD40 signalling pathway (120).

Although IL-4 stimulates switching of mouse B cells to both IgE and IgG1 and by human B cells to both IgE and IgG4, differences exist in the kinetics of switching to the different isotypes, the concentrations of IL-4 that are required to induce switching and the requirement for costimuli. There is a 12 to 16 hours delay in the generation of most IgE responses, as compared to the IgG1 response, by mouse B cells cultured with LPS plus IL-4 (121). Similarly, human B cells stimulated with IL-4 plus anti-CD40 antibody secrete detectable IgG4 approximately 2 days earlier than they secrete detectable IgE (122). Both observations are consistent with the interpretation that switch from IgM to IgE typically involves an initial switch to an IgG isotype and then a second switch to IgE, as already discussed in the previous section. Both IL-4 and IL-13 are also produced by mast cells and basophils upon appropriate stimulation (123). A variety of cytokines can modulate IL-4 and IL-13 mediated IgE synthesis. IgE synthesis can be enhanced by the

cytokines IL-5 and IL-6 in vitro. An involvement of TNF- $\alpha$  and its receptors CD120a and CD120b for the induction of IgE synthesis in vitro has also been suggested (124). CD23, the low affinity receptor for IgE, is upregulated on B cells by IL-4 and also plays a role in the induction of IgE response (101). Some monoclonal antibodies to this receptor inhibit the IgE response of human peripheral blood mononuclear cells cultured with IL-4 alone or with IL-4 plus hydrocortisone (127).

A number of different compounds have been identified that specifically inhibit IgE responses. The inhibitory effects of these compounds vary, however, depending on the costimulus that is employed to induce the IgE response. IFN- $\gamma$  inhibits germline  $\epsilon$  mRNA expression and IgE secretion by human peripheral blood mononuclear cells cultured with IL-4 (125, 146). IFN- $\gamma$  has no effect, however, on IgE secretion by human B cells cultured with IL-4 plus anti-CD40 antibody. IFN- $\alpha$  also inhibits IgE secretion by human peripheral blood mononuclear cells cultured with IL-4 (117, 146), and by human B cells cultured with IL-4 plus Epstein-Barr virus (126). Another cytokine, IL-12, has been reported to suppress IgE secretion by human B cells stimulated with IL-4 plus hydrocortisone, indirectly by inducing IFN- $\gamma$  (128).

### **1.8 IgE and Allergy**

Prausnitz and Küstner first demonstrated the presence of a factor in the blood of allergic subjects which when transferred to the skin of non-allergic individuals rendered them sensitive to allergens (129). This substance was identified as a cytophilic antibody in the late 1960s by Ishizaka and Ishizaka (130), but the lack of human cells that produce it in sufficient amounts was a serious drawback for its further investigation. It could nevertheless, be separated from the known immunoglobulins IgM, IgG, IgA and was named IgE for the erythema that allergens provoke in sensitive skin (129). The discovery of rat immunocytomas by Bazin and his colleagues (131), together with a rare human

myeloma reported by Johansson and Bennich (132), was a major breakthrough that provided the first tangible evidence for the existence of IgE (133). The protein produced by these cell lines afforded a standard for the measurement of IgE concentration in blood as well as material for the first structural studies. These cells were also the source of messenger RNA for the  $\epsilon$ -chain cDNA cloning and the starting point for some of the later structural studies of IgE (129).

The word allergy comes from a Greek term that means altered reactivity and thus includes all the mechanisms of hypersensitivity. The most common allergic diseases are asthma, allergic rhinitis, atopic dermatitis and food allergies, but the most dangerous is anaphylactic shock, usually provoked by insect stings or parenteral medication. Allergy in one form or another afflicts more than 20 percent of the population, and is generally caused by the overproduction of IgE in response to common environmental antigens, such as those present in pollen, food, house dust mites, animal danders, fungal spores, and insect venoms. IgE is produced only in mammals and is one of the five classes of human antibody. It constitutes a minuscule fraction of the total immunoglobulins in serum (50-300 ng/ml as compared with 10 mg/ml of IgG) and is therefore of little help in neutralizing antigens. However, its action is powerfully amplified by the receptors to which it binds.

The interaction between IgE and its high affinity receptor (Fc $\epsilon$ RI) on mast cells and basophils is a key step in allergic response. When a multivalent allergen associates with Fc $\epsilon$ RI-bound IgE it crosslinks the receptor molecules on the cell membrane, triggers degranulation of the cell and causes a rapid release of stored mediators, notably histamine, and further stimulates the synthesis and secretion of cytokines that attract and activate inflammatory cells. Fc $\epsilon$ RI has recently been discovered also on Langerhans cells (134), eosinophils and activated monocytes, but its biological function in these cell types has not been completely elucidated (135).

Early studies by Nissim and colleagues (136) had indicated that the high affinity receptor binding site of the IgE molecule can be assigned to the  $\epsilon$  H-chain constant region, since isolated Fc $\epsilon$  fragments (C $\epsilon$ 2-C $\epsilon$ 4), obtained by limited proteolysis of IgE, were able to bind to mast cells with an affinity similar to that of the intact molecule. However, fragmentation of the Fc $\epsilon$  into smaller pieces destroyed its receptor binding capacity (136). In addition, it has been shown that maintenance of the native conformation of IgE is important in its binding to the Fc $\epsilon$ RI (137). Studies in rodents demonstrated that a region in the cleft between the C $\epsilon$ 2 and C $\epsilon$ 3 is protected from proteolysis when bound to the Fc $\epsilon$ RI (138). The precise site on the IgE molecule that interacts with the Fc $\epsilon$ RI was further elucidated using recombinant DNA technology. Cloned C $\epsilon$  gene segments of both human (139, 140) and mouse IgEs (141, 142) were expressed in bacteria (143) and mammalian cells (136) as complete molecules, recombinant peptides or chimeras containing both rodent and human domains. Functional studies of these molecules provided direct evidence that the first twelve amino acids of C $\epsilon$ 3 are required for binding to Fc $\epsilon$ RI, but also showed that other residues in C $\epsilon$ 3 or C $\epsilon$ 4 influence this binding. Similar results were obtained from mapping studies with anti-IgE monoclonal antibodies (144). More recently, based on a model of the IgE Fc $\epsilon$ 3 (which is homologous to the second constant domain of IgG), homology scanning mutagenesis and replacement of individual residues were used to determine the specific amino acid residues in human IgE binding to human Fc $\epsilon$ RI (145). The amino acids were found to be localised in three loops, which form a putative ridge on the most exposed side of the Fc $\epsilon$ 3 domain of IgE and include a number of charged residues suggesting that the binding is mediated primarily by electrostatic interaction.

Activation of inflammatory cells by the products of mast cell degranulation induces the expression of the "low affinity" IgE receptor, Fc $\epsilon$ R2, also known as CD23, on eosinophils, monocytes, and Langerhans cells (146). This molecule is constitutively expressed on B lymphocytes and has been implicated in the regulation of the IgE

response (129, 134). Like in the case of FcεRI, studies with monoclonal anti-IgE antibodies and recombinant or chimeric IgE molecules pointed to Cε3 as the site of FcεRII interaction (147, 154). Studies with recombinant IgE confirmed that the Cε3 domain is involved in binding and also indicated that this domain must be dimeric since a single Cε3 did not bind to FcεRII. These studies also localized the IgE binding region in the vicinity of the glycosylated residue Asn 371, but showed that the carbohydrate components of IgE are not required for this interaction.

### **1.8a Alternative Spliced Forms of Human IgE**

Only one active gene coding for the ε heavy chain is present in humans. The ε heavy chain gene consists of four C region exons (CH1-CH4) and two membrane exons; the latter encode the transmembrane and cytoplasmic parts of membrane-bound IgE. Alternative splicing of sequences employing novel donor and acceptor sites 3' to the last ε heavy chain domain leads to the formation of multiple ε mRNA variants. These different ε mRNA variants have been detected in all human IgE producing cells i.e in the human IgE producing myeloma U266, and its subclones SKO-007 and AF10, in peripheral blood lymphocytes (PBLs) stimulated to produce IgE with IL-4 and anti-CD40 mAb, in human B cells spontaneously producing IgE isolated from patients with hyper-IgE immunodeficiency syndrome or atopic dermatitis, from fresh cells obtained from nasal washes of normal subjects challenged with diesel exhaust particles, and from unstimulated PBLs (148-152), demonstrating that these alternatively spliced isoforms occur naturally in non-atopic and atopic humans (Fig. 1.8). The different εmRNAs encode two membrane (εCH4-M1-M2 and εCH4-M1'-M2) and five potentially secreted (εCH4-S, εCH4\*, εCH4'-I, εCH4-M2' and εCH4-M2") ε-heavy chains. The secretory isoforms include the classical secretory IgE H chain (εCH4-S) and four isoforms which lack either portions of the CH4 domain (εCH4\* and εCH4'-I) or contain additional amino

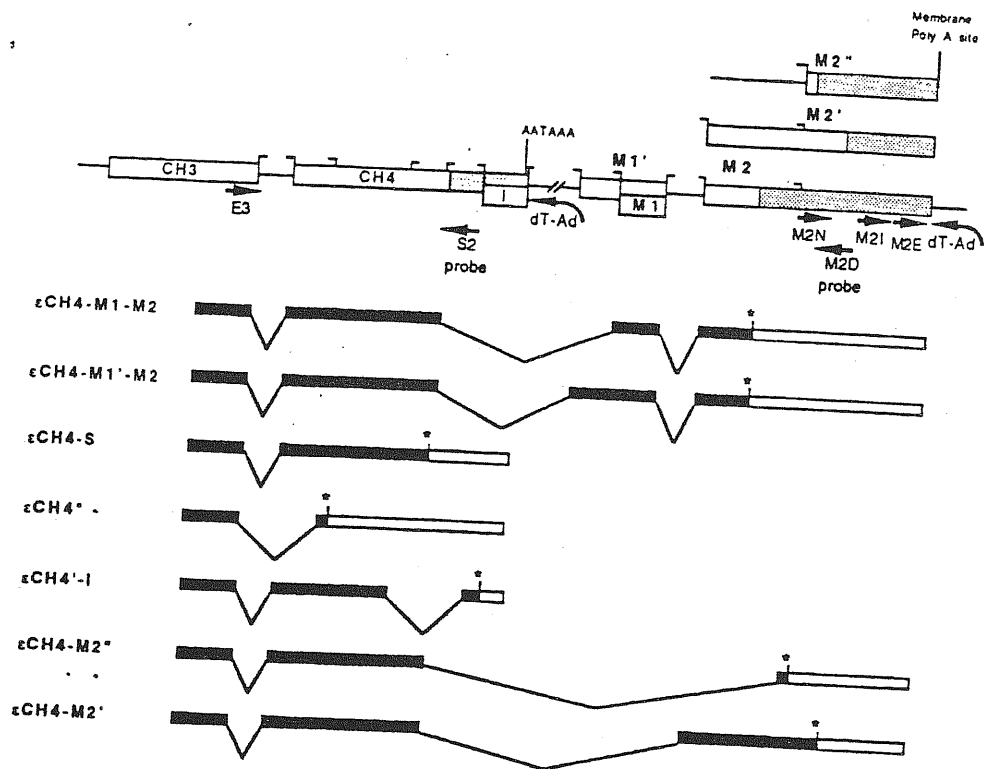


**Figure 1.8:** Diagrammatic summary of 3' ends of various  $\epsilon$  mRNA species detected in reverse transcriptase PCR experiments. A schematic representation of the 3' end of the *Ce* gene is shown at the top. Open boxes represent coding sequences, shadowed boxes represent 3' untranslated regions. In the diagram of the alternatively spliced  $\epsilon$  transcripts, filled and open boxes correspond to translated and untranslated regions, respectively. Stop codons are indicated by asterisks. The names of each of the splice variant is indicated on the left.



acids in their carboxy termini encoded by different parts and reading frames of the M2 exon ( $\epsilon$ CH4-M2' and  $\epsilon$ CH4-M2").

It was of great interest whether these novel mRNAs encode functional proteins and whether these various forms of IgE play distinct roles in the immune response. With the exception of the classical secreted and membrane form, analysis of the U266 cellular extracts and supernatants did not confirm the existence of proteins corresponding to the alternatively spliced  $\epsilon$  mRNA species suggesting that these isoforms are either inefficiently translated and/or rapidly degraded. To investigate the expression of these isoforms in the absence of competition for translational and other protein processing factors Batista et al introduced independently the modified human  $\epsilon$  H chain genes, corresponding to the  $\epsilon$ CH4-S,  $\epsilon$ CH4\*,  $\epsilon$ CH4'-I,  $\epsilon$ CH4-M2' and  $\epsilon$ CH4-M2" mRNA isoforms in the mouse plasmacytoma cell line J558L (152). All isoforms were found to be efficiently translated in the myeloma cells, but with the exception of  $\epsilon$ CH4-S and  $\epsilon$ CH4-M2" forms, their protein products were absent in the supernatants. Pulse-chase experiments showed that the  $\epsilon$ CH4\*,  $\epsilon$ CH4'-I,  $\epsilon$ CH4-M2' forms failed to assemble into H<sub>2</sub>L<sub>2</sub> dimers and were intracellularly retained and degraded. Immunofluorescence analysis suggested that the site of retention is the ER, since none of them were found to be compartmentalized within the Golgi. All these forms assemble into HL monomers that retain the specificity for the antigen, but fail to assemble into HL dimers. The absence of the complete CH4 domain in  $\epsilon$ CH4\* or the carboxyl terminal part of it in  $\epsilon$ CH4'-I could explain the inability to form HL dimers since this domain has been shown to be necessary for  $\epsilon$  H-chain dimerization (153). In the case of the  $\epsilon$ CH4-M2' form, which contains the complete  $\epsilon$  CH4 domain (except for the last two amino acids), the presence of the large M2' domain could prevent dimerization of the two H-chains. This data suggests that the  $\epsilon$ CH4\*,  $\epsilon$ CH4'-I and  $\epsilon$ CH4-M2' forms are only byproducts of alternative splicing in the C $\epsilon$  locus, and most likely, without functional significance.

Regarding the  $\epsilon$ CH4-M2' form the results of Batista et al were in marked contrast to those reported by Zhang et al., who found that it is secreted in a patient with myeloma and in AF10, a subclone of the U266 cell line (151). Batista et al., however did not detect it in the U266. It is unlikely that this discrepancy is a result of the differentiation state of the cells as observed for membrane and secreted forms of IgM (154), because all cells are of myeloma origin, although there may be differences in the subclones used by both groups. Recently Lyczak et al. confirmed the results obtained by Batista et al in the J558L myeloma but found the M2' form to be correctly assembled and secreted in another murine myeloma cell line Sp2/0 (155). They postulate a cell line-dependent regulation of secretion.

The  $\epsilon$ CH4-M2" in contrast, was found to be efficiently secreted by both plasma cells (J558L and Sp2/0) and B lymphocytes (155, 156). Batista et al have characterised it further and have designated it as the second secreted IgE isoform ( $\epsilon$ S2). The  $\epsilon$ S2 H chain is only six amino acids longer than the classical secreted IgE H chain ( $\epsilon$ S1) and contains a C-terminal cysteine, which is a characteristic sequence feature of  $\mu$  and  $\alpha$  H chains. However, unlike IgM and IgA, they found that the  $\epsilon$ S2 C-terminal cysteine does not induce polymerization of H<sub>2</sub>L<sub>2</sub> molecules, rather it creates a disulfide bond between the two H chains that increases the rate of association into covalently bound H<sub>2</sub>L<sub>2</sub> monomers. This C-terminal cysteine also does not function as an intracellular retention element because the  $\epsilon$ S2 isoform was found to be secreted in amounts equal to that of the  $\epsilon$ S1, both in B-lymphocytes and plasma cells. The  $\epsilon$ S2 H chains secreted by B lymphocytes differed from the  $\epsilon$ S1 H chains in the extent of glycosylation. Also, there was a difference in glycosylation between B-lymphocytes and plasma cells for both the isoforms. This could have a potential functional significance as recent studies have shown that the serum of allergic patients contains polyclonal IgE antibodies that differ in the degree of sialylation and possibly in effector functions. Only a portion of these IgE glycoforms bind the  $\epsilon$ BP, a  $\beta$ -galactoside-binding lectin that has been implicated in the

binding of IgE to mast cells, Langerhans cells, and neutrophils (157-159). Also, recent studies with recombinant human IgE-Fc fragments have shown that the extent of glycosylation also affects the affinity of IgE for the FcεRII (160). The biological function of the εS2 isoform, the regulation of its expression, and its role in atopic diseases are important issues that need to be studied further.

## **CHAPTER 2**

## MATERIALS AND METHODS

### 2.1 RNA and DNA samples

The murine IgE producing B cell lymphoma cell line I29e<sup>+</sup> was maintained in DMEM supplemented with 5% (v/v) fetal calf serum, penicillin (100 U/ml), streptomycin (100 µg/ml) and 50 µM β-mercaptoethanol. Spleens were excised from BALB/c mice, mechanically disrupted and the cells were dispersed in cold PBS.

Total cellular RNA was isolated using the acid guanidinium thiocyanate procedure (176). High molecular weight genomic DNA was isolated from mouse splenocytes by standard methodology (177).

### 2.2 3'-End Amplification of ε cDNA

The 3' ends of ε mRNAs were amplified using the RACE technique (178). 3 µg of total cellular RNA from I29e<sup>+</sup> cells were reverse transcribed with the Gene Amp RNA PCR kit (Perkin Elmer Cetus, Norwalk, CT) using an oligo(dT)<sub>15</sub>-adaptor (dT-Ad, 5'-GACTCGAGTCGACATCGATTTTTTTTTTTTTTTT-3') as primer. Thirty five cycles of PCR were next done on the RT sample with the M23/Ad (M23, 5'-TCCACACCGATGCAGGATACA-3'; Ad: 5'-GACTCGAGTCGACATCGA-3') and the M25/Ad primer pairs (M25, 5'-AGACCTTCCAAGACTATGCCA-3'). The PCR reactions were carried out with 1 min of denaturation at 95°C, 1 min of annealing at 58°C and 2 min of extension at 72°C. The specificity of the obtained products was confirmed by Southern Blot analysis with the M22 oligonucleotide (M22, 5'-CCTATGCCCTGGTCTGGAGGAT-3').

### 2.3 Cloning and Sequencing

PCR fragments obtained by amplification of cDNA from I29ε<sup>+</sup> cells and mouse splenocytes were purified from 1% agarose gels by electroelution. The recovered DNA fragments were ligated in the SmaI site of pUC18 (Pharmacia LKB, Uppsala, Sweden) and used to transform E. coli strain DH5-α. At least three positive clones from each transformation were sequenced using the T7 Sequencing kit (Pharmacia LKB).

### 2.4 PCR amplification of unknown 3' flanking DNA

The sequence of the 3' flanking region of the membrane locus poly(A) site was determined by analyzing "misprimed" or "jumping" PCR artefacts which were generated using primers complementary to sequences from the M2 exon and several non-specific primers unrelated to the mouse Cε gene (162, 168). Briefly, PCR reactions were performed with 1 μg genomic DNA, 50 pmol of M2 exon primer (M23), 50 pmol of non-specific primer, 200 μmol of each dNTP, 0.5 U Taq polymerase and 10 μl of 10X PCR buffer in a total volume of 100 μl. Thirty five cycles of denaturation at 95°C for 1 min, annealing at 58°C for 1 min and extension at 72°C for 2 min were performed. The PCR artefacts containing the sequence of interest were selected in semi-nested PCRs in which 2 μl of the first PCRs were reamplified with the internal primer M25 and the same non-specific primer from the first reaction. The specific PCR products were identified by Southern Blot analysis with the internal oligonucleotide M22, and were cloned and sequenced as described above. The obtained sequences were confirmed by PCR amplification of genomic DNA with primers from the known and new sequence, followed by cloning and sequencing of both strands of the PCR products.

## 2.5 Northern Blot Hybridizations

20  $\mu\text{g}$  samples of total I29 $\epsilon^+$  RNA were separated by electrophoresis in 1% agarose gels containing 6% formaldehyde, transferred to nylon membranes (Hybond-N, Amersham, UK) by overnight capillary blotting in 20X SSC and fixed with UV light. The filters were hybridized with three different probes generated by restriction enzyme digestion or PCR amplification of cloned Ce gene fragments. The m $\epsilon$ C probe was a 543 bp (HindIII/BstXI) fragment containing part of the CH3 and CH4 exons. The M1 probe was a 135 bp PCR fragment encompassing the complete M1 exon. The M2 probe was a 399 bp BstXI/AvaI fragment starting 66 nucleotides downstream of the first poly(A) signal. The probes were labeled with [ $\alpha$ - $^{32}\text{P}$ ]dCTP (Amersham, UK) using the Oligolabeling kit (Pharmacia, LKB). Hybridizations were carried out overnight at 42°C in 5XSSPE/0.5%SDS/5XDenhardt's/50% formamide/100  $\mu\text{g}/\text{ml}$  salmon sperm DNA. Filters were washed in 2XSSC/0.1% SDS at 42°C and autoradiographed.

## 2.6 RT-PCR analysis of $\epsilon$ transcripts

Two micrograms of splenocyte or I29 $\epsilon^+$  RNA were reverse transcribed with the Gene Amp RNA PCR kit using oligo-dT<sub>(15)</sub> as primer. Thirty five cycles of PCR were done on each RT sample with the E41 (5'-AAGTG ATCCA TGAGG CACTT CA-3') and the M28 (5'-TCCAT CCCAT GAAGA GGTCT-3') or M30 (5'-CCAGA GACAA AGTAG GACTG-3') oligonucleotide under the following conditions: 1 min denaturation at 95°C, 1 min annealing at 64°C and 2 min extension at 72°C. The RT and PCR analyses were performed in accordance with the instructions of the manufacturer. The specificity of the obtained PCR products was confirmed by Southern blot analysis with an oligonucleotide probe (M27, 5'-AACTCAGAGTCTAGAGCT-3') or a PCR probe from the M2 exon. The PCR probe was obtained by amplifying a cloned M2 exon fragment with

oligonucleotides M29 (5'-GCTTCAGACCTCTGGTC-3') and M26 (5'-TTCCTGAGACAGTGTACAT-3'). Positive bands were cloned and sequenced as described above.

The efficiency of amplification of the alternatively spliced  $\epsilon$  mRNA species was investigated by performing experiments with known quantities of corresponding cloned fragments. Maxi preparations of the plasmid DNAs were purified with a QIAGEN plasmid kit (Qiagen, Germany) and the concentrations were determined by spectrophotometry. The three plasmids were mixed together in different relative amounts and PCR amplified as described above.

## **2.7 Cell lines and transfections**

The WEHI 231 B-cell lymphoma (ATCC, Rockville, USA) was maintained in DMEM supplemented with 10% FCS, penicillin (100 U/ml), streptomycin (100  $\mu$ g/ml) and 50  $\mu$ M 2-mercaptoethanol. The A20 B-cell lymphoma (ATCC, Rockville, USA) was maintained in RPMI + 10% FCS, and the same components listed above. Transfections were performed by electroporation.  $2 \times 10^6$  cells were washed, resuspended in 500  $\mu$ l cold PBS, mixed with linearized DNA (15  $\mu$ g in 20  $\mu$ l H<sub>2</sub>O) and electroshocked using the Bio-Rad Gene Pulser at 250 volts and 960  $\mu$ F. After 5 min on ice, the cells were suspended in 50 ml DMEM/10% FCS/gentamicin and transferred to five 96-well plates. Selective medium containing 800  $\mu$ g/ml of G418 (Geneticin, Life Technologies, Inc., Gaithersburg, MD) was added 24 h later for selection of the clones. Cells were cloned by limiting dilution and positive clones were identified by immunofluorescence.



## 2.8 Construction of vectors for the expression of the $\epsilon$ CH4-M1-M2 and $\epsilon$ CH4-M1'-M2 H-chains

An Aat II/Kpn I fragment from Hu-pSVC $\epsilon$  (179) (kindly provided by Dr. M. Neuberger), containing the mouse immunoglobulin H-chain enhancer and promoter, a mouse anti-NIP VH segment and the entire human genomic C $\epsilon$  gene, was subcloned in a plasmid derived from pRc/CMV (Invitrogen, San Diego, USA) in which the cytomegalovirus promoter and the fd portion had been deleted. This new plasmid (pCIG-C $\epsilon$ ) contains a single Kpn I site downstream of the C $\epsilon$  gene and was used for the construction of the two alternatively spliced membrane  $\epsilon$  species.

To construct the pCIG-C $\epsilon$ CH4-M1'-M2, a PCR fragment obtained by amplifying cDNA from PBL with oligonucleotides E3 (E3, 5'-CATGC GGTCCA CGACC AAGAC-3') located in the CH3 exon of the C $\epsilon$  gene and M2d (M2d, 5'-TGGGTGCCGGGCCCTCCTTGGC-3') which is located in the 3' untranslated region of the C $\epsilon$  gene was cloned in the Sma I site of pUC18. A Bbs I-Kpn I fragment from this plasmid, which contained part of CH4, the M1' and the M2 exon until the Kpn I site was subcloned in pUC18 $\Delta$ C $\epsilon$ S. (pUC18 $\Delta$ C $\epsilon$ S contains the 3' part of the CH1 exon, the second intron, the CH2 exon, the third intron, and the CH3 and CH4 exons joined together). The Bgl II-Kpn I fragment from this modified plasmid now containing the M1' and M2 exon was used to replace the same fragment in the pCIG-C $\epsilon$ , generating the pCIG-C $\epsilon$ CH4-M1'-M2 which was used for transfection.

The pCIG-C $\epsilon$ CH4-M1-M2 vector was similarly constructed by replacing the Bgl II/Kpn I fragment of pCIG-C $\epsilon$ CH4-M1'-M2 with a corresponding fragment containing the M1 instead of the M1' exon (Fig. 3.2.3).

## 2.9 Flow cytometric analysis

The expression of surface IgE was examined by flow cytometry on a FACScan, (Becton Dickinson and Co., Mountain View, CA, USA). Briefly,  $1 \times 10^6$  cells were stained with rabbit anti-human IgE ( $\epsilon$  chain) (DAKO) in PBS+3% BSA for one hour at  $4^\circ\text{C}$ , washed with cold PBS containing azide and then incubated with FITC-conjugated swine anti rabbit IgG (DAKO) for one hour again at  $4^\circ\text{C}$ . After extensive washing the cells were analyzed for surface staining using the FACScan.

## 2.10 Immunoprecipitations

Metabolic labeling and immunoprecipitations were performed as previously described (181). Briefly,  $5 \times 10^6$  cells/ml were labeled with [ $^{35}\text{S}$ ]methionine (Amersham, Amersham, UK) at 100-250  $\mu\text{Ci/ml}$  (1Ci=37 GBq) and chased with cold methionine for the indicated times. The cells were washed with PBS and lysed by addition of cold cell lysis medium (50mM Tris pH 8.0, 150 mM NaCl, 5mM  $\text{MgCl}_2$ , 1% NP-40 and 1mM PMSF). For the pulse-chase experiments, 50% of the cells from each cell line were lysed immediately after labeling, while the remaining cells were incubated for additional period of time with an excess of cold methionine. Cell lysates were immunoprecipitated with rabbit immunoglobulins to human IgE ( $\epsilon$  chains) or rabbit immunoglobulins to mouse IgM ( $\mu$  chains) (DAKO, Glostrup, Denmark) and purified by protein A-sepharose. The samples were analyzed by SDS-PAGE in the presence or absence of mercaptoethanol, as indicated in the figure legends. Treatments of labeled supernatants with Recombinant N-glycosidase F (PNGase F) and Endoglycosidase H (Endo H) were performed according to the protocols provided by the manufacturer (New England Biolabs, Beverly, MA).

## 2.11 Surface biotinylation and immunoprecipitation of IgE and IgM

### BCRs

Twenty million cells were washed twice with PBS and incubated in 1 ml of PBS containing 0.5 mg/ml of Sulfo-NHS-biotin (Pierce) at room temperature for 15 min. Free succinimide groups were blocked by the addition of 10 ml of non supplemented medium at room temperature for 10 min. Cells were washed twice with PBS and resuspended in 500  $\mu$ l lysis buffer containing: 1 % digitonin (Sigma-Aldrich Chemical Co.); 50 mM Tris-HCl, pH 7.5; 150 mM NaCl; 5 mM EDTA; and the protease inhibitors PMSF (1 mM) , aprotinin (10  $\mu$ g/ml), and leupeptin (10  $\mu$ g/ml), all from Sigma. Lysates were incubated on ice for 30 min and centrifuged at 10,000g for 30 min at 4°C. The supernatants were precleared three times with 30  $\mu$ l of protein A agarose beads (Gibco-BRL) at 4°C for 30 min. Immunoprecipitations were performed by incubating the lysates with 6  $\mu$ l of rabbit immunoglobulins to human IgE ( $\epsilon$  chains) (DAKO), rabbit immunoglobulins to mouse IgM ( $\mu$  chains) (DAKO), or goat immunoglobulins to human IgE ( $\epsilon$  chains) (Kirkegaard & Perry), at 4°C for 60 min. 20  $\mu$ l of protein A agarose were then added and incubated for a further 30 min at 4°C. The Ig- $\alpha$ /Ig- $\beta$  heterodimer was immunoprecipitated using a polyclonal antibody against Ig- $\alpha$ , kindly provided by Dr. J. C. Cambier (National Jewish Centre for Immunology and Respiratory Medicine, Denver, CO., USA). Beads were preincubated with 10 mg/ml bovine serum albumin for 20 min and washed three times with lysis buffer before use. The beads were pelleted by centrifugation (the supernatants were saved for reprecipitation) and washed twice with high salt lysis buffer (50 mM Tris pH 7.5, 500 mM NaCl, 5 mM EDTA, 0,2% digitonin, plus inhibitors) and twice with low salt buffer (50 mM Tris pH 7.5, 150 mM NaCl, 5 mM EDTA, 0.2% digitonin, plus inhibitors). For re-precipitation, supernatants were precleared twice with 30  $\mu$ l beads before adding a different primary antibody.

### 2.12 In vitro kinase assay

Immunoprecipitates from digitonin lysates were resuspended in kinase buffer (50 mM Tris pH 7.5, 10 mM  $MnCl_2$ , 1 mM EDTA, 1 mM sodium orthovanadate (Sigma), 1 % digitonin, plus inhibitors) containing 10  $\mu Ci$  [ $\gamma^{32}P$ ] (Amersham), and incubated at room temperature for 5 min. The reaction was terminated by addition of kinase buffer containing 50 mM EDTA and the pellets were collected by centrifugation before resuspending in SDS-PAGE reducing sample buffer. The samples were boiled and electrophoresed on a 10 % SDS-PAGE. The gel was dried without fixing and autoradiographed at  $-70^\circ C$ .

### 2.13 Detection of tyrosine phosphorylated proteins by western blotting

Tyrosine phosphorylated proteins were detected as previously described (181). Briefly,  $4 \times 10^6$  cells were resuspended in 0.5 ml of DMEM medium and stimulated with either goat anti-human IgE ( $\epsilon$  chain) (Kirkegaard & Perry) (20  $\mu g/ml$ ) or anti-mouse IgM (5  $\mu g/ml$ ) at  $37^\circ C$  for the indicated periods of time. After washing twice with ice-cold PBS containing 1 mM sodium orthovanadate, cells were lysed with 100  $\mu l$  of Triton X-100 lysis buffer containing 20 mM Tris-HCl (pH 8.0), 137 mM NaCl, 10 % glycerol, 1 % Triton X-100, 2 mM EDTA, plus inhibitors and 1 mM sodium orthovanadate. After incubation for 10 min on ice, the supernatants were cleared by centrifugation at 10000g for 15 min at  $4^\circ C$ . Subsequently, 30  $\mu l$  of supernatant was subjected to 10% SDS-PAGE and Western blotting. The PVDF membrane (Amersham) was incubated with the antiphosphotyrosine monoclonal antibody PY20 (Transduction Laboratories), followed by horseradish peroxidase-coupled anti mouse Ig antibody (DAKO). The bound antibodies were visualized by the enhanced chemiluminescence (ECL) detection system (Amersham).

### 2.14 Cellular Proliferation Assay

Two B-cell transfectomas that expressed comparable levels of m<sub>L</sub>IgE and m<sub>S</sub>IgE were cultured in triplicate in 96-well plates at a cell density of 2x10<sup>4</sup>/well. The cells were incubated for 24 hours with various amounts of goat anti-human IgE (ε chain) (Kirkegaard & Perry) in 0.2 ml medium. Proliferation was determined by incorporation of [methyl-<sup>3</sup>H]thymidine (1μCi per well, 94.0 Ci/mmol, Amersham). After 14 hours of incubation cells were harvested, and levels of incorporated [<sup>3</sup>H]thymidine were measured by scintillation counting.

### 2.15 Apoptosis assay

The assay was performed using the ApoAlert Annexin V Apoptosis kit (Clontech). Two B-cell transfectomas that expressed comparable levels of m<sub>L</sub>IgE and m<sub>S</sub>IgE were cultured in 24-well plates at a cell density of 1x10<sup>5</sup>/well. The cells were incubated for 24 hours with 20μg/ml of goat anti-human IgE (ε chain) (Kirkegaard & Perry) in 0.5 ml medium. The WEHI cells were incubated as above with 10μg/ml of rabbit anti-mouse IgM (DAKO). The cells were washed with PBS and resuspended in 200μl of binding buffer provided in the kit, next 10μl of annexin V-FITC was added to a final concentration of 1μg/ml. The cells were then incubated in the dark for 15 min at room temperature, before their analysis by flow cytometry.

### 2.16 Internalization Assay

Internalization was also measured by flow cytometry as previously described (66, 204). Both the transfected cell lines were stained with FITC-conjugated rabbit anti-human IgE

(DAKO) at 4°C for 30 min in PBS/1%FCS. After washing, all samples except for positive control (no internalization) were resuspended in prewarmed medium and incubated for 60 min at 37°C. The reaction was stopped by adding ice-cold PBS/FCS containing 0.1% sodium azide. The fluorescence was then analyzed using a Becton-Dickinson FACScan.

## CHAPTER 3

## RESULTS

### Section 1

#### 3.1.0 Identification and characterization of murine immunoglobulin $\epsilon$ mRNAs and their polyadenylation sites

##### 3.1.1 Introduction

*The C $\epsilon$  gene is the penultimate gene at the immunoglobulin (Ig) heavy (H) chain locus in both mice and humans, and encodes the constant region part of the IgE H-chain molecules. It is composed of four constant region exons (CH1-CH4) and two membrane exons that encode the membrane-proximal, transmembrane and cytoplasmic parts of membrane IgE (149, 150, 152, 161). In humans, the second membrane exon (M2) contains a long 3' untranslated region (1046 bp) and an AGTAAA polyadenylation signal sequence which differs from the consensus AATAAA found in the second membrane exon of all other human Ig H-chain genes (162-164). This rather inefficient poly(A) signal could in part determine the low levels of expression of membrane  $\epsilon$  transcripts and the extremely low number of human peripheral blood lymphocytes (PBL) expressing surface IgE.*

*The human C $\epsilon$  gene also appears to be peculiar in its capacity to produce a number of  $\epsilon$  mRNAs that are generated by alternative splicing between the last two constant region exons and the two membrane exons (148-152, 162, 165, 166). Many of these isoforms are apparently just aberrant by-products of alternative splicing which are unable to form properly assembled IgE molecules (152). However, one of this variants, referred to as the  $\epsilon_{S2}$ , was found to be secreted with the same efficiency as the classical secreted  $\epsilon_{S1}$  H-*



chain (157). This isoform contains only six additional amino acids which are added by splicing to an internal acceptor splice site in the M2 exon.

Considering the possible functional differences of the human IgE isoforms, it would be important to investigate whether similar isoforms exist in other species. If so, these species could serve as useful animal models to determine the biological effects of the various IgEs. We focused our study on the mouse C $\epsilon$  gene whose sequence had previously been characterised until the stop codon of the second membrane exon (141). This gene shares considerable homology with the human C $\epsilon$  gene in the 3' part (the CH4, M1 and M2 exons), although to a lower extent than the other genes from the Ig H-chain locus (141). Northern blot analysis of IgE-producing mouse hybridoma cells has shown that the mouse C $\epsilon$  gene is transcribed into a major RNA species corresponding to the secretory form and two minor species corresponding to membrane form(s) of the  $\epsilon$  chain (141, 168). The latter species could have been generated by alternative splicing of membrane-exon sequences or by differential usage of two poly(A) sites.

We have addressed these issues by analyzing the  $\epsilon$  mRNAs produced by freshly isolated murine splenocytes and by a murine IgE producing lymphoma. Using RT/PCR and sequence analysis we identified five alternatively spliced  $\epsilon$  transcripts in the mouse. We also determined the complete 3' untranslated region sequence of the mouse C $\epsilon$  gene and identified and characterised the two poly (A) sites of the murine membrane  $\epsilon$  locus.

### **3.1.2 Characterization of the two murine membrane $\epsilon$ mRNA polyadenylation sites**

The poly (A) sites of the mouse membrane  $\epsilon$  transcripts were identified by RACE-PCR analysis of total cellular RNA isolated from the IgE expressing B-cell lymphoma I29e<sup>+</sup>. Total RNA from I29e<sup>+</sup> was reverse transcribed using a 35-base oligonucleotide

containing 15dT residues and an adaptor sequence with three endonuclease recognition sites that are found infrequently in genomic DNA (dT/Ad). In order to identify the poly (A) sites, the resulting cDNA (negative strand) was then amplified with an oligonucleotide that contained only the adaptor sequence (Ad) and two oligonucleotides located in the M2 exon (primers M23 and M25 from Fig. 3.1.1). The PCR products were analysed by Southern blot with an internal radiolabeled oligonucleotide from the same exon (primer M22). Two strong bands of ~ 700bp and ~ 1200 bp and a weak band of ~900 bp hybridized to this oligonucleotide, suggesting that the transcripts containing the M2 exon use more than one polyadenylation site. Cloning and sequencing of the above fragments showed that the two major bands represent differentially polyadenylated  $\epsilon$  transcripts, whereas the weak ~900 bp fragment was a heteroduplex of the two species. This analysis also yielded the complete sequence of the 1.17 kb 3' untranslated region of the M2 exon (shown in Fig. 3.1.2).

Analysis of the 3' untranslated region sequence showed that the M2 exon contains two polyadenylation signals. The first one is an AGTAAA hexanucleotide located 743 bp downstream from the beginning of the M2 exon and 9 nt upstream from a CA dinucleotide where mRNA cleavage and poly(A) addition had occurred. The second polyadenylation signal is an AAGAAA hexanucleotide located 486nts further downstream. The transcripts that used this polyadenylation signal were cleaved at a GA dinucleotide located 17 nt after the hexamer.

To further characterise the polyadenylation signal of the transcripts from the membrane  $\epsilon$  locus and to investigate the presence of other potential polyadenylation signals we analyzed the genomic composition of the region downstream of the poly (A) site. The sequence of the genomic DNA flanking the poly (A) site in the 3' direction was obtained by using a modification of a PCR-based chromosome walking technique (168). This procedure takes advantage of the PCR artefacts that are generated by primer misannealing and "jumping PCR" when the reaction is performed in the absence of

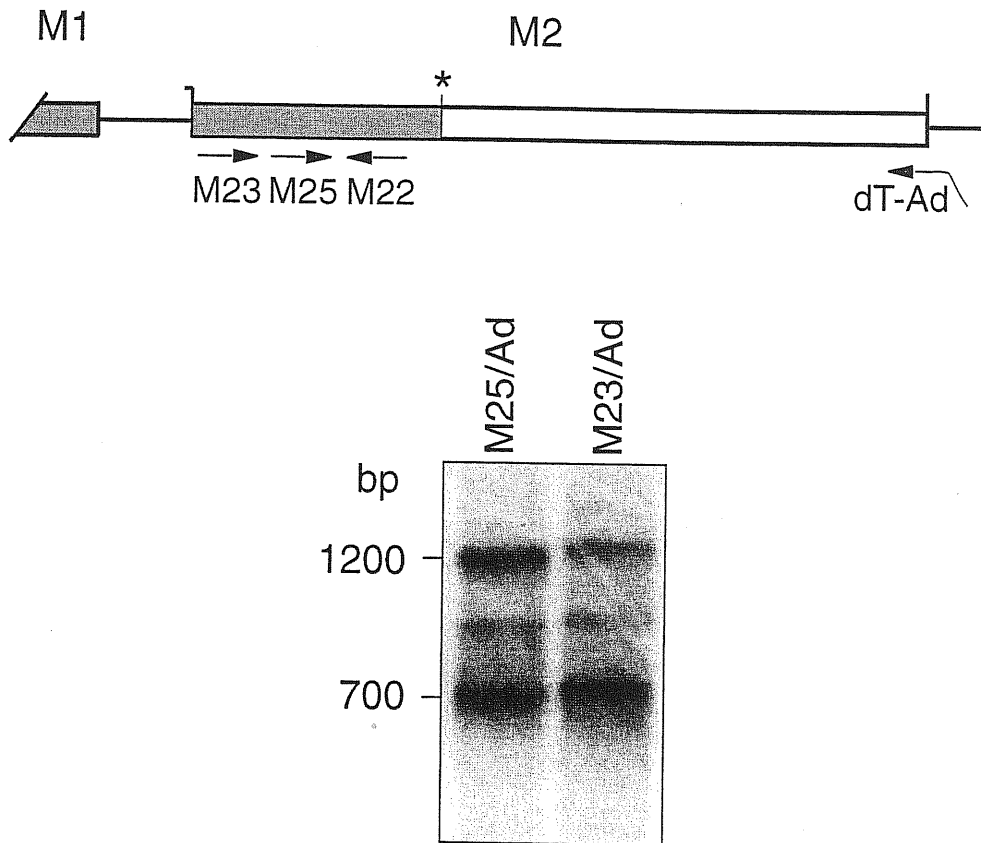


**Figure 3.1.1:** RACE-PCR analysis of  $\epsilon$  transcripts containing M2 exon sequences. The location of the RT/PCR primers (M23, M25 and dT-Ad) and the oligonucleotide that was used for the hybridization (M22) are indicated. Asterik indicates the stop codon in the M2 exon. Filled and open boxes represent coding and 3' untranslated regions, respectively. The lower panel shows an autoradiogram from the RACE-PCR analysis of I29 $\epsilon^+$  mRNA.



correct template. The artefacts containing the sequence of interest were selected and further amplified in a seminested PCR to obtain the sequence of genomic DNA which lied outside the boundary of the known sequence of the C $\epsilon$  locus.

In this way, 836 nt of M2 exon 3' flanking region sequence was obtained (Fig. 3.1.2). The sequence was determined by sequencing both strands of three independent PCR products. Only a few discrepancies were noted between the sequences, which were apparently due to Taq polymerase errors. The consensus sequence (from two identical sequences) was subsequently confirmed by cloning and sequencing a PCR product obtained by amplification of mouse genomic DNA with a primer located in the M2 exon (M23) and a primer derived from the 3' end of the new sequence (M26 in Fig. 3.1.2). This sequence has been submitted to the EMBL database under the following accession number: X99259. Analysis of this sequence showed that a GT rich region is located 14 nt downstream to the site of cleavage and polyadenylation of the second poly(A) signal.

### **3.1.3 Both poly (A) signals are used by the membrane $\epsilon$ transcripts**

The  $\epsilon$  mRNA species produced by I29 $\epsilon^+$  cells were investigated by Northern blot analysis using three different probes corresponding to distinct parts of the C $\epsilon$  gene. The m $\epsilon$ C probe contained CH3 and CH4 exon sequences and was used to detect all  $\epsilon$  mRNAs. As shown in Figure. 3.1.3, this probe hybridised to three mRNA species. The smallest, most intensely hybridising mRNA was ~ 1.9 kb long and corresponded in size to the secretory type of  $\epsilon$  mRNA. The two larger  $\epsilon$  mRNA species had molecular sizes of 2.7 and 3.2 kb and both of them also hybridised to the probe containing the complete M1 exon. The difference in size between these two mRNAs was consistent with the distance between the two polyadenylation sites, indicating that they corresponded to differentially polyadenylated membrane  $\epsilon$  mRNAs. This was confirmed with a probe located in the

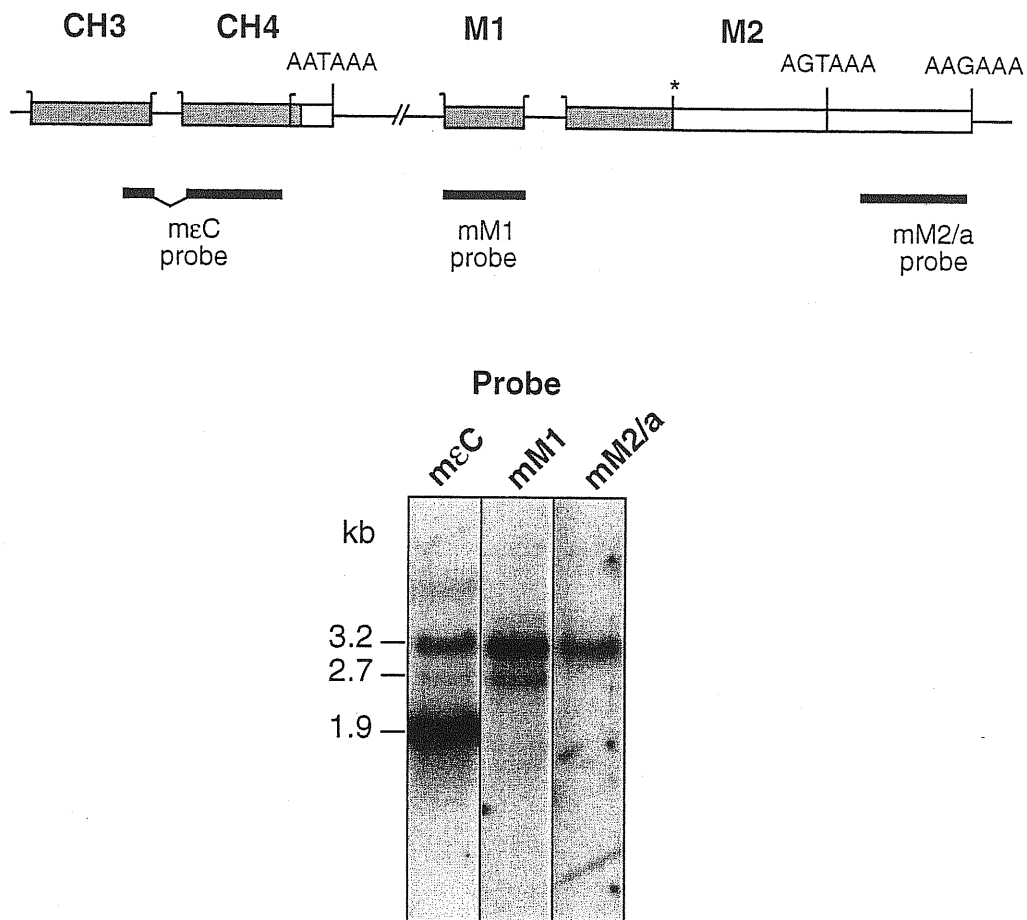


**Figure 3.1.3:** Northern Blot analysis of murine  $\epsilon$  mRNAs. Upper panel shows the schematic representation of the 3' end of the murine  $\epsilon$  gene and the position of the probes used for hybridization. Bottom panel shows an autoradiogram with the predominant  $\epsilon$  mRNA species expressed by the IgE producing lymphoma I29 $\epsilon^+$ .

region between the two poly(A) sites, which hybridised only to the 3.2 kb transcript. Interestingly, the 3.2 kb transcript appeared to be more abundant than the 2.7 kb species (as judged by the hybridisation signals obtained with the m $\epsilon$ C and mM1 probes), suggesting that the second poly(A) signal is more active than the first one.

### **3.1.4 Alternatively spliced membrane exon transcripts are produced by I29 $\epsilon^+$ cells and mouse splenocytes**

In recent studies we and others have shown that the human C $\epsilon$  gene produces a number of alternatively spliced  $\epsilon$  mRNA molecules (148-152, 162, 165, 166). To investigate if similar events occur in the mouse C $\epsilon$  locus, RT-PCR analysis was done on RNA extracted from the murine IgE secreting lymphoma (I29 $\epsilon^+$ ) and from freshly isolated mouse splenocytes. The cDNAs were amplified with primers located in the CH4 exon (E41) and at the end of the M2 3' untranslated region (M28) (Fig. 3.1.4a). Three bands of approximately 1.4 kb, 1.3 kb and 0.5 kb were obtained from both cell types, all of which hybridized with an M2 exon PCR fragment spanning the region between oligonucleotides M29 and M26 (Fig. 3.1.4b).

Cloning and sequencing of the PCR fragments showed that they represent four different  $\epsilon$  mRNA species (Figures 3.1.4). The first one corresponded to the classical membrane species whose structure had been predicted based on splice sites consensus sequences. This species (m $\epsilon$ CH4-M1-M2) is spliced from the CH4 exon donor site, located 23 nt upstream of the CH4 stop codon, to the acceptor site of the M1 exon, and subsequently from the M1 to the M2 exon. One of the novel mRNAs designated m $\epsilon$ CH4-M1-M2\* was obtained from the same band as the m $\epsilon$ CH4-M1-M2 splice product. This RNA spliced to a new acceptor splice site in the M2 exon located 30 nt downstream to the splice site of the m $\epsilon$ CH4-M1-M2 form. Since there is no shift in the reading frame, this second

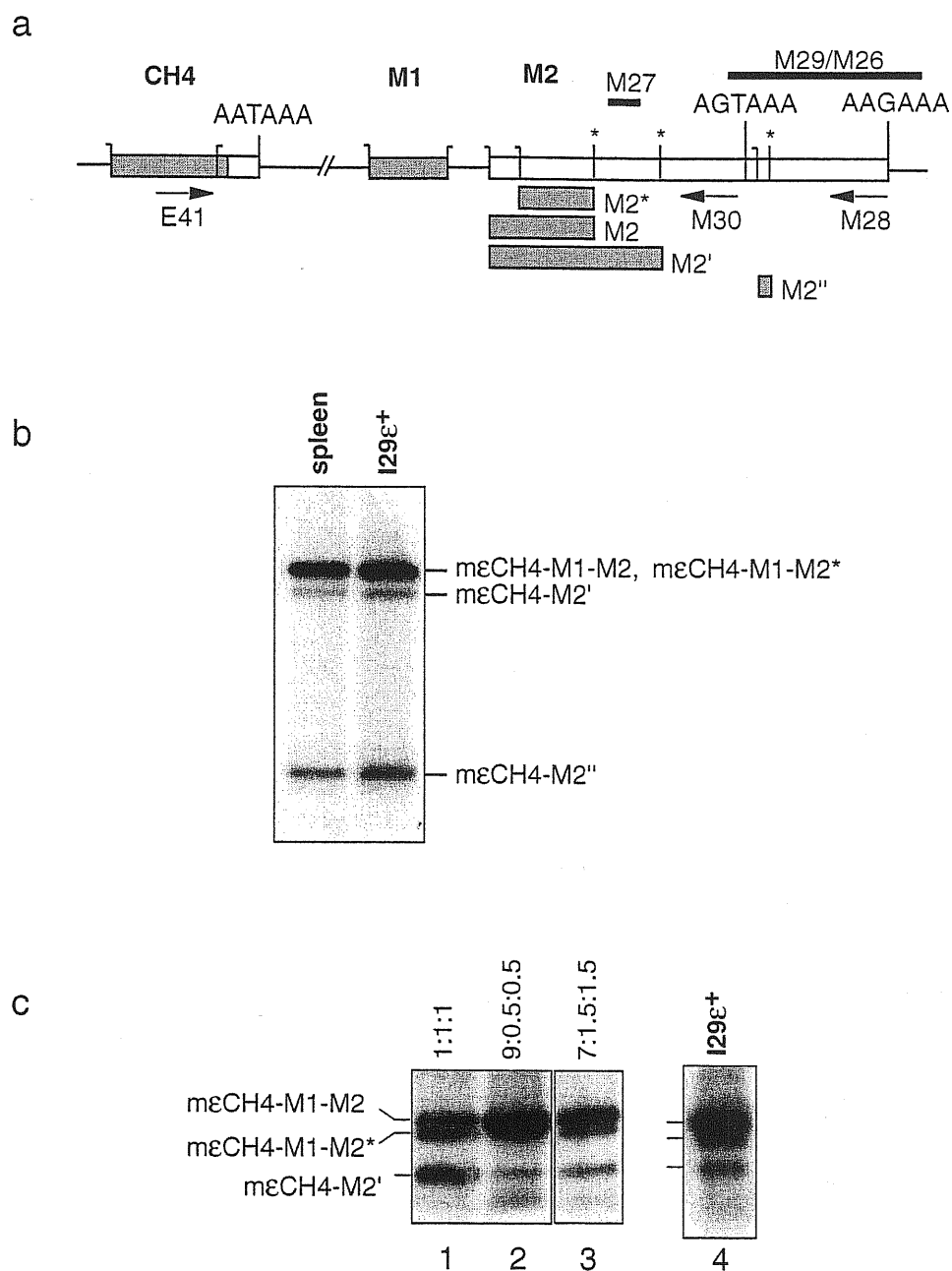


**Figure 3.1.4:** Detection of alternatively spliced murine  $\epsilon$  mRNAs in  $I29E^+$  cells and normal mouse splenocytes. a) Schematic representation of the 3' end of the  $C\epsilon$  gene with the location of splice sites, stop codons and primers used for PCR amplification (E41, M30 and M28). The four different coding regions derived from the M2 exon are indicated below the exon. b) RT-PCR products obtained by amplification with oligonucleotides E41 and M28. The M29/M26 probe was used for the Southern Blot hybridization. The identity of each band in the autoradiogram is indicated. c) Quantification of the relative amounts of  $m\epsilon CH4$ -M1-M2,  $m\epsilon CH4$ -M1-M2\* and  $m\epsilon CH4$ -M2' transcripts in  $I29E^+$  cells (lane 4). The  $\epsilon$  cDNA was amplified with the E41/M30 primer pair and hybridized with the M27 oligonucleotide. Standards containing known quantities of cloned fragments corresponding to the  $m\epsilon CH4$ -M1-M2,  $m\epsilon CH4$ -M1-M2\* and  $m\epsilon CH4$ -M2' variants were amplified under the same conditions (lanes 1-3). The relative amount of plasmid DNA in each standard ( $m\epsilon CH4$ -M1-M2 :  $m\epsilon CH4$ -M1-M2\* :  $m\epsilon CH4$ -M2') is indicated above each lane.



membrane isoform should end at the same stop codon as the classical membrane isoform, but should be 10 aa shorter in the cytoplasmic domain (Fig. 3.1.2).

The m $\epsilon$ CH4-M2' mRNA species was spliced directly from the donor splice site of the CH4 exon to the acceptor site of the M2 exon. This resulted in a mRNA which lacked the entire M1 exon. The absence of the M1 exon in this form resulted in a shift of the M2 exon reading frame. The new reading frame of this exon (M2') encodes 59 aa in contrast to the 27 residues of the M2 exon in the m $\epsilon$ CH4-M1-M2 isoform (Fig. 3.1.2).

The fourth  $\epsilon$  mRNA species (m $\epsilon$ CH4-M2'') revealed another novel splice site located within the M2 exon. This acceptor splice site is located in the 3' untranslated region of the M2 exon, 728 nt downstream of the stop codon from the M2 reading frame and 631 nt downstream from the stop codon of the M2' reading frame. Thus, this species lacks completely the amino-acid sequences encoded by the M1 and M2 or M2' exons, but contains eight other amino-acids encoded by a small exon designated M2'' (Fig. 3.1.2).

Since the PCR strategy used in the above assay would not have detected  $\epsilon$  transcripts that were polyadenylated at the first poly(A) site, we did an additional RT/PCR experiment in which a primer upstream of the first poly(A) site (M30) was used together with the CH4 exon primer (Fig. 3.1.4a). Three bands corresponding in size to the m $\epsilon$ CH4-M1-M2, m $\epsilon$ CH4-M1-M2\* and m $\epsilon$ CH4-M2' species were obtained, indicating that these alternatively spliced transcripts can be polyadenylated at either site (Fig. 3.1.4c, lane 4). The m $\epsilon$ CH4-M2'' species was not detected in this experiment because the M2'' exon is located downstream to the first poly(A) site. The band corresponding to the m $\epsilon$ CH4-M1-M2 isoform was of the strongest intensity, suggesting that this is the most abundant membrane  $\epsilon$  transcript. To investigate if the PCR strategy gives a true estimate of the relative amounts of the alternatively spliced  $\epsilon$  transcripts, we performed experiments with standards containing different relative amounts of cloned DNA fragments corresponding to the m $\epsilon$ CH4-M1-M2, m $\epsilon$ CH4-M1-M2\* and m $\epsilon$ CH4-M2' species (analysis of three representative standards is shown in Fig. 3.1.4c, lanes 1-3). These experiments showed

that the three  $\epsilon$  species are amplified with equal efficiency. Analysis of I29 $\epsilon^+$  mRNA gave a similar value as the standard containing m $\epsilon$ CH4-M1-M2, m $\epsilon$ CH4-M1-M2\* and m $\epsilon$ CH4-M2' plasmids at a 9:0.5:0.5 ratio, respectively, indicating that the m $\epsilon$ CH4-M1-M2 species is approximately 10 times more abundant than the other two species.

## RESULTS

### SECTION 2

#### 3.2.0 Characterization, expression and functional analysis of the two membrane isoforms of human IgE

##### 3.2.1 Introduction

*The following section describes the expression and function of the IgE molecules encoded by the two types of human membrane  $\epsilon$  transcripts. These two  $\epsilon$  mRNA species differ only in the 5' part of the first membrane exon that encodes the extracytoplasmic membrane proximal domain (Fig. 3.2.1a). The longer variant  $m_L$ IgE ( $\epsilon$  CH4-M1'-M2) contains 156 extra nucleotides as a consequence of alternative splicing between the donor splice site at the 3' end of the CH4 exon and the upstream acceptor splice site in the M1 exon. Thus, the two putative membrane proteins have the same constant  $\epsilon$  region and the same transmembrane and cytoplasmic domains, but differ in a 52 amino acids segment which is present only in the long membrane IgE variant (Fig. 3.2.1b). The long membrane transcript was initially described as the predominant  $\epsilon$  mRNA species in humans, because it was found at significantly higher levels than the short species in IL-4 plus anti-CD40 stimulated peripheral blood lymphocytes (PBLs) and in IgE-producing myeloma cell lines (149, 151). The presence of the putative protein products of the short membrane transcript which is homologous to the murine membrane  $\epsilon$  transcript has not been investigated, and it is unclear whether this  $\epsilon$  transcript has any functional significance or it is just a by-product of alternative splicing in the C $\epsilon$  locus. Furthermore, the  $\epsilon$  mRNA splicing pattern could be a characteristic of transformed plasma-cell lines or a consequence of in vitro culture conditions and might not be representative of the splicing pattern that occurs in vivo.*

*We have addressed these issues by analyzing the membrane  $\epsilon$  mRNAs produced by unstimulated PBL. The properties of the protein products of the two membrane  $\epsilon$  transcripts were then investigated by construction of IgE H-chain expression vectors and examination of their expression and function in transfected cell lines.*

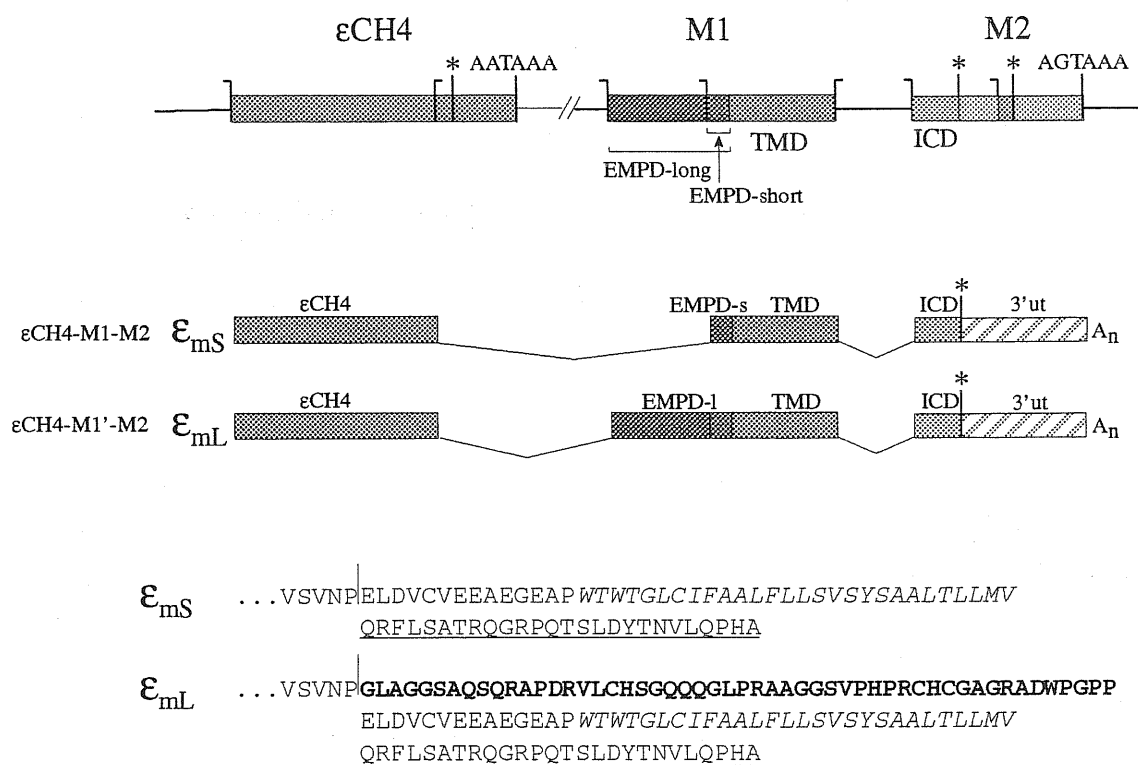


Figure 3.2.1: Schematic representation of the two membrane IgE H-chain isoforms. (a) Diagram of the 3' part of the C $\epsilon$  gene and the pattern of alternative splicing that generates the  $\epsilon$ CH4-M1-M2 and  $\epsilon$ CH4-M1'-M2 membrane transcripts. Shaded boxes represent coding sequences and striped boxes represent 3' untranslated regions; stop codons are indicated by asterisks. (b) Amino-acid sequence of the carboxyl-terminus of the short ( $\epsilon$ CH4-M1-M2) and long ( $\epsilon$ CH4-M1'-M2)  $\epsilon$  chains. The extra 52 amino-acids present in the extracytoplasmic membrane-proximal domain of the long  $\epsilon$  chain are in bold.

### 3.2.2 Investigation of the expression of the two membrane $\epsilon$ mRNA species in PBL.

We analyzed the expression of the two membrane isoforms in unstimulated PBL obtained from 20 random blood donors. RT-PCR analysis was done on each sample with an oligonucleotide complementary to a sequence in the  $\epsilon$ CH4 exon (E4Y) and an oligonucleotide in the M2 exon (M2W). The first PCR was then reamplified in a semi-nested PCR with an internal 5'-<sup>32</sup>P-end-labeled oligonucleotide in the  $\epsilon$ CH4 exon (E4Z), and the primer M2W. The PCR products were then analyzed on denaturing polyacrylamide gels (Fig. 3.2.2). The short membrane isoform  $m_S$ IgE ( $\epsilon$  CH4-M1-M2) which is homologous to the murine membrane transcript was detected in about one third of the PBL samples and in some cases it was the only  $\epsilon$  mRNA species present. In contrast, the long membrane isoform ( $\epsilon$  CH4-M1'-M2) was detected in only three samples (Fig. 3.2.2). These data suggested that the expression of the two membrane  $\epsilon$  mRNAs may depend on the stage of B cell differentiation, and that their protein products might be functional (162). Hence, we decided to investigate the properties of the protein products of these two transcripts by constructing IgE H-chain expression vectors and examining their expression in transfected cell lines.

### 3.2.3 Expression of $m_S$ IgE and $m_L$ IgE

To investigate the properties of the two membrane IgE isoforms, we generated two chimeric mouse/human  $\epsilon$ -chain gene constructs which contained the mouse  $V_H$  segment from an Ab with anti-NIP specificity and the human  $C\epsilon$  region with a carboxyl terminus corresponding to the  $m_L$ IgE or the  $m_S$ IgE isoform. A schematic diagram of the two constructs is depicted in Fig. 3.2.3. The two constructs were created by amplifying cDNA from PBL with oligonucleotides located in the CH3 exon and in the 3' untranslated

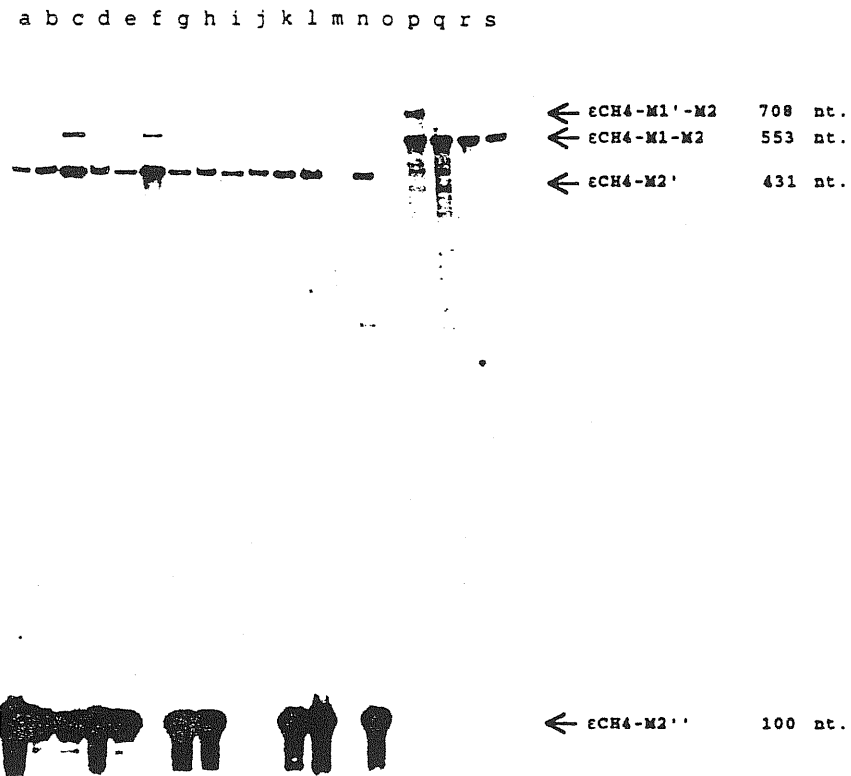


**Figure 3.2.2:** RT-PCR analysis of membrane  $\epsilon$  transcripts expressed by PBL. The samples were amplified in a semi-nested radioactive PCR and analyzed by denaturing polyacrylamide gel electrophoresis.

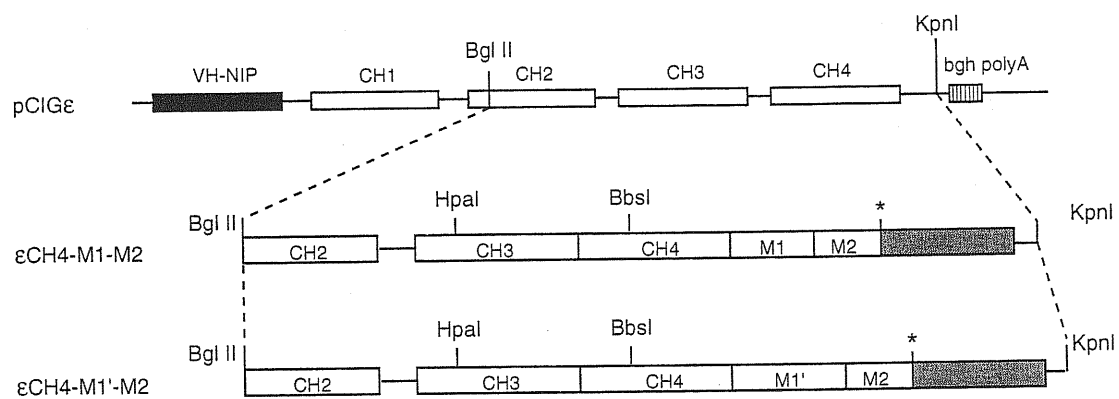


**Figure 3.2.3:** Diagram of the chimeric mouse V<sub>H</sub>-NIP/Cε membrane gene constructs. The 3' ends of the two membrane ε isoforms were cloned in their cDNA form (starting from the CH3 exon) into pCIG-Cε, using the indicated restriction enzyme sites.

region of the M2 exon of C $\epsilon$  gene. Hence, the 3' ends of both constructs were in a cDNA form as shown in the Fig. 3.2.3. This ensured that only one kind of alternative spliced form will be produced in the transfected cells. The two constructs were independently transfected into a murine B cell lymphoma, WEHI-231, which resembles phenotypically an immature B cell as it expresses sIgM and low amounts of Ia but no detectable sIgD or Fc receptor. G418 resistant transfectants were selected for the expression of mIgE by immunofluorescence. RT-PCR analysis using membrane long or short specific primers ensured that the WEHI transfectomas expressed only the desired isoform. Also, the transfected cell lines were stained with a membrane long IgE specific antibody (207). This antibody strongly stained only the WEHI-m<sub>L</sub>IgE cells and not the WEHI-m<sub>S</sub>IgE transfectomas (data not shown).

### 3.2.4 Assembly and Transport of m<sub>S</sub>IgE and m<sub>L</sub>IgE

In order to investigate the assembly and transport of the m<sub>L</sub>IgE and m<sub>S</sub>IgE isoforms we performed pulse-chase studies in the WEHI cell lines. Cells were given a 15' pulse with [<sup>35</sup>S]methionine and then chased for 1, 2, 3 and 4 hours. mIgE was immunoprecipitated from the WEHI-m<sub>S</sub>IgE or WEHI-m<sub>L</sub>IgE cell extracts and analyzed on a non reducing 6% SDS-PAGE (Fig. 3.2.4a). Two major species of more than 240 kDa were observed in both cell lines, demonstrating that both membrane isoforms are assembled into H<sub>2</sub>L<sub>2</sub> molecules. During the course of the chase the quantity of immunoprecipitated proteins remained the same, indicating that there is no intracellular degradation of either membrane isoform. The accumulation of higher molecular weight species in the course of the chase suggested that both proteins are terminally glycosylated during their transport to the cell surface. This was confirmed by treatment of the immunoprecipitated material with Endoglycosidase H (Endo H) which cleaves N-linked high mannose oligosaccharides of glycoproteins before they arrive in the medial Golgi, but fails to cleave terminally



processed carbohydrate moieties. The digested material was run on a 10% reducing gel. As shown in Fig. 3.2.4b, after Endo H treatment two  $\epsilon$  species were observed in each case (i) a 60 ( $m_S$ IgE) or 65 ( $m_L$ IgE) kDa species corresponding to Endo H sensitive  $\epsilon$  chains that carried unprocessed high mannose carbohydrates and (ii) an 87 ( $m_S$ IgE) or 90 ( $m_L$ IgE) kDa species corresponding to mature  $\epsilon$  chains that bore processed N-linked carbohydrates which were resistant to the enzyme. These species should correspond to the completely processed membrane proteins. In the WEHI- $m_L$ IgE transfectoma only 20-30% of the newly synthesized membrane  $\epsilon$  chains were of the mature processed type after 4 hours chase (Fig.3.2.4). This was similar to the rate of transport observed for the endogenous mouse mIgM. Interestingly, three to four times more  $m_S$ IgE H-chains were present in the mature form after the same period of time. This clearly demonstrated that the  $m_S$ IgE is more efficiently transported to the cell surface than the  $m_L$ IgE, or even the endogenous mIgM.

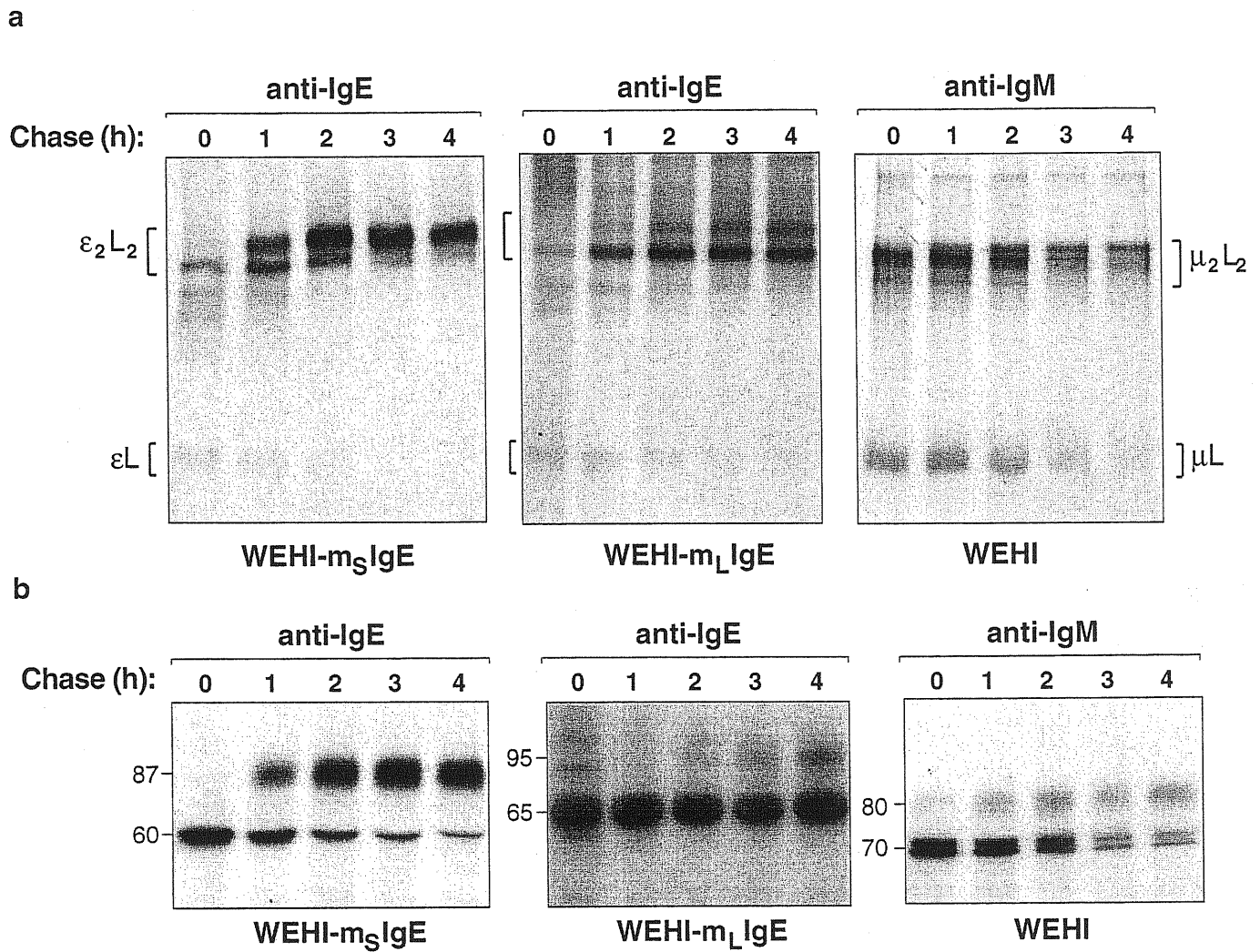


**Figure 3.2.4:** Assembly and transport of  $m_L$ IgE and  $m_S$ IgE. WEHI- $m_S$ IgE, WEHI- $m_L$ IgE, and wild-type WEHI cells were pulse-labeled with [ $^{35}$ S]methionine for 15 min. and chased for the indicated times in the presence of excess cold methionine. Cellular extracts were immunoprecipitated with the indicated antibodies and (a) analyzed on a non-reducing 6% SDS-PAGE or (b) treated with Endo H and separated on reducing 10% SDS-PAGE.

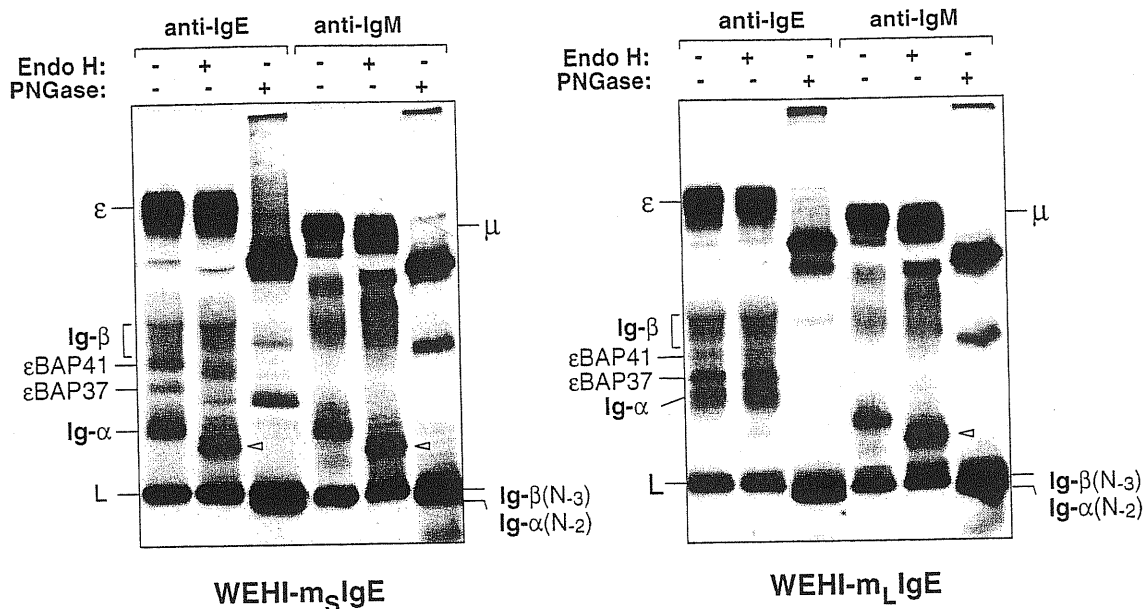
### 3.2.5a Characterization of IgE-BCR components

Antigen receptors on B lymphocytes are expressed on the plasma membrane as a complex of disulfide-bonded Ig H and L chains that are noncovalently associated with at least two other glycoproteins, Ig- $\alpha$  (CD79a) and Ig- $\beta$  (CD79b) (70). These proteins form a disulfide-linked heterodimer which appears to be a prerequisite for the transport and cell-surface expression of the membrane-bound Igs (mIg) (52-54, 169).

To characterize the IgE-BCR and to determine the  $m_S$ IgE and  $m_L$ IgE associated proteins we immunoprecipitated the IgE antigen receptor complex from digitonin lysates of surface biotinylated WEHI- $m_S$ IgE and WEHI- $m_L$ IgE cells. The relatively mild detergent digitonin preserves the non-covalent association between the Ig- $\alpha$  and Ig- $\beta$  and the Ig H and L chain. The immunoprecipitations were performed in duplicate using two different anti-human IgE antibodies [rabbit anti-human IgE (DAKO) and goat anti-human IgE (KPL)]. As a control, the endogenous IgM-BCR was subsequently immunoprecipitated from the same cell extracts. The immunoprecipitated material was resolved on a 10% SDS-PAGE under reducing conditions (Fig. 3.2.5a). Analysis of the mIgM complex yielded the expected characteristic pattern of an 80kDa band corresponding to the  $\mu$  H chain, a 25 kDa band corresponding to the L chain, and the 32 and 40-47 kDa bands corresponding to Ig- $\alpha$  and Ig- $\beta$  polypeptides, respectively. A similar pattern was observed after immunoprecipitation of the  $m_S$ IgE- and  $m_L$ IgE-BCRs, indicating that Ig- $\alpha$  and Ig- $\beta$  chains are also present in these receptors. This was confirmed by analysis of the material that was dissociated from the immunoprecipitated IgE-BCRs by treatment with Nonidet P-40. (NP-40 being a stronger detergent disrupts the association between the receptor and Ig- $\alpha$  /Ig- $\beta$ ). Reprecipitation of this material with an anti-Ig- $\alpha$  specific antiserum produced only the Ig- $\alpha$  and Ig- $\beta$  subunits (Fig. 3.2.5b). The Ig- $\beta$  subunit was of the same molecular mass in the three BCRs, whereas the Ig- $\alpha$  of

the  $m_L$ IgE ( $m_L$ IgE- $\alpha$ ) showed a slower mobility than the IgM- $\alpha$  and  $m_S$ IgE- $\alpha$  (Fig. 3.2.5). Slower mobility of the Ig- $\alpha$  chain has also been observed in the case of the IgD-BCR. This difference has been shown to be the consequence of different terminal glycosylation of the two N-glycosylation sites in the polypeptide (169-171). In order to establish if this is the case with the  $m_L$ IgE- $\alpha$ , immunoprecipitated materials were treated with endoglycosidases. Figure 3.2.5a shows that Endo H treatment decreased the molecular weight of the IgM and  $m_S$ IgE associated Ig- $\alpha$  polypeptides. On the other hand, the  $m_L$ IgE- $\alpha$  remained at the same position, indicating that both glycosylation sites are terminally glycosylated. Treatment with PNGase, which cleaves all sugar residues, eliminated the difference in size between the different Ig- $\alpha$  polypeptides.

a



b

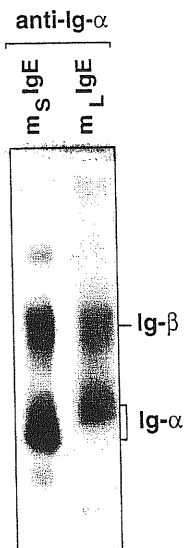


**Figure 3.2.5:** Immunoprecipitation of BCRs from biotin-labeled cell-surface proteins. WEHI-m<sub>S</sub>IgE and WEHI-m<sub>L</sub>IgE were surface biotinylated and treated with digitonin lysis buffer to preserve the BCR complexes. (a) Lysates were treated first with anti-IgE and then with anti-IgM sera to immunoprecipitate the IgE-BCR and endogenous IgM-BCR complexes, respectively. Immunoprecipitated material was treated with Endo H or PNGase as indicated, and analyzed by reducing 10% SDS-PAGE. Arrow-heads indicate the position of the Ig-α polypeptide after removal of one of the two N-linked carbohydrate moieties by Endo H. Ig-α(N-2) and Ig-β(N-3) correspond to the Ig-α and Ig-β polypeptides after removal by PNGase of the 2 or 3 N-linked carbohydrate moieties, respectively. (b) Reimmunoprecipitation of the Ig-α/Ig-β heterodimer dissociated by NP-40 from the m<sub>S</sub>IgE-BCR and m<sub>L</sub>IgE-BCR. The immunoprecipitation was done with an anti Ig-α serum and analyzed on a 10% SDS-PAGE under reducing conditions.

### 3.2.5b Detection of two new proteins associated with IgE-BCRs

Two additional proteins of 37 and 41 kDa were detected in the m<sub>S</sub>IgE-BCR and m<sub>L</sub>IgE-BCR immunoprecipitations (Fig. 3.2.5a). The immunoprecipitations were again performed in digitonin lysates of surface biotinylated cells. These proteins were not present in the IgM-BCR and were immunoprecipitated with either of the two anti-IgE Abs, indicating that they are specifically associated with mIgE. The relative amount of these IgE-BCR associated proteins (further referred to as εBAP37 and εBAP41) was different in the two IgE-BCRs, with significantly lower quantities of εBAP41 in the m<sub>L</sub>IgE-BCR. These proteins were not immunoprecipitated with the anti-Ig-α antiserum, indicating that they are not covalently-associated to Ig-α or antigenically related to this polypeptide (Fig. 3.2.5b).

### 3.2.5c Two-dimensional analysis of the IgE-BCR components

To further characterize the components of the IgE-BCRs, two dimensional analysis of anti-IgE immunoprecipitated material was performed on digitonin lysates from biotinylated WEHI-m<sub>S</sub>IgE and WEHI-m<sub>L</sub>IgE cells. The analysis was done on a 10% SDS-PAGE under non-reducing conditions in the first dimension and reducing conditions in the second (Fig. 3.2.6). In addition to the bands corresponding to ε<sub>2</sub>L<sub>2</sub> and εL, a complex of around 75 kDa was present in the non-reducing PAGE analysis of the m<sub>S</sub>IgE-BCR. A slightly higher M.W. complex (80 kDa) was detected in the m<sub>L</sub>IgE-BCR. In the second dimension these complexes dissociated into free Ig-α and Ig-β chains. This experiment also indicated that the εBAP37 and εBAP41 proteins form a disulfide bound complex (εBAP37/41) which in the non-reducing PAGE analysis of the m<sub>S</sub>IgE-BCR migrated distinctly from the Ig-α/Ig-β heterodimer. In the m<sub>L</sub>IgE-BCR the εBAP37 apparently formed a homodimer which co-migrated with the Ig-α/Ig-β complex.

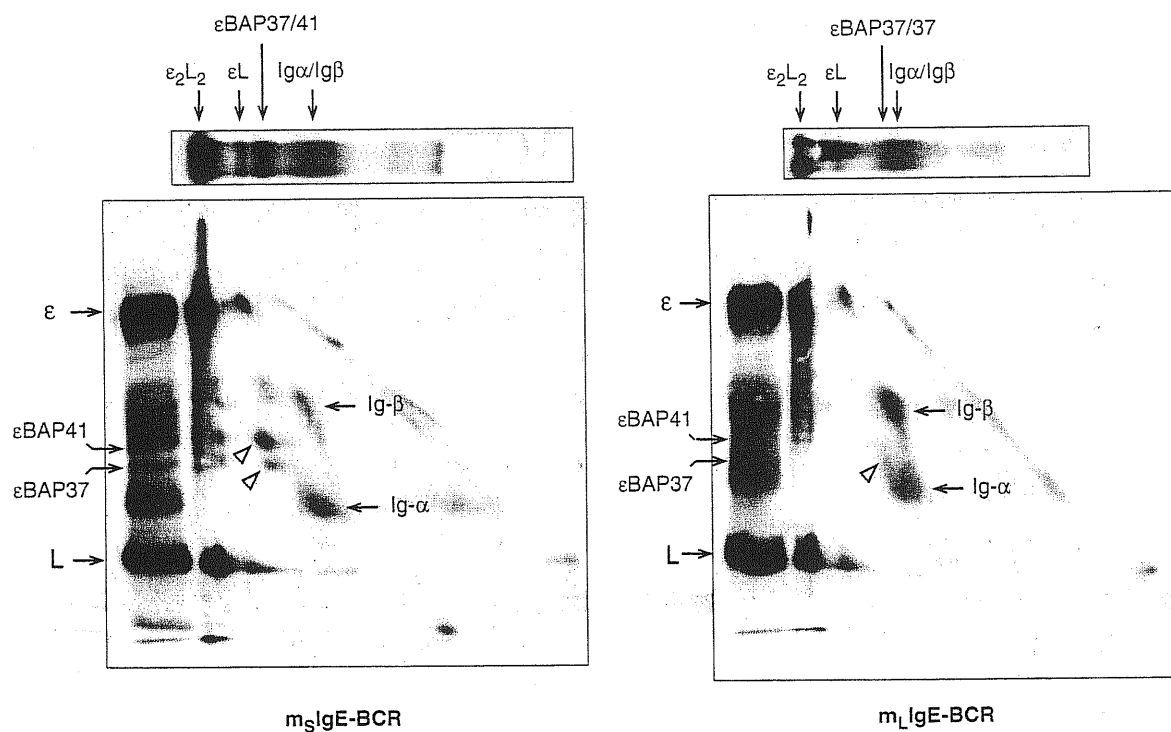


**Figure 3.2.6:** Bidimensional analysis of surface-biotinylated IgE-BCRs. Anti-IgE immunoprecipitates from the two transfectomas were analyzed by bidimensional (non-reducing/reducing) PAGE. The migration of the same material run only under reducing conditions or non-reducing conditions is shown in the left lane of each gel or as a separate lane on top of each gel, respectively. Arrow-heads indicate the position of the dissociated  $\epsilon$ BAP37 and  $\epsilon$ BAP41 proteins. The other components of the IgE-BCRs are indicated in the figure.

### 3.2.6 *In vitro* phosphorylation of IgE-BCR associated proteins

The Ig- $\alpha$ /Ig- $\beta$  heterodimer non-covalently associated with the mIg has been shown to be the signal transduction unit of the BCR (182-186). The heterodimer is involved in the coupling of the BCR to several protein tyrosine kinases (PTKs) expressed in B cells, such as the src-related PTKs Lyn, Fyn, Lck, and Blk, and the cytoplasmic PTK Syk (186-191). Signal transduction through the cross-linked BCR involves the rapid activation of these enzymes which phosphorylate several substrate proteins in B cells including the Ig- $\alpha$ /Ig- $\beta$  heterodimer (191).

To investigate if the IgE-BCRs contain receptor associated protein kinases capable of phosphorylating the Ig- $\alpha$ /Ig- $\beta$  heterodimers, as shown for the IgM-, IgD- and IgG-BCRs (172), we performed an *in vitro* kinase assay ( $[\gamma\text{-}^{32}\text{P}]\text{ATP}$  labeling) on immunoprecipitated BCRs. The immunoprecipitations were again performed on digitonin lysates from unlabeled cells. The endogenous IgM-BCR from both transfectomas was analyzed as an internal control. The phosphorylated receptor components were then analyzed by 10% reducing SDS-PAGE and autoradiography. As shown in Fig. 3.2.7, bands corresponding to the Ig- $\alpha$  and Ig- $\beta$  proteins were found to be phosphorylated when incubated with  $[\gamma\text{-}^{32}\text{P}]\text{ATP}$  in all three BCRs. The identity of these bands was again confirmed by treatment with Endo H and PNGase F. The two newly identified  $\epsilon$ BAPs were not detected in this *in vitro* assay, suggesting that they are not substrates for the BCR-associated protein kinases.



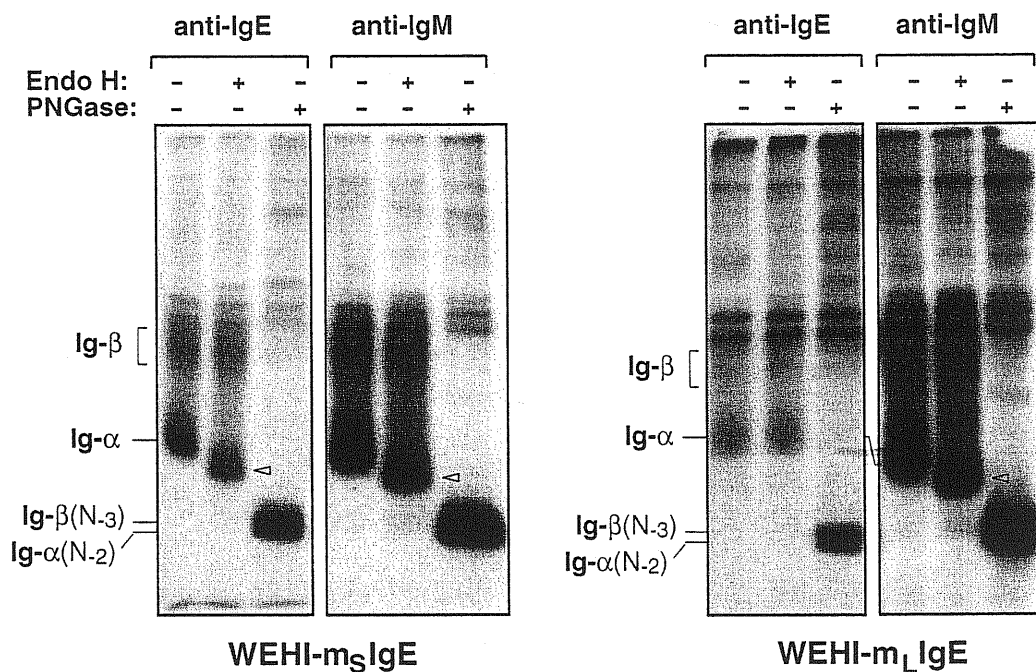


**Figure 3.2.7:** *In vitro* phosphorylation of BCR associated proteins. IgE-BCR and IgM-BCR from the WEHI-m<sub>5</sub>IgE and WEHI-m<sub>L</sub>IgE transfectomas were immunoprecipitated, incubated with [ $\gamma^{32}$ P]ATP and analyzed on reducing 10% SDS-PAGE. Treatment with Endo H or PNGase is indicated on top of each gel. Arrow-heads, Ig- $\alpha$ (N-2) and Ig- $\beta$ (N-3) as in legend to Figure 3.2.5.

### 3.2.7 Protein tyrosine phosphorylation upon crosslinking of the IgE-BCRs

The current models of signal transduction from the antigen receptors on B and T cells suggest that the activation of PTKs is the first event following the aggregation of the receptor (205, 206). Other events, like the activation of PLC $\gamma$ , and the generation of the secondary messengers diacylglycerol (DAG) and inositol-1,4,5 triphosphate (InsP3) occur further downstream in the signalling cascades from the BCR. Aggregation of the BCR results in activation of PTK, phosphorylation of the receptor subunits Ig- $\alpha$  and Ig- $\beta$ , and coupling of the receptor to different signalling elements. Signal terminators and the identity of the BCR transducer elements remains to be elucidated. These could be both serine-threonine-kinases and tyrosine phosphatases (206).

To analyze the activation of protein tyrosine kinases (PTKs) upon engagement of the IgE-BCRs, we used transfectant cell lines (WEHI-m<sub>L</sub>IgE and WEHI-m<sub>S</sub>IgE) that expressed comparable levels of m<sub>L</sub>IgE and m<sub>S</sub>IgE (Fig. 3.2.8). The expression of surface IgE was examined by flow cytometry on a FACScan, using rabbit anti-human IgE, and FITC-conjugated swine anti-rabbit IgG. Wild type WEHI cells were analyzed in parallel as control.

The three cell lines were incubated for different periods of time (1-40 min) in the presence of either anti-IgE or anti-IgM. The PTK activation in these cells was monitored by the increase in tyrosine phosphorylation of PTK substrate proteins in total Triton X-100 cell lysates. Equal amounts of lysates were electrophoresed on a 10% reducing gel and the blot was probed with an antiphosphotyrosine monoclonal antibody, PY20. Cross-linking the IgM-BCR or the IgE-BCRs resulted in a similar pattern of phosphorylation, indicating that all three BCRs induce the phosphorylation of the same substrate proteins. However, the kinetics of phosphorylation of the two IgE-BCRs was

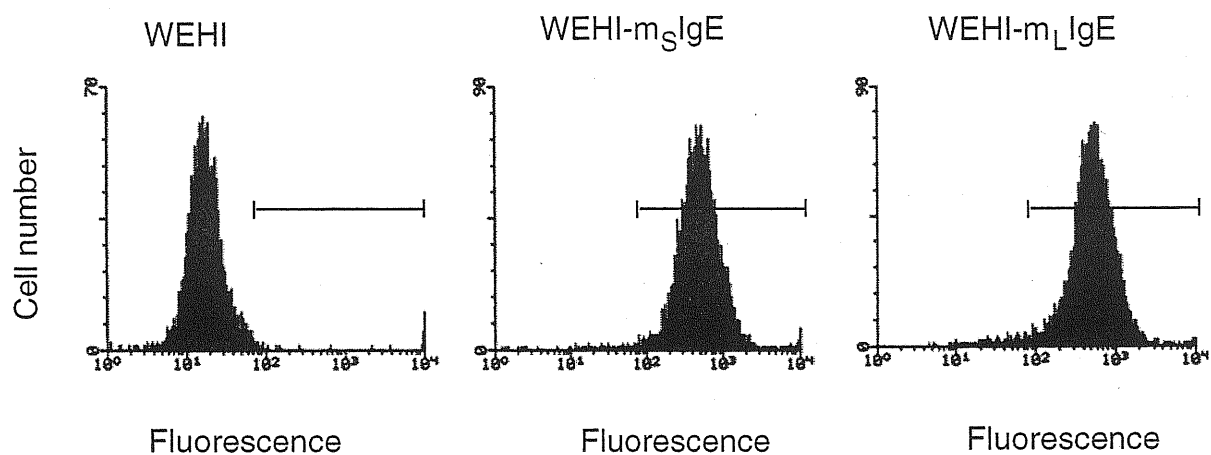


**Figure 3.2.8:** Quantitation of m<sub>S</sub>IgE-BCR and m<sub>L</sub>IgE-BCR levels on the surface of transfected WEHI cells. The level of surface IgE was determined in each cell line by fluorescent flow cytometry analysis with a rabbit anti-human IgE antibody and FITC-conjugated swine anti-rabbit IgG.

quite different. After crosslinking the m<sub>L</sub>IgE-BCR the substrate phosphorylation reached its maximum in 1 min and drastically declined within 5 min (Fig. 3.2.9). In contrast, in the m<sub>S</sub>IgE-producing transfectant the substrate phosphorylation still increased after 1 min of stimulation and reached its maximum after 5 min. Increased tyrosine phosphorylation was still evident after 40 min., although for several polypeptides it had declined. These data showed that the kinetics of protein tyrosine phosphorylation induced by receptor crosslinking is significantly different for the two IgE-BCRs.

In subsequent experiments we observed that the kinetics of tyrosine phosphorylation were independent of the amount of IgE expressed on the cell surface. Analysis of WEHI-m<sub>S</sub>IgE and WEHI-m<sub>L</sub>IgE clones expressing different amounts of IgE-BCR showed a difference only in the intensity of the signal, whereas the kinetics of both receptors remained the same (data not shown). Moreover, crosslinking of the endogenous IgM-BCR in the two transfectants and in wild type WEHI cells showed the same kinetics of tyrosine phosphorylation, and was consistent with published data (173). These experiments excluded the possibility that the differences in signal transduction between the two IgE-BCRs were due to peculiarities of the transfected cell lines rather than the type of mIgE.

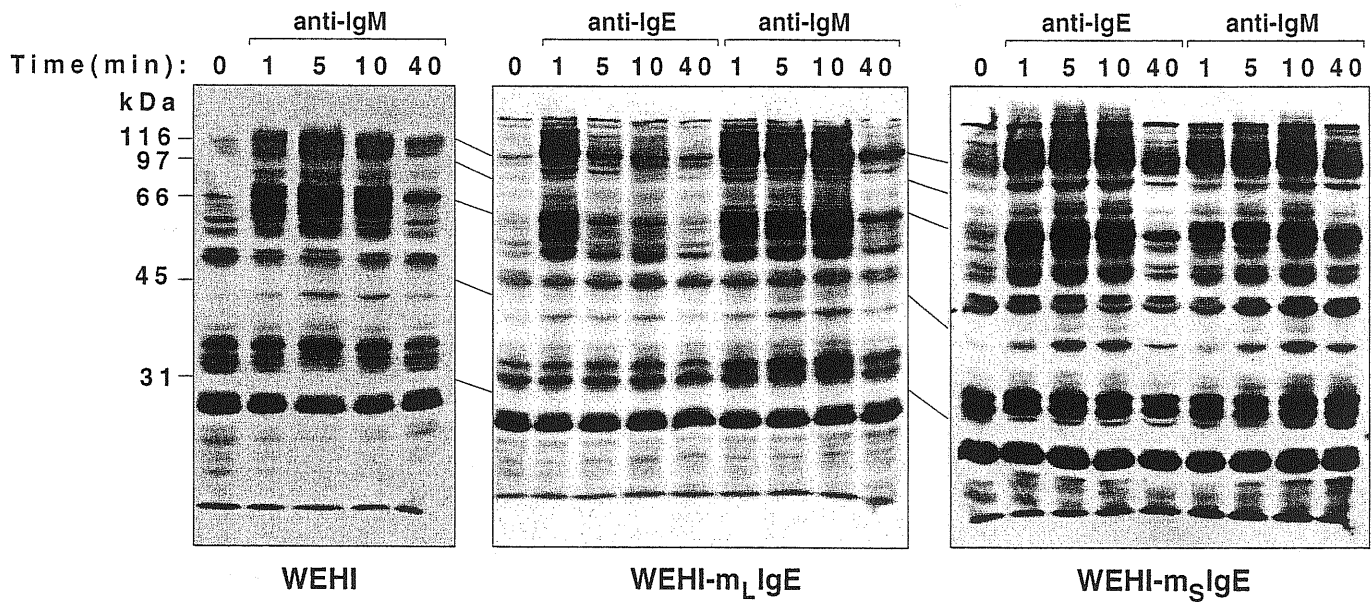


**Figure 3.2.9:** Kinetics of PTK substrate phosphorylation upon crosslinking of the m<sub>5</sub>IgE-BCR, m<sub>1</sub>IgE-BCR and IgM-BCR. Wild-type WEHI, WEHI-m<sub>1</sub>IgE or WEHI-m<sub>5</sub>IgE cells were incubated for various times with anti-IgE or anti-IgM antibodies, as indicated on top of each gel. Cellular extracts were then prepared and tyrosine phosphorylated proteins detected by immunoblotting with an anti-phosphotyrosine mAb.

### 3.2.8 Cellular responses induced by crosslinking of m<sub>S</sub>IgE- and m<sub>L</sub>IgE-BCR

Crosslinking of the endogenous IgM-BCR in WEHI cells leads to their growth inhibition (174). On the other hand, crosslinking of the IgD-BCR in WEHI cells transfected with a  $\delta$  chain does not affect their proliferation (175). In order to investigate whether signaling through the IgE-BCRs has an effect on cellular proliferation, WEHI-m<sub>S</sub>IgE and WEHI-m<sub>L</sub>IgE cells were grown for 24 hours in the presence of various concentrations of anti-IgE Ab and were subsequently incubated for 14 hours with [<sup>3</sup>H] thymidine. A marked inhibition in proliferation was observed only in the WEHI-m<sub>S</sub>IgE transfectoma, whereas crosslinking of the m<sub>L</sub>IgE had no effect (Fig. 3.2.10). The above results indicate that different cellular responses can occur after IgE-BCR signaling, depending on the type of mIgE expressed on the cell surface.

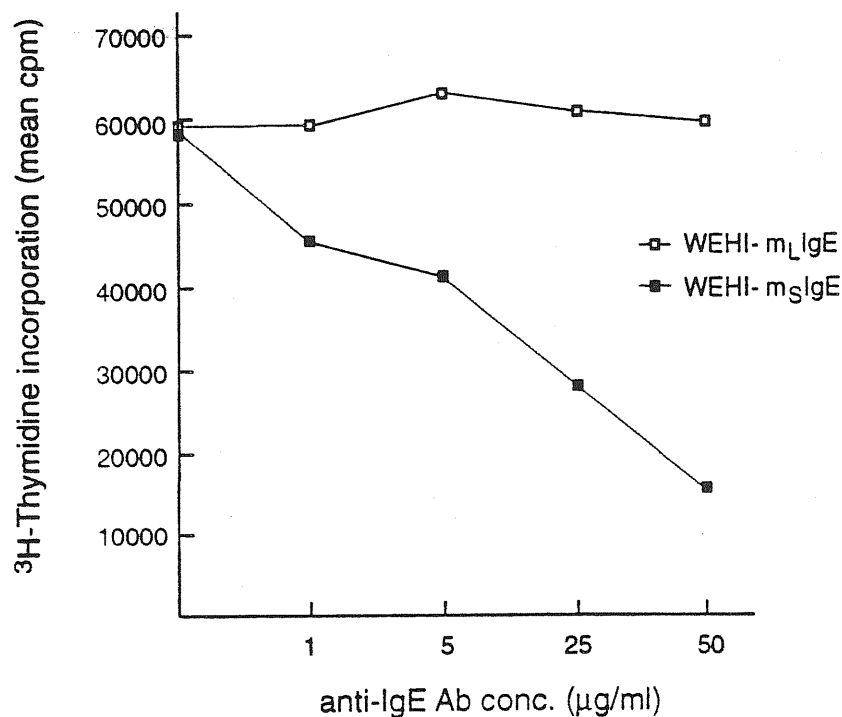


**Figure 3.2.10:** Proliferation of WEHI-m<sub>L</sub>IgE and WEHI-m<sub>S</sub>IgE cells after crosslinking of mIgE.  $2 \times 10^4$  cells were incubated with 0, 1, 5, 25 or 50 µg/ml of polyclonal anti-human IgE anti-serum. Results show one representative of three separate experiments with similar results. Each point represents an average of triplicate cultures (SEM < 5%).

### 3.2.8b Apoptosis assay for monitoring cell-death.

To investigate further whether the inhibition of cellular proliferation induced by crosslinking the m<sub>5</sub>IgE BCR was due to cell death by apoptosis, the two transfectomas were grown as before for 24 hours in the presence of anti-human IgE antibody, the cells were then stained with annexin V-FITC to detect apoptotic cells. Staining by annexin V-FITC is based on the observation that, soon after initiating apoptosis, most cell types translocate the membrane phospholipid phosphatidylserine (PS) from the inner face of the plasma membrane to the cell surface. Once on the cell surface, PS can be easily detected by staining with an FITC conjugate of annexin V, a protein that has a strong natural affinity for PS. As shown in Fig. 3.2.11, treatment of the WEHI-m<sub>5</sub>IgE transfectoma with anti-IgE antibody led to an increase in the population of cells with dramatically increased annexin V-binding. The effect was similar to the one seen if the endogenous mouse IgM on the WEHI is crosslinked with anti-IgM antibody (Fig. 3.2.11). However, in contrast there was no such increase in annexin-V binding population of WEHI-m<sub>L</sub>IgE cells. Therefore, this result indicates that the inhibition of cellular proliferation by m<sub>5</sub>IgE BCR is likely to be mediated by apoptosis.

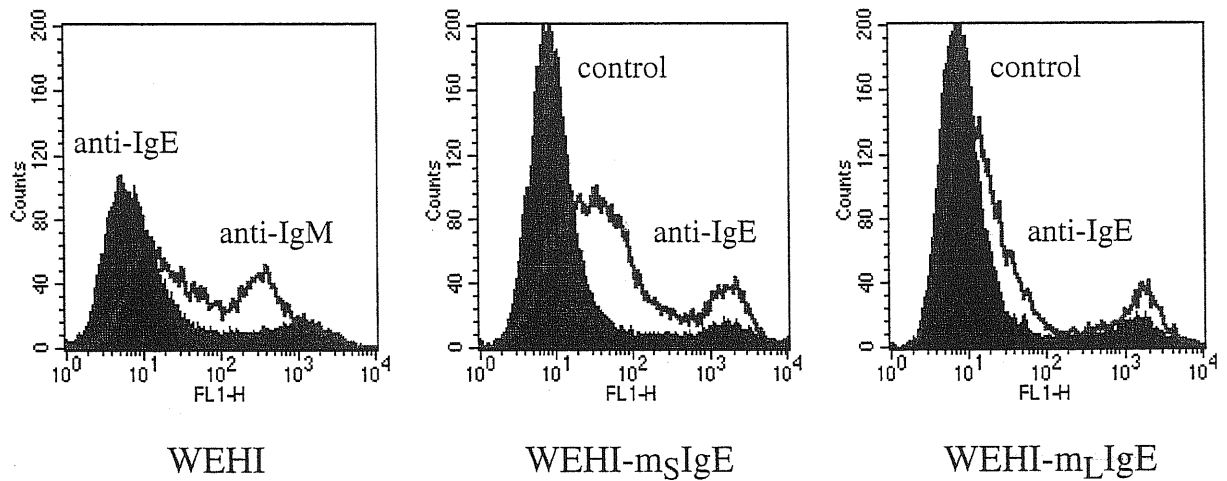


**Figure 3.2.11:** Apoptosis assay for monitoring cell death. Wild-type WEHI, WEHI-m<sub>L</sub>IgE or WEHI-m<sub>S</sub>IgE cells were incubated for 24 hours with anti-IgM or anti-IgE antibodies, (crosslinked) or without any antibody (uncrosslinked). The cells were then incubated for 15 min. with 1 $\mu$ g/ml of Annexin V-FITC in binding buffer, and 20,000 cells were analyzed by FACS. The histogram plot shows an overlay of crosslinked (solid line) over uncrosslinked cells (filled histograms).



### 3.2.9 Internalization of the two IgE-BCRs

An important physiological function of the BCR is endocytosis of bound antigen. Endocytosis leads to internalization of the antigen that is bound to BCR and its subsequent degradation; peptides derived from the degraded antigen are then transported back to the B-cell surface in association with major histocompatibility complex (MHC) class II molecules for subsequent presentation to T cells (65, 66). Internalization of the two IgE receptors was measured by incubating the cells with fluorescein isothiocyanate (FITC)-conjugated rabbit anti- $\epsilon$  antiserum and following incubation at 37°C, determining the decrease in cell-associated fluorescence (66, 204).

The two WEHI transfectomas were pretreated with fluorescein isothiocyanate (FITC)-conjugated anti human IgE antibody at 4°C and subsequently incubated in culture medium for 60 minutes at 37°C. The remaining FITC-molecules on the surface were then detected with the FACScan. The FITC fluorescence rapidly diminishes with the acidification that accompanies endocytosis. Since, the same FITC-conjugated anti-human IgE was used for both the transfectomas, any residual dissociation of the antibody at 37°C was same for both cell lines. Also, cells incubated at 37°C, with the FITC-anti-human IgE but in the presence of 0.1% sodium azide (no internalization) showed no significant difference in their fluorescence from those incubated at 4°C (positive control); thereby indicating that there is very little dissociation of antibody at 37°C (data not shown). The percent internalization was calculated by expressing the residual mean fluorescence as a percentage of the zero time value. As shown in Fig. 3.2.13, after crosslinking with the antibody, the residual amount of  $m_s$ IgE molecules on the surface of WEHI- $m_s$ IgE cells is approximately twice as much as that on the surface of WEHI- $m_L$ IgE cells. This result seems to indicate that the two IgE-BCRs also differ in their rate of internalization, with the  $m_L$ IgE BCR being faster and probably more efficient than the  $m_s$ IgE BCR.

## Internalization assay of the short and long IgE-BCR

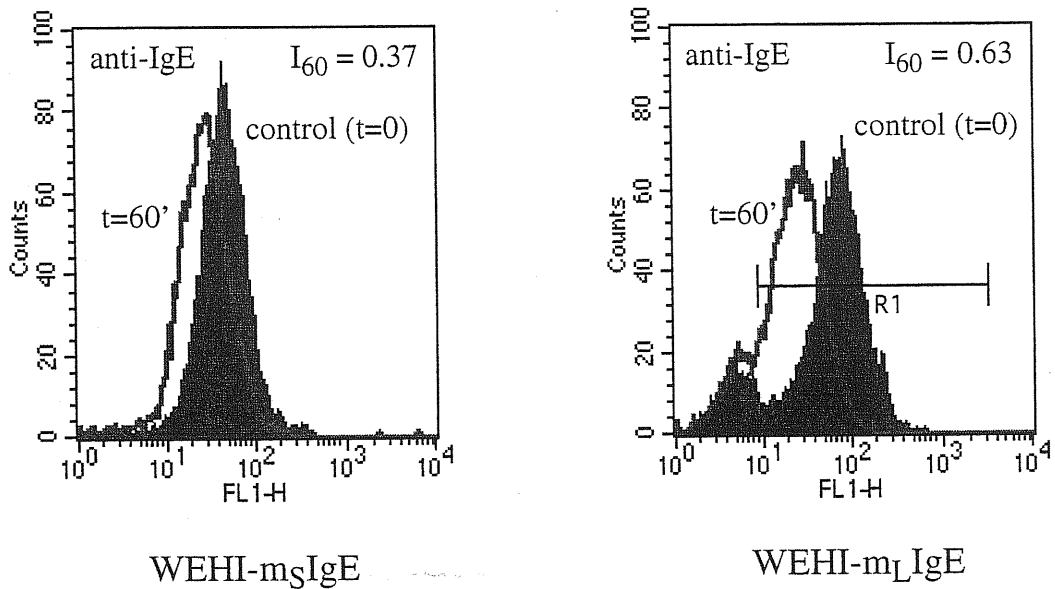


**Figure 3.2.12:** Internalization of IgE-BCRs. The two WEHI transfectomas were stained on the surface with FITC-rabbit anti-human IgE and then incubated for 60 min. at  $37^\circ\text{C}$ . Remaining FITC molecules were detected on the surface with a FACScan and mean values of FACScan histograms (10,000 cells/sample) were then used for calculation of percentage internalization. Cells stained with FITC-anti human IgE without incubation at  $37^\circ\text{C}$  were the positive control (filled histogram) and cells after 60 min of internalization (solid line).

## SECTION 3

### RESULTS

#### 3.3.0 Characterization of the two IgE isoforms in mature B cells

##### 3.3.1 Expression of the two IgE-BCRs in A20 cells

The results of the previous section prompted us to study the properties of the two IgE-BCRs in more mature B cells which have undergone Ig H chain class switching. We chose A20 a mouse B cell lymphoma because these cells express endogenous IgG2a that can serve as a positive control (68). A20 cells also efficiently present antigen through IgG2a, and crosslinking IgG2a produces an increase of intracellular  $Ca^{2+}$  (68). Furthermore, A20 cells transfected with IgM have been shown to be competent to signal through either IgM or IgG2a (68).

The constructs for the two IgE isoforms were independently transfected in the A20 cells by electroporation and G418 resistant transfectants were selected for the expression of mIgE by immunofluorescence (Fig. 3.3.1).

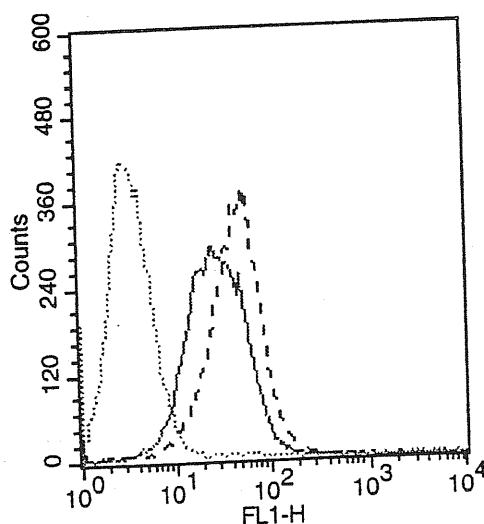


**Figure 3.3.1:** Expression of  $m_S$ IgE-BCR and  $m_L$ IgE-BCR levels on the surface of transfected A20 cells. The level of surface IgE was determined in each cell line by fluorescent flow cytometry analysis with a rabbit anti-human IgE antibody and FITC-conjugated swine anti-rabbit IgG. A20 untransfected (dotted line); A20- $m_S$ IgE (striped line) and A20- $m_L$ IgE (solid line) are shown.

### 3.3.2 Characterization of the IgE-BCR components on A20 cells

To characterize the IgE-BCR and to look for the existence of the  $\epsilon$ BAPS in these cells, we immunoprecipitated the IgE antigen receptor complex from digitonin lysates of surface biotinylated A20- $m_S$ IgE and A20- $m_L$ IgE cells. The immunoprecipitated material was resolved on a 10% SDS gel under reducing conditions (Fig. 3.3.2). Analysis of the  $m_L$ IgE complex yielded again the characteristic pattern of heavy and light chain and the B cell specific proteins Ig- $\alpha$  (32 kDa) and Ig- $\beta$  (37–39 kDa). The Ig- $\alpha$  associated with the  $m_L$ IgE was again of a higher molecular weight than that associated with  $m_S$ IgE (Fig. 3.3.2). Like in the WEHI, this difference was also due to different terminal glycosylation of the two N-glycosylation sites in the polypeptide, indicating that association of differentially glycosylated form of Ig- $\alpha$  is independent of the differentiation state of B cells. In contrast, the  $\epsilon$ BAPS were not found to be associated with the IgE BCRs on the surface of A20 cells, suggesting a differentiation dependent association.

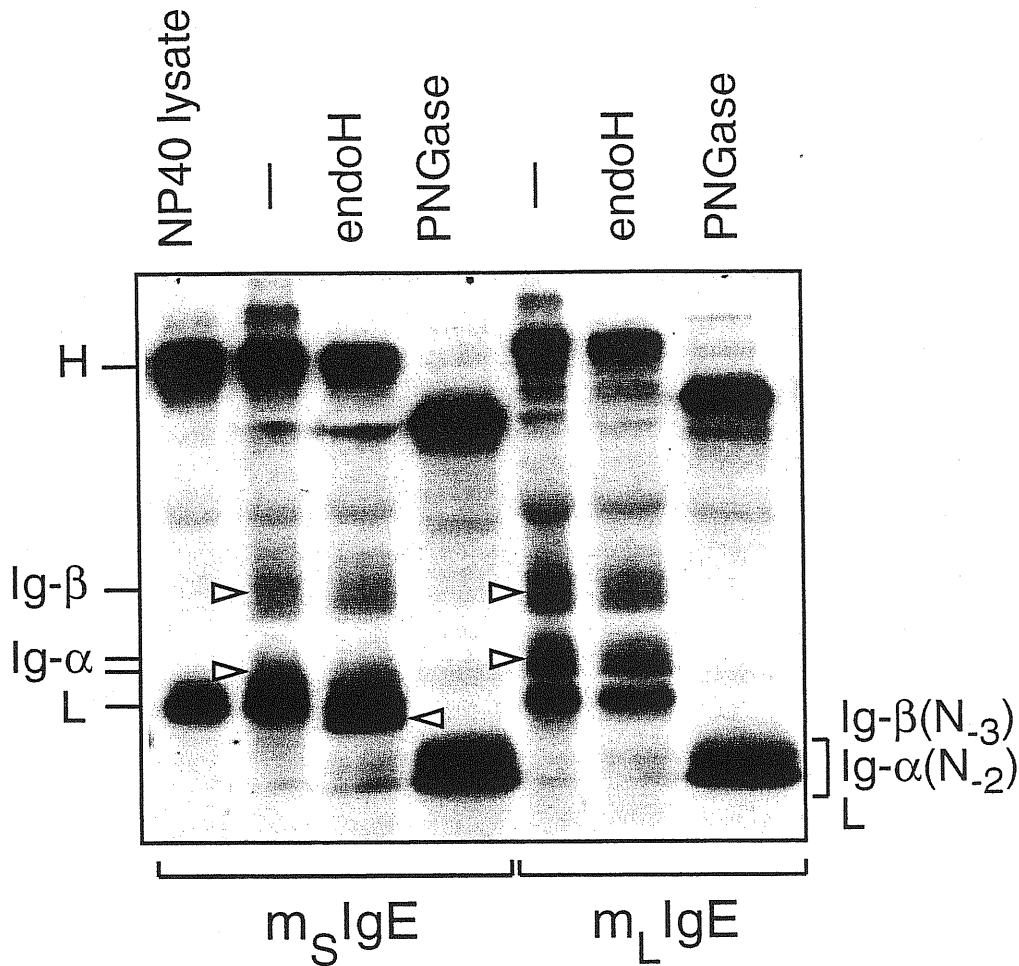


**Figure 3.3.2:** Immunoprecipitation of BCRs from biotin-labeled cell-surface proteins. A20- $m_S$ IgE and A20- $m_L$ IgE were surface biotinylated and treated with digitonin lysis buffer to preserve the BCR complexes. Lysates were treated with anti-IgE, to immunoprecipitate the IgE-BCR. Immunoprecipitated material was treated with Endo H or PNGase as indicated and analyzed by reducing 10% SDS-PAGE. Arrow-heads indicate the position of the Ig- $\alpha$  polypeptide after removal of one of the two N-linked carbohydrate moieties by Endo H. Ig- $\alpha$ (N-2) and Ig- $\beta$ (N-3) correspond to the Ig- $\alpha$  and Ig- $\beta$  polypeptides after removal by PNGase of the 2 or 3 N-linked carbohydrate moieties, respectively.

### 3.3.3 Protein tyrosine phosphorylation upon crosslinking of the IgE-BCRs on A20 cells.

In order to analyze the activation of protein tyrosine kinases upon crosslinking the IgE-BCRs expressed on A20 cells, we used transfected cell lines (A20-m<sub>S</sub>IgE and A20-m<sub>L</sub>IgE ) that expressed comparable levels of the two mIgEs. The two cell lines were incubated for different periods of time (1-40 min) in the presence of anti-IgE antibody. The PTK activation in these cells was monitored by the increase in tyrosine phosphorylation of PTK substrate proteins in Triton X-100 cell lysates. The lysates were run on a 10% reducing gel, and the blot was probed with an anti-phosphotyrosine antibody. Crosslinking of the two IgE BCRs resulted in the increase in phosphorylation of a different set of substrate proteins between the two IgE BCRs. However, the kinetics of phosphorylation of the two IgE-BCRs remained the same (Fig. 3.3.3). The above result was in marked contrast to that obtained in the WEHI, in which both the IgE BCRs upon crosslinking induced the phosphorylation of the same set of substrate proteins, but they differ in the kinetics of tyrosine phosphorylation. The fact that in A20 the two IgE BCRs phosphorylate a different set of substrate proteins but with the same kinetics, implies that in these cells as well, the two IgE BCRs signal differently, and may induce different cellular responses.

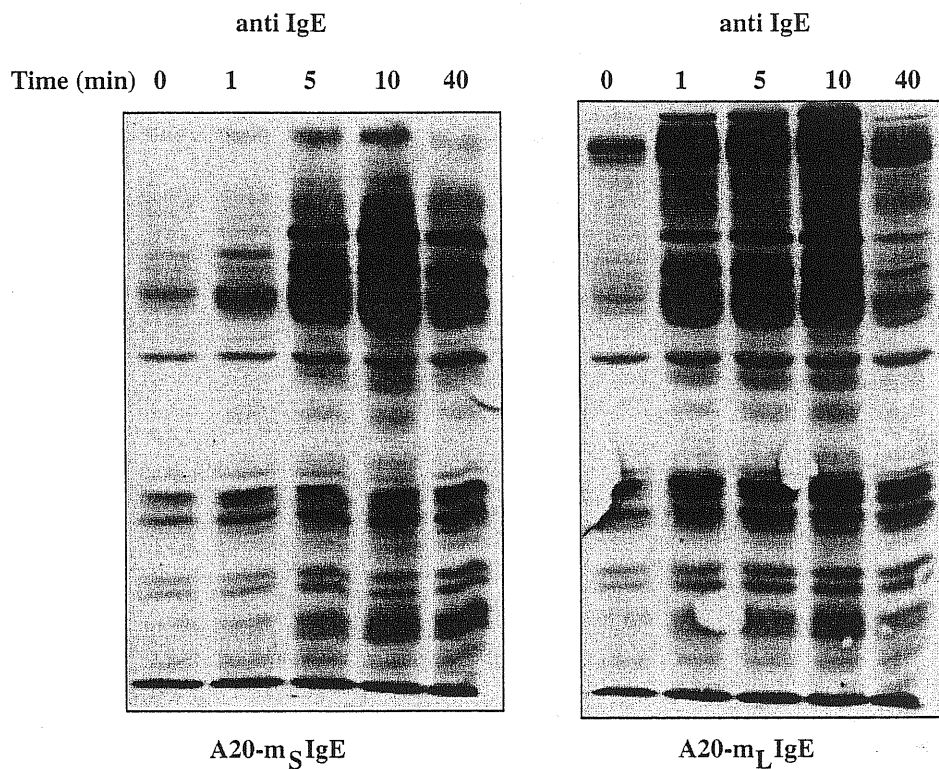


Figure 3.3.3: Kinetics of PTK substrate phosphorylation upon cross-linking of the m<sub>S</sub>IgE-BCR, m<sub>L</sub>IgE-BCR. A20-m<sub>L</sub>IgE or A20-m<sub>S</sub>IgE cells were incubated for various times with anti-IgE antibody, as indicated on top of each gel. Cellular extracts were then prepared and tyrosine phosphorylated proteins detected by immunoblotting with an anti-phosphotyrosine mAb.

## **CHAPTER 4**



## DISCUSSION

During terminal B cell differentiation to plasma cells a switch from production of membrane-bound to secreted immunoglobulin occurs (154, 192, 193). The production of these two types of Ig H chains is regulated by differential splicing and polyadenylation of primary H chain transcripts (39, 40). The membrane and secretory H chain isoforms differ only in their C-termini, where they contain a hydrophobic or hydrophilic sequence respectively. The pattern of splicing is more complex in the case of human IgE, since a number of alternatively spliced  $\epsilon$  transcripts have been detected in all human IgE producing cells examined to date, demonstrating that they occur naturally in non-atopic and atopic humans (150-152, 165). These variants encode two membrane forms of IgE and four putative secreted isoforms (Figure 1.8).

It has been previously demonstrated that the  $\epsilon$  mRNA variant pattern is not fixed either in vivo or in vitro. Addition of diesel exhaust particle (DEP)-derived polyaromatic hydrocarbons to B cells stimulated to produce IgE leads to a significant alteration in the relative ratios of each of the  $\epsilon$  variants. The four isoforms CH4-M1'-M2, CH4-M2', CH4-M2'', and CH4-S all increased from about 22-33 fold over basal levels and the total amount of  $\epsilon$  mRNA obtained after DEP challenge increased nearly 28-fold compared with prechallenge levels (165). Also, more recently it has been shown that biological processes in vivo (i.e., parasitic infection or atopy) or biologic activities in vitro (i.e., IL-10 and cross-linking the low affinity receptor for IgE (FcERII or CD23) involved in IgE regulation can also control the production of different variants (194). Cells from subjects with high levels of serum IgE secondary to parasitic infection or atopy spontaneously produced higher relative levels of the  $\epsilon$ CH4-M2'  $\epsilon$  mRNA variant, lower relative amounts of both the membrane and  $\epsilon$ CH4-M2'' secreted variants, and very low levels of the  $\epsilon$ CH4'-I variant (194). When transfected in the mouse myeloma and lymphoma cells, many of these isoforms ( $\epsilon$ CH4-M2',  $\epsilon$ CH4\*,  $\epsilon$ CH4-I) were unable to form properly

assembled IgE molecules, and were degraded intracellularly, with the exception of one of the variants ( $\epsilon$ CH4-M2") referred to as  $\epsilon_{S2}$  which was found to be secreted with the same efficiency as the classical secreted  $\epsilon$ CH4-S ( $\epsilon_{S1}$ ) (152, 156). The significance of the mouse transfectoma results has been recently confirmed by the finding that both secreted isoforms are co-expressed in a human IgE secreting myeloma U266, in human sera and tonsils. The  $\epsilon_{S2}$  form has also been shown to functionally engage the high affinity receptor of IgE (unpublished results, Roberto Lorenzi; our lab). The above results corroborate the hypothesis that humans have two functional secreted IgE isoforms.

#### *4.1 Characterization of the two murine membrane $\epsilon$ mRNA polyadenylation sites*

Since functional differences among the various  $\epsilon$  mRNAs may provide important insights into the immunobiology of diseases involving immediate hypersensitivity, we wanted to investigate if alternatively spliced forms also exist in other species. We focused our study on the mouse C $\epsilon$  gene whose sequence had previously been characterized until the stop codon of the second membrane exon (141). Also, Northern blot analysis of IgE producing mouse hybridoma cells had shown that the mouse C $\epsilon$  gene is transcribed into a major RNA species corresponding to the secreted form and two minor species corresponding to membrane form(s) of the  $\epsilon$  chain (141, 167). These could either have been generated by alternative splicing of membrane-exon sequences or by differential usage of two poly(A) sites.

Therefore, we characterized the poly(A) signals of the murine membrane  $\epsilon$  transcripts. For this, we determined the complete sequence of the 3' untranslated region of these transcripts and 836 nucleotides (nt) of new sequence downstream of the second polyadenylation site. The first poly(A) signal used by the mouse membrane  $\epsilon$  transcripts is an AGTAAA hexamer located 743 nt downstream from the beginning of the M2 exon.

The site of cleavage and polyadenylation is a CA dinucleotide located 9 nt further downstream. Though the AGTAAA hexamer is not identical to the consensus AATAAA and has only 30% of its activity (195), it has been found in a number of eukaryotic genes. Most interestingly, this hexamer constitutes the polyadenylation signal sequence of human membrane  $\epsilon$  transcripts (162). However, in contrast to humans, the first mouse poly(A) site does not contain the conserved (G+T) rich element. The absence of this element could further weaken this poly(A) site, since even changes in the position of the (G+T) rich regions have been shown to result in a dramatic reduction of 3' end processing activity (196).

Unlike the human C $\epsilon$  gene, the mouse M2 exon contains another poly(A) signal sequence located 486 nt downstream to the first hexamer. This AAGAAA signal sequence is even less frequently found in eukaryotic genes, and has been attributed only 6% of the polyadenylation activity of the consensus AATAAA (195). However, this distal poly(A) site contains a 21 nt long (G+T) rich region which is located 14 nt downstream to the cleavage site. The presence of this element could strengthen the 3' end processing activity of the distal poly(A) site and could account for the Northern blot data in the mouse IgE producing B cell lymphoma (I29e<sup>+</sup>) which showed that this site is preferentially utilised by the membrane  $\epsilon$  transcripts.

Differential polyadenylation of membrane transcripts is also a feature of other mouse Ig H-chain genes. The mouse C $\delta$  gene contains two distal poly(A) sites that give rise to two types of membrane  $\delta$  transcripts, whereas three poly(A) sites are present in the second membrane exon of the mouse C $\alpha$  gene (39, 40). The striking feature of the murine membrane  $\epsilon$  poly(A) signals is that both of them (AGTAAA and AAGAAA) are different from the consensus AATAAA and ATTAAA sequences and have a much lower polyadenylation activity, whereas all other mouse and human Ig H chain genes, with the exception of human C $\epsilon$ , contain the consensus sequence. The presence of inefficient

poly(A) signals in the membrane C $\epsilon$  locus could constitute an additional aspect in the regulation of IgE production, preventing high level expression of membrane  $\epsilon$  transcripts.

#### *4.2 Alternatively spliced forms of $\epsilon$ mRNA are expressed in a mouse IgE producing lymphoma and in normal B cells.*

We also investigated the type of  $\epsilon$  mRNA expressed by a mouse IgE-producing lymphoma cell line and by normal mouse splenocytes. This allowed us to define the structure of the membrane exons and the positions of splice sites within them. We show that the predicted splice sites in the CH4, M1 and M2 exons are active and that two novel acceptor splice sites are present within the M2 exon. As in humans, utilization of these splice sites generates a number of  $\epsilon$  mRNA variants which contain membrane-exon sequences (Figure 4.1). Estimation of their relative amounts with a quantitative RT/PCR assay indicated that these alternatively spliced transcripts are expressed at substantially lower levels than the classical membrane IgE isoform (m $\epsilon$ CH4-M1-M2).

The pattern of splicing that produces the newly described murine variants is rather similar to the one of the human  $\epsilon$  locus, although none of the variants bears significant amino acid homology to their human counterparts (Figure 4.1). One of the new  $\epsilon$ mRNAs is produced by splicing of the CH4 exon to a novel acceptor splice site inside the M2 exon. This splicing generates an alternative membrane variant of murine IgE (m $\epsilon$ CH4-M1-M2\*) that is 10 aa shorter in the cytoplasmic domain than the classical m $\epsilon$ CH4-M1-M2 form. This is opposite to what has been observed in humans, where the two membrane variants differ in the length of the extracellular membrane-proximal domain (150, 157, 163). The other two alternatively spliced  $\epsilon$ mRNAs exclude the M1 exon and splice directly into the M2 exon. One of them (m $\epsilon$ CH4-M2') splices to the first acceptor site of the M2 exon and generates an mRNA that encodes an IgE H-chain 52 aa longer than the classical secreted protein (m $\epsilon$ CH4-S). This form is analogous to the M2' form in



humans, which contains an additional 134 aa tailpiece that prevents its assembly and secretion (152). The second form that excludes the M1 exon is produced by splicing of CH4 to a previously undescribed acceptor splice site inside the M2 exon, between the two poly(A) sites. This isoform (mεCH4-M2") is of considerable interest since it is analogous to the human εCH4-M2" transcript which encodes the secreted εS<sub>2</sub> isoform (156). Both human and mouse εCH4-M2" transcripts are generated by splicing to a novel exon, the coding region of which encodes eight amino acids in the human and seven in the mouse. The mouse mεCH4-M2" form is exactly of the same size as the classical secreted mεCH4-S since the number of amino acids replaced at the carboxy terminal are identical. In contrast, the human εCH4-M2" isoform is six amino acids longer than the classical secreted form. The human and mouse M2" exons do not share any sequence homology, although there is a similar net charge of the carboxyl terminal tails encoded by these two exons (Figure 4.2). Furthermore, whereas the human εCH4-M2" transcript is readily detectable by Northern Blot analysis, the same is not true for the mouse εCH4-M2" variant, which implies that the mouse M2" form is significantly less represented.

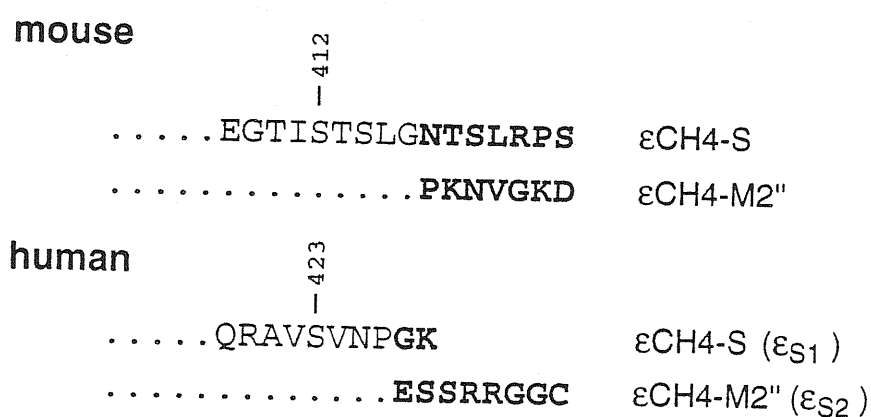


**Figure 4.2:** Comparison of the carboxyl-terminal sequences of the classical secretory mouse ε heavy chain (mεCH4-S) and the novel murine mεCH4-M2" variant with the human secretory isoforms εS<sub>1</sub> and εS<sub>2</sub>. Dots indicate amino acid identity. The carboxyl-terminal tail unique to each isoform is shown in bold. Numbers are relative to the first residue of Cε.

In conclusion, we have shown that alternative splicing of membrane exon sequences also occurs in the mouse Cε locus. This finding is different from what has been reported for the rat Cε gene, in which only one type of membrane transcript was observed (197). It is noteworthy that mice, unlike humans, express only one membrane isoform which resembles the short membrane isoform of the humans. The mouse in fact lacks the 156 nt that are unique to the long membrane isoform of the humans. There is significant homology, however, between mouse and humans in the remaining parts of the molecule as shown in Figure 4.3.

### The mouse and human membrane IgE

	extracellular
mouse	ELDLQDL C I E E V E G E E L E
human	***V---*V** <u>A</u> ***- <u>AP</u>
	transmembrane
mouse	ELWTSICVFITLFLLSVSYGATVTVL
human	<u>WT</u> **GL*I* <u>AA</u> *****S* <u>AL</u> *L*
	cytoplasmic
mouse	KVKWVLSTPMQDTPQTFQDYANILQTRA
human	<u>M</u> * <u>QRF</u> ** <u>ATR</u> * <u>GR</u> *** <u>SL</u> **T*V** <u>PH</u> *

**Figure 4.3:** Comparison of the M1 and M2 exons of the classical membrane isoform of the mouse (mεCH4-M1-M2) with the short membrane isoform in the humans (hεCH4-M1-M2). Asteriks indicate amino acid identity. The dissimilar amino acids are underlined.

### 4.3 A tale of two receptors

Humans have two types of membrane  $\epsilon$  transcripts which differ only in the 5' part of the first membrane exon (M1) that encodes the extracellular membrane proximal domain and the transmembrane domain (Figure 3.2.1a). The longer variant  $m_L$ IgE ( $\epsilon$ CH4-M1'-M2) contains 156 extra nucleotides as a consequence of alternative splicing between the donor splice site at the 3' end of the CH4 exon and the upstream acceptor splice site in the M1 exon. These extra nucleotides encode an additional 52 amino acids in the extracellular membrane proximal domain, which are lacking in the short isoform ( $\epsilon$ CH4-M1-M2).

Since the long membrane transcript in the humans was described as the predominant membrane  $\epsilon$  mRNA species, because it was found at significantly higher levels than the short species in IL-4 plus anti-CD40 stimulated peripheral blood lymphocytes (PBLs) and in IgE producing myeloma cell lines (149, 151), we wanted to see the pattern of expression of these two isoforms in unstimulated PBLs. The surprising observation that the short membrane isoform is expressed significantly by unstimulated PBLs (Figure 3.2.2) led us to investigate the properties of this isoform and to compare it with the long membrane isoform.

We demonstrate here for the first time the existence of two functional human IgE B-cell receptors that are generated by alternative splicing. Although both receptors were found to be correctly assembled, transported to the cell surface, and capable of signal transduction upon receptor engagement, a number of differences were noted between them that could only be attributed to the different extracellular membrane proximal domains.

The first difference was in the rate of their transport to the plasma membrane. The transit time of the  $m_L$ IgE was much longer, since only 20% of the molecules were found to be terminally glycosylated within 3h of their synthesis, whereas almost all of the  $m_S$ IgE molecules were converted into the mature form during this period. Interestingly, a



different rate of transport has also been shown for IgM and IgD with a shorter transit time for the former (198). In our experiments the endogenous IgM was transported at a similar rate as the  $m_L$ IgE, indicating that the transport of the  $m_S$ IgE is extremely efficient.

Both mIgE isoforms were found to associate into complete BCR complexes that contain the Ig- $\alpha$ /Ig- $\beta$  heterodimer as well as the PTKs involved in their phosphorylation. However, a difference was also noted in the pattern of glycosylation of the associated Ig- $\alpha$ ; when associated with  $m_S$ IgE the Ig- $\alpha$  polypeptide had only one of the sites terminally glycosylated and resistant to Endo H cleavage, whereas, when associated with  $m_L$ IgE, both sites were resistant to the enzyme. This is identical to what has been reported for IgM and IgD, which associate with partially or completely processed Ig- $\alpha$ , respectively (169, 170). Several possibilities have been considered to explain the difference in glycosylation of the Ig- $\alpha$  polypeptide associated with IgD, including the length of the extracellular membrane proximal domain, the presence of inter-chain disulfide bonds in this region and the transit time of the complex through the Golgi (171). These possibilities could also account for the different processing of the IgE-associated Ig- $\alpha$  polypeptides, since, analogous to IgD, the  $m_L$ IgE contains a much longer extracellular domain than the  $m_S$ IgE, has three extra cysteines in this region and also has a lower rate of transport to the cell surface.

#### ***4.4 The association of BCR associated proteins ( $\epsilon$ BAPs) with IgE***

An unexpected observation in this study was the finding that both IgE-receptors associate with two novel BCR associated proteins ( $\epsilon$ BAP37 and  $\epsilon$ BAP41) that were not associated with the endogenous IgM-BCR of the WEHI lymphoma. Their association with the IgE-receptors appeared to be very specific, since they were co-precipitated with two different anti-IgE antisera. BCR associated proteins which are specifically associated with particular isotypes have been described before. BAP32 and BAP37 are known to be

exclusively associated with IgM (199), and BAP29 and BAP31 are preferentially associated with IgD molecules (200). BAP32 has been identified to be mouse prohibitin and BAP37 was found to be highly homologous to BAP32. Since prohibitin was identified as an inhibitor of cell proliferation, its association with mIgM but not mIgD has been thought to explain the different biological events elicited after engagement of each receptor. BAP31 on the other hand, has recently been identified as a representative of a novel class of sorting protein that controls anterograde transport of certain membrane proteins from the ER to the Golgi complex (203). The BAPs associated with both mIgM and mIgD are intracellular proteins, and are coprecipitated with the immunoglobulins only in Triton X-100 and Nonidet P-40, but not in digitonin lysates. It has also been shown that the transmembrane domain of mIgM determines the specificity of the interaction with BAP32/prohibitin and BAP37 (199, 200).

There are a number of characteristics which distinguish the  $\epsilon$ BAPs from the above described proteins: They have an extracellular domain which was labeled in the cell-surface biotinylation experiment, implying that they are membrane proteins unlike the BAPs associated with IgM and IgD. Both proteins were glycosylated, and they form disulfide-bonded homo or heterodimers depending on which of the two IgE BCRs they associate with. The  $\epsilon$ BAP41 appeared to be underrepresented in the m<sub>L</sub>IgE-BCR, suggesting that the longer extracellular membrane-proximal domain affects the association of  $\epsilon$ BAP41 to the BCR or its accessibility to biotinylation. At present we do not know which domain(s) of IgE impart the specificity of the interaction with the two BAPs. The possibility that it could also be via the cytoplasmic domain cannot be ruled out, since IgE in contrast to IgM and IgD has a longer cytoplasmic domain (28 aa in IgE vs 3 in IgM/D) (70) which may contribute to confer selective association. Also, we do not know whether the  $\epsilon$ BAPs play a role in the difference in signal transduction and cellular responses observed between the two IgE-BCRs on WEHI cells.

#### *4.5 Functional differences between the two IgE-BCRs*

Functional differences between the two IgE BCRs was analysed by looking at tyrosine phosphorylation, cellular proliferation and internalization.

The most striking difference between the two IgE-BCRs was related to the response elicited by their crosslinking. Both receptors appeared to activate the same PTKs, as judged by the pattern of tyrosine phosphorylation. However, a clear difference was noted in the maximal phosphorylation time point as well as in the duration of the response. More specifically, the phosphorylation induced via the  $m_L$ IgE-BCR reached its maximum after 1 min of receptor engagement and declined within the following 5 min. In contrast, the signal induced by crosslinking of the  $m_S$ IgE-BCR reached its maximum after 5 min and remained for a prolonged period. Differences in the kinetics of the response have also been observed for the IgM- and IgD-BCRs (181). Experiments with these receptors or receptor chimeras have indicated that the extracellular membrane-proximal and/or transmembrane domains influence the duration of the response (181). Since in the IgE-BCRs the difference resides only in the extracellular membrane-proximal domain, it can be concluded that this region determines the kinetics of protein tyrosine phosphorylation upon receptor engagement. The mechanisms through which this could occur are unknown at present, but could be mediated through the association and/or interaction with the different Ig- $\alpha$  glycoforms or other proteins of the BCR-complex.

The different kinetics of signal transduction through the IgE-BCRs were associated with different cellular responses of the WEHI transfectomas. Crosslinking of the  $m_S$ IgE-BCR led to growth inhibition, whereas signaling through the  $m_L$ IgE-BCR had no effect on cellular proliferation. These cellular responses are analogous to those observed after signaling through the IgM- and IgD-BCRs in WEHI cells (175). In this case the IgM-BCR, which like  $m_S$ IgE has a short extracellular spacer, is capable of transmitting a growth inhibitory signal. A difference was also noted in the rate of

internalization of the two IgE-BCRs, with the m<sub>L</sub>IgE-BCR being faster than the m<sub>S</sub>IgE-BCR.

In conclusion, we have shown that both human mIgE isoforms assemble into functional B-cell receptors. When expressed on immature B-cells, such as the WEHI lymphoma, the two IgE-BCRs transmit qualitatively distinct signals after crosslinking.

Work is in progress to determine the properties of these two receptors in human B cells, and in particular we are interested to see: (1) the association of the two εBAPs in human B cells, (2) to identify them and then to study their function in these cells. We transfected the two membrane IgE constructs in a variety of different human B cell lines (Ramos, BJAB, WILCL, TAK3). However, we had no expression of either of the two membrane isoforms in any of the B cell lines. We suspect that our chimeric (mouse/human) heavy chain does not assemble with the human light chain. At present, work is in progress to modify these constructs and to obtain human B cell clones expressing the two IgE isoforms.

However, it should also be noted here that B-cells co-expressing IgM and IgE have been detected in peripheral blood (201, 202). Clearly, it would be of interest to determine the type of mIgE expressed by these cells and whether the two mIgE-BCRs can be co-expressed by the same cell, and if so what is the final outcome of signalling through these receptors. The final outcome of signalling may depend on the relative expression of the two isoforms with respect to each other, and at the differentiation state of the B cell. It could be that Ag-induced signalling through m<sub>S</sub>IgE-BCR generates a negative signal that results in deletion of the B cell. In contrast, by this hypothesis, signalling through m<sub>L</sub>IgE-BCR generates signals positive for activation of B cell that also interfere with negative signals simultaneously generated through m<sub>S</sub>IgE-BCR. Such studies should further delineate the relevance of having two receptors with identical specificity for the ligand and may allow characterization of additional components of the BCR signal-transduction pathways.

## CONCLUSIONS

The work presented here focused on the molecular, biochemical and functional characterization of membrane IgE isoforms. Recent studies on the human C $\epsilon$  gene produces a number of alternatively spliced heavy chain transcripts of which some encode functional IgE isoforms. The first part of the study presented here shows that differentially processed  $\epsilon$  mRNA variants also exist in the mouse and are generated by differential polyadenylation and alternative splicing of primary  $\epsilon$  chain transcripts. The two poly(A) sites of the mouse membrane transcripts were identified in the present study by RACE-PCR analysis. The first poly(A) site is located 743 nt downstream from the beginning of the second membrane exon (M2) and contains the same non-consensus AGTAAA signal sequence as the single poly(A) site of the human membrane transcripts. The second poly(A) site is located almost 500 nt further downstream and is characterized by an AAGAAA hexamer. This poly(A) site contains a (G+T) rich element downstream to the site of cleavage and polyadenylation, and is preferentially utilised by the membrane  $\epsilon$  transcripts. Additional diversity of  $\epsilon$  transcripts is generated by alternative splicing between the last constant region exon (CH4) and the two membrane exons (M1 and M2). The alternatively spliced transcripts include two variants that skip the first membrane exon and encode  $\epsilon$  heavy chains that lack the transmembrane domain. The third variant is generated by splicing to an internal site in M2 and codes for a membrane isoform that is 10 amino acids shorter in the cytoplasmic domain than the classical membrane IgE. Although little amino-acid sequence homology exists between the murine  $\epsilon$  chain isoforms and their human counterparts, the pattern of splicing is rather conserved between the two species. (*Shubha Anand, Facundo D Batista, Tatiana Tkach, Dimitar G Efremov and Oscar Burrone. (1997) Multiple transcripts of murine immunoglobulin  $\epsilon$  membrane locus are generated by alternative splicing and differential usage of two polyadenylation sites. Mol. Immunol. 34, 175*)

The second part of this study shows for the first time the existence of two functional human IgE B cell receptors that are generated by alternative splicing. The human C $\epsilon$  gene expresses two membrane IgE heavy (H) chain mRNAs which differ in the sequence that encodes their extracellular membrane-proximal domain. In the long IgE isoform (m<sub>L</sub>IgE) this domain contains a stretch of 52 amino acids which are absent in the short variant (m<sub>S</sub>IgE). We generated B-cell transfectoma cell lines that express these two isoforms and show that both types of mIgE form functional B-cell antigen receptors (BCR). Both

receptors associate with the Ig- $\alpha$ /Ig- $\beta$  heterodimer, as well as with protein kinases that are capable of phosphorylating this complex. Upon their crosslinking, both receptors can activate protein tyrosine kinases that phosphorylate the same substrate proteins. Both IgE receptors also associate with two novel proteins that do not bind to mIgM. Apart from these similarities, the two IgE-BCRs show several differences of which some are analogous to the differences between the IgM- and IgD-BCRs. First, the m<sub>S</sub>IgE is transported to the cell surface at a higher rate than the m<sub>L</sub>IgE. Second, the two IgE-BCRs associate with differently glycosylated Ig- $\alpha$  proteins: the m<sub>L</sub>IgE associates with the completely glycosylated form, whereas the m<sub>S</sub>IgE associates with an Ig- $\alpha$  glycoform that is partially sensitive to EndoH. Third, the kinetics of protein tyrosine phosphorylation induced by receptor crosslinking is significantly different for the two IgE-BCRs. Finally, crosslinking of the m<sub>S</sub>IgE-BCR leads to growth inhibition of the B-cell transfectoma, whereas signaling through the m<sub>L</sub>IgE-BCR does not affect the cellular proliferation. These data show that the two human membrane IgE isoforms assemble into functionally distinct antigen receptors which can induce different cellular responses. (*Facundo D Batista, Shubha Anand, Gianni Presani, Dimitar G Efremov and Oscar Burrone. (1996) The two membrane isoforms of human IgE assemble into functionally distinct B- cell antigen receptors. J. Exp. Med. 184, 2197*).

## BIBLIOGRAPHY

1. Kabat, E.A., Wu, T.T., Reid-Miller, M., Perry, H.M., and Gottesman, K.S. (1987). *Sequences of proteins of immunological interest*. US Dept. Health & Human Services, Washington, D. C.
2. Kabat, E. A. (1982). Antibody diversity versus antibody complimentary. *Pharm. Rev.*, 34, 23.
3. Nissinoff, A., Hopper, J. E., and Spring, S.B. (1975). *The antibody molecule*. Academic Press, New York.
4. Koshland, M.E. (1989). The immunoglobulin helper: The J chain. In *Immunoglobulin genes* (ed. T. Honjo, F.W. Alt, and T.H. Rabbits), p. 345. Academic Press, New York.
5. Tonegawa, S. (1983). Somatic generation of antibody diversity. *Nature*, 302, 575.
6. Livant, D., Blatt, C., and Hood, L. (1986). One heavy chain variable region gene segment subfamily in the BALB/c mouse contains 500-1000 or more members. *Cell*, 47, 461.
7. Brodner, P.H., Osman, G.E., Mackle, J.J., and Lalor, T.M. (1988). The organization of the mouse IgH-V locus. *J. Exp. Med.*, 168, 2261.
8. Kofler, R., Geley, S., Kofler, H., and Helmborg, A. (1992). Mouse variable region gene families: complexity, polymorphism and use in non-autoimmune responses. *Immunol. Rev.*, 128, 5.
9. Tutter, A., Brodeur, P., Shlomchik, M., and Riblet, R. (1991). Structure, map position, and evolution of two newly diverged mouse V<sub>H</sub> gene families. *J. Immunol.*, 147, 3215.
10. Rathbun, G. A., Capra, J.D., and Tucker, P. W. (1987). Organization of the murine immunoglobulin V<sub>H</sub> complex in the inbred strains. *EMBO J.*, 6, 2931.
11. Croce, C. M., Shander, M., Martinis, J., Cicurel, L., D' Ancona, G. G., Dolby, T. W., and Koprowski, H. (1979). Chromosomal location of the human genes for immunoglobulin heavy chains. *Proc. Natl. Acad. Sci. USA*. 76, 3416.
12. Ichihara, Y., Matsuoka, H., and Kurosawa, Y. (1988). Organization of human immunoglobulin heavy chain diversity gene loci. *EMBO J.*, 7, 4141.
13. Matsuda, F., Shin, E. K., Hirabayashi, Y., Nagaoka, H., Yoshida, M. C., Zong, S. Q., and Honjo, T. (1988). Organization of variable region segments of the human immunoglobulin heavy chain : duplication of the D5 cluster within the locus and interchromosomal translocation of variable region segments. *EMBO J.*, 7, 1047.
14. Walter, M. A., Surti, U., Hofker, M. H., and Cox, D. W. (1990). The physical organization of the human immunoglobulin heavy chain gene complex. *EMBO J.*, 9, 3303.
15. van Dijk, K. W., Mortari, F., Kirkham, P. M., Schroeder, H. W., and Milner, E. C. (1993). The human immunoglobulin V<sub>H</sub> 7 segment gene family consists of a small polymorphic group of six to eight gene segments dispersed throughout the V<sub>H</sub> locus. *Eur. J. Immunol.*, 23, 832.
16. Rathbun, G., Berman, J., Yancopoulos, G., and Alt, F. W. (1989). Organization and expression of the mammalian heavy-chain variable-region locus. In *Immunoglobulin genes* (ed. T. Honjo, F. W. Alt, and T. H. Rabbits), p. 63. Academic Press, New York.

17. Liu, C.-P., Tucker, P. W., Mushinski, F. and Blattner, F. R. (1980). Mapping of the heavy chain genes of mouse immunoglobulins M and D. *Science*, 209, 1348.
18. Tucker, P.W., Lui, C.-P., Mushinski, F. and Blattner, F.R. (1980). Mouse immunoglobulin D: Messenger RNA and genomic DNA sequences. *Science*, 209, 1353.
19. Maki, R., Roeder, W., Trauhecker, A., Sidman, C., Wabl, M., Rascke, L., and Tonegawa, S. (1981). The role of DNA rearrangement and alternate RNA processing in the expression of immunoglobulin  $\delta$  genes. *Cell*, 24, 353.
20. Blattner, F. R. and Tucker, P. W. (1984). The molecular biology of immunoglobulin D. *Nature*, 307, 417.
21. Mather, E. L., Nelson, K. J., Haimovitch, J., and Perry, R. P. (1984). Mode of regulation of immunoglobulin  $\mu$  and  $\delta$ -chain expression varies during B-lymphocyte maturation. *Cell*, 36, 329.
22. Roes, J. and Rajewsky, K. (1991). Cell autonomous expression of IgD is not essential for the maturation of conventional B cells. *Int. Immunol.*, 3, 1367.
23. Nitschke, L., Kosco, M. H., Kohler, G., and Lamers, M. C. (1993). Immunoglobulin D-deficient mice can mount normal immune responses to thymus-independent and -dependent antigens. *Proc. Natl. Acad. Sci. USA*, 90, 1887.
24. Roes, J. and Rajewsky, K. (1993). Immunoglobulin D (IgD)- deficient mice reveal an auxillary receptor function for IgD in antigen-mediated recruitment of B cells. *J. Exp. Med.*, 177, 45.
25. Shimizu, A. and Honjo, T. (1984). Immunoglobulin class switching. *Cell*, 36, 801.
26. Snapper, C. M. and Finkelman, F. D. (1993). Immunoglobulin class switching. In *Fundamental immunology* (ed. W. E. Paul), p. 837. Raven Press, New York.
27. Flanagan, J. G., and Rabbitts, T. H. (1982). Arrangement of human immunoglobulin heavy chain constant region genes implies evolutionary duplication of a segment containing  $\gamma$ ,  $\epsilon$  and  $\alpha$  genes. *Nature*, 300, 709.
28. Selsing, E., Durdik, J., Moore, M. W., and Persiani, D. M. (1989). Immunoglobulin  $\lambda$  genes. In *Immunoglobulin genes* (ed. T. Honjo, F. W. Alt, and T. H. Rabbits), p. 111. Academic Press, New York.
29. McBride, O. W., Heiter, P. W., Hollis, G. F., Swan, D., and Leder, P. (1982). Chromosomal location of human kappa and lambda immunoglobulin light chain constant region gene. *J. Exp. Med.*, 155, 1480.
30. Vasicek, T. J. and Leder, P. (1990). Structure and expression of the human immunoglobulin  $\lambda$  genes. *J. Exp. Med.*, 172, 609.
31. Alt, F. W., Yancopoulos, G. D., Blackwell, T. K., Wood, C., Thomas, E., Boss, M., Coffman, R., Rosenberg, N., Tonegawa, S., and Baltimore, D. (1984). Ordered rearrangement of immunoglobulin heavy chain variable region segments. *EMBO J.*, 3, 1209.
32. Schlissel, M. S., Corcoran, L. M., and Baltimore, D. (1991). Virus transformed pre-B cells show ordered activation but not inactivation of immunoglobulin gene rearrangement and transcription. *J. Exp. Med.*, 173, 711.
33. Kitamura, D., and Rajewsky, K. (1992). Targeted disruption of mu chain membrane exon causes loss of heavy chain allelic exclusion. *Nature*, 356, 154.
34. Banerji, J., Olson, L., And Schaffner, W. (1983). A lymphocyte-specific cellular enhancer is located downstream of the joining region in immunoglobulin heavy chain genes. *Cell*, 33, 729.



35. Gillies, S. D., Morrison, S. L., Oi, V. T., and Tonegawa, S. (1983). A tissue-specific transcription enhancer element is located in the major intron of a rearranged immunoglobulin heavy chain gene. *Cell*, 33, 717.
36. Pettersson, S., Cook, G. P., Bruggemann, M., Williams, G. T., and Neuberger, M. S. (1990). A second B cell-specific enhancer 3' of the immunoglobulin heavy-chain locus. *Nature*, 344, 165.
37. Mills, F. C., Harindranath, N., Mitchell, M., and Max, E. E. (1997). Enhancer complexes located downstream of both human immunoglobulin C $\alpha$  genes. *J. Exp. Med.* 186, 845.
38. Yuan, D., Uhr, J. W., Knapp, M. R., Slavin, S., Strober, S., and Vitteta, E. S. (1979). Structural differences between  $\mu$  chain of the cell associated and secreted forms of immunoglobulin  $\mu$  chain. *Cell*, 20, 303.
39. Word, C. J., Mushinski, J. F., and Tucker, P. W. (1983). The murine immunoglobulin  $\alpha$  gene expresses multiple transcripts from a unique membrane exon. *EMBO J.* 2, 887.
40. Cheng, H. L., Blattner, F. R., Fitzmaurice, L., Mushinski, J. F., and Tucker, P. W. (1982). Structure of genes for membrane and secreted murine IgD heavy chains. *Nature*, 296, 410.
41. Manley, J. L., and Proudfoot, N. J. (1994). RNA 3' ends: formation and function-meeting review. *Genes and Dev.* 8, 259.
42. Picard, D. and Schaffner, W. (1984). A lymphocyte-specific enhancer in the mouse immunoglobulin  $\kappa$  gene. *Nature*, 307, 80.
43. Sharpe, M. J., Milstein, C., Jarvis, J. M., and Neuberger, M. S. (1991). Somatic hypermutation of immunoglobulin kappa may depend on sequences 3' of C kappa and occurs on passenger transgenes. *EMBO J.*, 10, 2139.
44. Betz, A. G., Milstein, C., Gonzalez-Fernandez, A., Pannel, R., Larson, T., and Neuberger, M. S. (1994). Elements regulating somatic mutation: Critical role for the intron enhancer/matrix attachment region. *Cell*, 77, 239.
45. Yancopoulos, G. D., and Alt, F. W. (1986). Regulation of the assembly and expression of variable region genes. *Annu. Rev. Immunol.*, 4, 339.
46. Rolink, A. and Melchers, F. (1991). Molecular and cellular origins of B lymphocyte diversity. *Cell*, 66, 1081.
47. Rajewsky, K. (1996). Clonal selection and learning in the antibody system. *Nature*, 381, 751.
48. Lassoued, K., Illges, H., Benlagha, K. and Cooper, M. D. (1996). Fate of surrogate light chains in B lineage cells. *J. Exp. Med.*, 183, 421.
49. Gong, S., and Nussenzweig, M. C. (1996). Regulation of an early developmental checkpoint in the B cell pathway by Ig $\beta$ . *Science*, 272, 411.
50. Torres, R. M., Flaswinkel, H., Reth, M. and Rajewsky, K. (1996). Aberrant B cell development and immune response in mice with a compromised BCR complex. *Science*, 272, 1804.
51. Ye, J., McCray, S. K. and Clarke, S. H. (1996). The transition of pre-BI to pre-BII cells is dependent on the V<sub>H</sub> structure of the  $\mu$  surrogate L chain. *EMBO J.* 15, 1524.
52. DeFranco, A.L. (1993). Structure and function of the B cell antigen receptor. *Annu. Rev. Cell. Biol.* 9, 377.
53. Hombach, J., Leclercq, L., Radbruch, A., Rajewsky, K., and Reth, M. (1988). A novel 34-kd protein co-isolated with the IgM molecule in surface IgM-expressing cells *EMBO. J.* 7, 3451.

54. Hombach, J., Tsubata, T., Leclercq, L., Stappert, H., and Reth, M. (1990). Molecular components of the B-cell antigen receptor complex of the IgM class. *Nature*, 43, 760.
55. Hermanson, G.G., Eisenberg, D., Kincadee, P. W., and Wall, R. (1988). B29: a member of the immunoglobulin gene superfamily exclusively expressed on beta-lineage cells. *Proc Natl. Acad. Sci. USA*. 85, 6890.
56. Sakaguchi, N., Kashiwamura, S., Kimoto, M., Thalmann, P., and Melchers, F. (1988). B lymphocyte lineage-restricted expression of mb-1, a gene with CD3-like structural properties. *EMBO J.* 7, 3457.
57. Lam, K.-P., Kühn, R., and Rajewsky, K. (1997). In vivo ablation of surface immunoglobulin on mature B cells by inducible gene targeting results in rapid cell death. *Cell*, 90, 1073.
58. Clark, M. R., Johnson, S. A. and Cambier, J. C. (1994). Analysis of Ig-alpha-tyrosine kinase interaction reveals two levels of binding specificity and tyrosine phosphorylated Ig-alpha stimulation of Fyn activity. *EMBO J.*, 13, 1911.
59. Flaswinkel, H. and Reth, M. (1994). Dual role of the tyrosine activation motif of the Ig-alpha protein during signal transduction via the B cell antigen receptor. *EMBO J.* 13, 83.
60. Smit, L., de Vries Smits, A. M., Bos, J. L., and Borst, J. (1994). B cell antigen receptor stimulation induces formation of a Shc-Grb2 complex containing multiple tyrosine phosphorylated proteins. *J. Biol. Chem.* 269, 20209.
61. Yao, X-R., and Scott, D. (1993). Antisense oligodeoxynucleotides to the Blk tyrosine kinase prevent anti-mu chain mediated growth inhibition and apoptosis in a B cell lymphoma. *Proc. Natl. Acad. Sci. USA.*, 90, 7946.
62. Takata, M., Sabe, H., Hata, A., Inazu, T., Homma, Y., Nukada, T., Yamamura, H. and Kurosaki, T. (1994). Tyrosine kinases lyn and syk regulate B cell receptor-coupled Ca<sup>2+</sup> mobilization through distinct pathways. *EMBO J.* 13, 1341.
63. Tuveson, D. A., Carter, R. H., Soltoff, S. P., and Fearon, D.T. (1993). CD19 of B cells as a surrogate kinase insert region to bind phosphatidylinositol 3-kinase. *Science*, 260, 986.
64. Gulbins, E., Langlet, C., Baier, G., Bonnefoy-Berard, N., Herbert, E., Altman, A. and Coggeshall, K. M. (1994). Tyrosine phosphorylation and activation of Vav GTP/GDP exchange activity in antigen receptor triggered B cells. *J. Immunol.* 152, 2123.
65. Patel, K. J., and Neuberger, M. S. (1993). Antigen presentation by the B cell antigen receptor is driven by the alpha/beta sheath and occurs independently of its cytoplasmic tyrosines. *Cell*, 74, 939.
66. Weiser, P., Reisterer, C., and Reth, M. (1994). The internalization of the IgG2a antigen receptor does not require the association with Ig-alpha and Ig-beta but the activation of protein tyrosine kinases does. *Eur. J. Immunol.* 24, 665.
67. Cherayil, B., Macdonald, K., Waneck, G. and Pillai, S. (1993). Surface transport and internalization of the membrane IgM H chain in the absence of the Mb-1 and B29 proteins. *J. Immunol.* 151, 11.
68. Shaw, A. C., Mitchell, R. N., Weaver, Y. K., Campos-Torres, J., Abbas, A. K., and Leder, P. (1990). Mutations of immunoglobulin transmembrane and cytoplasmic domains: effects on intracellular signalling and antigen presentation. *Cell*, 63, 381.
69. Parikh, V. S., Bishop, G. A., Liu, K. J., Do, B. T., Ghosh, M. R., Kim, B. S. and Tucker, P. W. (1992). Differential structure-function requirements of the transmembrane domain of the B cell antigen receptor. *J. Exp. Med.* 176, 1025.
70. Reth, M. (1992). Antigen receptors on B lymphocytes. *Annu. Rev. Immunol.*, 10, 97.

71. Knight, A. M., Lucocq, J. M., Prescott, A. R., Poonambalam, S., and Watts, C. (1997). Antigen endocytosis and presentation mediated by human membrane IgG1 in the absence of the Ig $\alpha$ /Ig $\beta$  dimer. *EMBO J.* 13, 3842.
72. Kaisho, T., Schwenk, F., and Rajewsky, K. (1997). The roles of g1 heavy chain membrane expression and cytoplasmic tail in IgG1 responses. *Science.*, 276, 412.
73. Achatz, G., Nitschke, L., and Lamers, M. C. (1997). Effect of transmembrane and cytoplasmic domains of IgE on the IgE response. *Science.*, 276, 409.
74. Pollock, B. A., Kearney, J. F., Vakail, M., and Perry, R. P. (1984). A biological consequence of variation in the site of D-to-J<sub>H</sub> gene rearrangement. *Nature*, 31, 376.
75. Sanz, I. and Capra, D. (1987). V<sub>K</sub> and J<sub>K</sub> gene segments of A/J Ars-A antibodies: Somatic recombination generates the essential arginine at the junction of the variable and joining regions. *Proc. Natl. Acad. Sci. USA.*, 84, 1085.
76. Davis, M. M., and Bjorkman, P. J. (1988). T-cell antigen receptor genes and T-cell recognition. *Nature*, 334, 395.
77. Gu, H., Förster, I. and Rajewsky, K. (1990). Sequence homologies, N sequence insertion and JH gene utilization in VHDHJH joining: implications for the joining mechanism and the ontogenetic timing of Ly1 B cell and B-CLL progenitor generation. *EMBO J.* 9, 2133.
78. Goodnow, C. C., Crosbie, J., Adelstein, S., Lavoie, T. B., Smith-Gill, S. J., Brink, R. A., Pritchard-Briscone, H., Wotherspoon, J. H., Loblay, R. H., and Raphael, K. (1988). Altered immunoglobulin expression and functional silencing of self-reactive B lymphocytes in transgenic mice. *Nature*, 334, 676.
79. Berek, C. and Milstein, C. (1987). Mutation drift and repertoire shift in the maturation of the immune response. *Immunol. Rev.* 96, 23.
80. Berek, C. and Ziegner, M. (1993). The maturation of the immune response. *Immunol. Today.* 14, 405.
81. Reynaud, C. A., Anquez, V., Dahan, A., and Weill, J. C. (1985). A single rearrangement event generates most of the chicken immunoglobulin light chain diversity. *Cell*, 40, 283.
82. Baltimore, D. (1981). Gene conversion: some implications for immunoglobulin genes. *Cell*, 24, 592.
83. Maizels, N. (1989). Might gene conversion be the mechanism of somatic hypermutation of mammalian immunoglobulin genes?. *Trends Genet.*, 5, 4.
84. MacLennan, I. C. M. (1994) Germinal Centers. *Annu. Rev. Immunol.* 12, 117.
85. Linton, P. J., Rudie, A., and Klinman, N. R. (1991). Tolerance susceptibility of newly generating memory B cells. *J. Immunol.* 146, 4091.
86. Schitteck, B., and Rajewsky, K. (1990). Maintenance of B-cell memory by long-lived cells generated from proliferating precursors. *Nature*, 346, 749.
87. Esser, C., and Radburch, A. (1990). Immunoglobulin class switching: molecular and cellular analysis. *Annu. Rev. Immunol.* 8, 717.
88. Stavnezer, J. (1996). Antibody class switching. *Adv. Immunol.* 61, 79.
89. Renshaw, B. R., Fanslow, W. C. I., Armitage, R. J., Campbell, K. A., Liggit, D., Wright, B., Davison, B. L., Maliszewski, C. R. (1994). Humoral immune response in CD40 ligand-deficient mice. *J. Exp. Med.*, 180, 1889.
90. Kawabe, T., Naka, T., Yoshida, K., Tanaka, T., Fujiwara, H., Suematsu, S., Yoshida, N., Kishimoto, T., and Kikutani, H. (1994). The immune responses in CD40-deficient mice: impaired immunoglobulin class switching and germinal center formation. *Immunity*, 1, 167.

91. Jacob, J., Kassir, R., and Kelsoe, G. (1991). *In situ* studies of the primary immune response to (4-hydroxy-3-nitrophenyl) acetyl. I. The architecture and dynamics of the responding cell populations. **J. Exp. Med.** 173, 1165.
92. Bottaro, A., Lansford, R., Xu, L., Zhang, J., Rothman, P., and Alt, F. W. (1994). S region transcription per se promotes basal IgE class switch recombination but additional factors regulate the efficiency of the process. **EMBO J.** 13, 665.
93. Jung, S., Rajewsky, K., and Radburch, A. (1993). Shutdown of class switch recombination by deletion of a switch region control element. **Science**, 259, 984.
94. Lorenz, M., Jung, S., and Radburch, A. (1995). Switch transcripts in immunoglobulin class switching. **Science**, 267, 1825.
95. Kenter, A. L., Wuerffel, R., Sen, R., Jamieson, C. E., and Merkulov, G. V. (1993). Switch recombination breakpoints occur at nonrandom positions in Sy tandem repeat. **J. Immunol.** 151, 4718.
96. Jack, H. M., McDowell, M., Steinberg, C. M., and Wabl, M. (1988). Circular DNA is excised by immunoglobulin class switch recombination. **Cell**, 62, 143.
97. DePinho, R., Kruger, K., Andrews, N., Lutzker, S., Baltimore, D., and Alt, F. W. (1984). Molecular basis of heavy-chain class switching and switch region deletion in an Abelson virus transformed cell line. **Mol. Cell. Biol.**, 4, 2905.
98. Obata, M., Kataoka, T., Nakai, S., Yamagishi, H., Takahashi, N., Yamawaki, K. Y., Nikaido, T., Shimizu, A., and Honjo, T. (1981). Structure of a rearranged gamma 1 chain gene and its implication to immunoglobulin class switch mechanism. **Proc. Natl. Acad. Sci. USA.**, 78, 2437.
99. Li, S. C., Rothman, P. B., Chan, C., Hirsch, D., and Alt, F. W. (1994). Expression of I $\mu$ -C $\gamma$  hybrid germline transcripts subsequent to Ig heavy chain class-switching. **Int. Immunol.**, 6, 491.
100. Jung, S., Siebenkotten, G., and Radburch, A. (1994). Frequency of immunoglobulin E class switching is autonomously determined and independent of prior switching to their classes. **J. Exp. Med.** 179, 2023.
101. Snapper, C. M., Finkelman, F. D., and Paul, W. E. (1988). Differential regulation of IgG1 and IgE synthesis by interleukin 4. **J. Exp. Med.** 167, 183.
102. Coffman, R. L., Seymour, B. W., Lebman, D. A., Hiraki, D. D., Christiansen, J. A., Shrader, B., Cherwinski, H. M., Savelkoul, H. F., Finkelman, F. D., and Bond, M. W. (1988). The role of helper T cell products in mouse B cell differentiation and isotype regulation. **Immunol. Rev.**, 102, 5.
103. Jabara, H. H., Schneider, L. C., Shapira, S. K., Alfieri, C., Moody, C. T., Kieff, E., Geha, R. S., and Vercelli, D. (1990). Induction of germ-line and mature C epsilon transcripts in human B cells stimulated with rIL-4 and EBV. **J. Immunol.**, 145, 3468.
104. Jabara, H. H., Fu, S. M., Geha, R. S., and Vercelli, D. (1990). CD40 and IgE: synergism between anti-CD40 monoclonal antibody and interleukin 4 in the induction of IgE synthesis by highly purified human B cells. **J. Exp. Med.** 172, 1861.
105. Jabara, H. H., Ahern, D. J., Vercelli, D., and Geha, R. S. (1991). Hydrocortisone and IL-4 induce IgE isotype switching in human B cells. **J. Immunol.** 147, 1557.
106. Lundgren, M., Persson, U., Larsson, P., Magnusson, P., Smith, C. I., Hammarstrom, L., and Severinson, E. (1989). Interleukin 4 induces synthesis of IgE and IgG4 in human B cells. **Eur. J. Immunol.** 19, 1311.
107. Kuhn, R., Rajewsky, K., and Muller, W. (1991). Generation and analysis of interleukin 4 deficient mice. **Science**, 254, 707.

108. Punnonen, J., Aversa, G., Cocks, B. G. et al. (1993). Interleukin-13 induces interleukin-4 independent IgG4 and IgE synthesis and CD23 expression by human B cells. *Proc. Natl. Acad. Sci. USA* 90, 3730.
109. Köhler, I., and Rieber, E. P. (1993). Allergy associated I $\epsilon$  and Fc $\epsilon$  receptor II (CD23b) genes activated via binding of an interleukin-4-induced transcription factor to a novel responsive element. *Eur. J. Immunol.* 23, 3066.
110. Ivashkiv, L. B. (1995). Cytokines and STATs: how can signals achieve specificity. *Immunity*, 3, 1.
111. Köhler, I., Alliger, P., Minty, A. et al (1994). Human interleukin 13 activates the interleukin 4 dependent transcription factor NF-IL-4 sharing a DNA binding motif with an interferon induced nuclear binding factor. *FEBS Lett.* 345, 187.
112. Delphin, S., and Stavnezer, J. (1995). Characterization of an IL-4 responsive region in the immunoglobulin heavy chain germline  $\epsilon$  promoter: regulation by NF-IL4, a C/EBP family member, and NF- $\kappa$ B/p50. *J. Exp. Med.* 181, 181.
113. Liao, F., Birshtein, B. K., Busslinger, M., and Rothman, P. (1994). The transcription factor BSAP (NF-HB) is essential for immunoglobulin germ-line  $\epsilon$  transcription. *J. Immunol.* 152, 2904.
114. Adams, B., Dörfler, P., Aguzzi, A., Kozmik, Z., Urbanek, P., Maurer-Fogy, I., and Busslinger, M. (1992). Pax-5 encodes the transcription factor BSAP and is expressed in B lymphocytes, the developing CNS, and adult testis. *Genes. Dev.* 6, 1589.
115. Thienes, C. P., DE Monte, L., Monticelli, S., Busslinger, M., Gould, H., and Vercelli, D. (1997). The transcription factor B cell specific activator protein (BSAP) enhances both IL-4 and CD40-mediated activation of the human  $\epsilon$  germline promoter. *J. Immunol.*, 158, 5874.
116. Rousset, F., Garcia, E., Banchereau, J. (1991). Cytokine induced proliferation and immunoglobulin production of human B lymphocytes triggered through their CD40 antigen. *J. Exp. Med.* 173, 705.
117. Gauchat, J. F., Henschow, S., Mazzel G. et al. (1993). Induction of human IgE synthesis in B cells by mast cells and basophils. *Nature*, 365, 340.
118. Lane, P., Traunecker, A., Hueble, S., Inui, S., Lanzavecchia, A., and Gray, A. (1992). Activated human T cells express a ligand for the human B cell associated antigen CD40 which participate in T cell dependent activation of B lymphocytes. *Eur. J. Immunol.* 1992, 2573.
119. Korthäuer, U., Graf, D., Mages, H. W. et al (1993). Defective expression of T-cell CD40 ligand causes X-linked immunodeficiency with hyper-IgM. *Nature*, 361, 539.
120. Weiss, S. J., Zeng, F. F., and Bonagura, V. R. (1996). Hyper-IgM syndrome (HIGMs): a B-cell defect. *J. Allergy Clin Immunol* 97, 393.
121. Mandler, R., Finkelman, F. D., Levine, A. D., and Snapper, C. M. (1993). IL-4 induction of IgE class switching by lipopolysaccharide-activated murine B cells occurs predominantly through sequential switching. *J. Immunol.* 150, 407.
122. Gascan, H., Gauchat, J. F., Aversa, G., Van Vlasselaer, P., and de Vries, J. E. (1991). Anti-CD40 monoclonal antibodies or CD4+ T cell clones and IL-4 induce IgG4 and IgE switching in purified human B cells via different signalling pathways. *J. Immunol.* 147, 8.
123. Burd, P. R., Thompson, W. C., Max, E. E., and Mills, F. C. (1995). Activated mast cells produce interleukin 13. *J. Exp. Med.* 181, 1371.
124. Worm, M., and Henz, B. M. (1997). Molecular regulation of human IgE synthesis. *J. Mol. Med.* 75, 440.

125. Berton, M. T., Uhr, J. W., And Vitetta, E. S. (1989). Synthesis of germ-line gamma 1 immunoglobulin heavy-chain transcripts in resting B cells: induction by interleukin 4 and inhibition by interferon gamma. *Proc. Natl. Acad. Sci. USA.* 86, 2829.
126. Thyphronitis, G., Banchereau, J., Heusser, C., Tsokos, G. C., Levine, A. D., and Finkelman, F. D. (1991). Kinetics of interleukin-4 induction and interferon gamma inhibition of IgE secretion by Epstein Barr virus infected human peripheral blood B cells. *Cell. Immunol.* 133, 408.
127. Chretien, I., Pene, J., Briere, F., Malefijt, D. R., Rousset, F., and de Vries, J. E. (1990). Regulation of human IgE synthesis. I. Human IgE synthesis in vitro is determined by the reciprocal antagonistic effects of interleukin 4 and interferon-gamma. *Eur. J. Immunol.* , 20, 243.
128. Kiniwa, M., Gately, M., Gubler, U., Chizzonite, R., Fargeas, C., and Delespesse, G. (1992). Recombinant interleukin-12 suppresses the synthesis of IgE by interleukin-4 stimulated human lymphocytes. *J. Clin. Invest.* 90, 262.
129. Sutton, B. J. and Gould, H. J. (1993). The human IgE network. *Nature*, 366, 421.
130. Ishizaka, K., and Ishizaka, T. (1967). Identification of gamma-E-antibodies as a carrier of reaginic activity. *J. Immunol.* 99, 1187.
131. Bazin, H., Beckers, A., and Querimjean, P. (1974). Three classes and four subclasses of rat immunoglobulins: IgM, IgA, IgE, IgG, IgG(2b), and IgG(2c). *Eur. J. Immunol.* 4, 44.
132. Johansson, S. G. O., and Bennich, H. (1967). Immunological studies of an atypical (myeloma) immunoglobulin. *Immunol.* 4, 44.
133. Metzger, H., Alcaraz, G., Hohman, R., Kinet, J., Pribluda, V., and Quarto, R. (1986). The receptor with high affinity for immunoglobulin E. *Annu. Rev. Immunol.*, 4, 419.
134. Wang, B., Rieger, A., Kilgus, O., Ochiai, K., Maurer, D., Fodinger, D., Kinet, J. P. and Stingl, G. (1992). Epidermal Langerhans cells express the high affinity receptor immunoglobulin E (Fc epsilon RI). *J. Exp. Med.* 175, 1285.
135. Bieber, T. (1994). FcεRI on human Langerhans cells : a receptor in search for new functions. *Immunol. Today*, 52, 52.
136. Nissim, A., Helene, J., and Eshhar, Z. (1991). Mapping of the high affinity Fcε receptor binding site to the third constant region domain of IgE. *EMBO J.* 10, 101.
137. Rousseaux-Prevost, R., Rousseaux, J., Bazin, H., and Biserte, G. (1984). Differential reduction of the inter-chain disulfide bonds of rat immunoglobulin E: relation to biological activity. *Mol. Immunol.* 21, 233.
138. Perez-Montfort, R., and Metzger, H. (1982). Proteolysis of soluble IgE-receptor complexes: localization of sites on IgE which interact with the Fc receptor. *Mol. Immunol.* 19, 1113.
139. Flanagan, J. G., and Rabbitts, T. H. (1982). The sequence of human immunoglobulin epsilon heavy chain constant region gene, and evidence for three non-allelic genes. *EMBO J.* 1, 655.
140. Nishida, Y., Miki, T., Hisajima, H., and Honjo, T. (1982). Cloning of human immunoglobulin epsilon chain genes: evidence for multiple C epsilon genes. *Proc. Natl. Acad. Sci. USA.* 79, 3833.
141. Ishida, N., Ueda, S., Hayashida, H., Miyata, T., and Honjo, T. (1982). The nucleotide sequence of the mouse immunoglobulin epsilon gene: comparison with the human epsilon gene sequence. *EMBO J.* 1, 1117.

142. Liu, F. T., Albrandt, K., Sutcliffe, J. G., and Katz, D. H. (1982). Cloning and nucleotide sequence of mouse immunoglobulin epsilon chain cDNA. *Proc. Natl. Acad. Sci. USA.* 79, 7852.
143. Liu, F. T., Albrandt, K., Bry, C. G., and Ishizaka, T. (1984). Expression of a biologically active fragment of human IgE epsilon chain in *Escherichia coli*. *Proc. Natl. Acad. Sci. USA.* 81, 5369.
144. Baniyash, M., Kehry, M., and Eshhar, Z. (1988). Anti-IgE monoclonal antibodies directed at the Fc epsilon receptor binding site. *Mol. Immunol.* 25, 705.
145. Presta, L., Shields, R., O'Connell, L., Lahr, S., Porter, J., Gorman, C., and Jardieu, P. (1994). The binding site on human IgE for its high affinity receptor. *J. Biol. Chem.* 269, 26368.
146. Grangette, C., Gruart, V., Ouaisi, M. A., Rizvi, F., Delespesse, G., Capron, A., and Capron, M. (1989). IgE receptor on human eosinophils (FcεRII). Comparison with B cell CD23 and association with an adhesion molecule. *J. Immunol.* 143, 3580.
147. Conrad, D. H. (1990). FcεRII/CD23: the low affinity receptor for IgE. *Annu. Rev. Immunol.* 8, 623.
148. Hellman, L. (1993). Characterisation of four novel ε chain mRNA and a comparative analysis of genes for immunoglobulin E in rodents and man. *Eur. J. Immunol.*, 23, 159.
149. Peng, C., Davis, F. M., Sun, L. K., Liou, R. S., Kim, Y. W., and Chang, T. W. (1992). A new isoform of human membrane-bound IgE. *J. Immunol.*, 148, 129.
150. Zhang, K., Max, E. E., Cheah, H. H., and Saxon, A. (1994). Complex alternative RNA splicing of ε-immunoglobulin transcripts produces mRNAs encoding four potential secreted protein isoforms. *J. Biol. Chem.*, 269, 456.
151. Zhang, K., Saxon, A., and Max, E. E. (1992). Two unusual forms of human immunoglobulin E encoded by alternative RNA splicing of ε heavy chain membrane exon. *J. Exp. Med.*, 176, 233.
152. Batista, F.D., Efremov, D. G., and Burrone, O. R. (1995). Characterisation and expression of alternatively spliced IgE heavy chains transcripts produced by peripheral blood lymphocytes. *J. Immunol.* 154, 209.
153. Vercelli, D., Helm, B., Marsh, P., Padlan, E., Geha, R. S., and Gould, H. (1989). The B cell binding site on human immunoglobulin E. *Nature*, 338, 649.
154. Sitia, R., Neuberger, M., and Milstein, C. (1987). Regulation of membrane IgM expression in secretory B cells: translational and post-translational events. *EMBO J.*, 6, 3969.
155. Lyczak, J. B., Zhang, K., Saxon, A., and Morrison, S. L. (1996). Expression of novel secreted isoforms of human immunoglobulin E proteins. *J. Biol. Chem.* 271, 3428.
156. Batista, F.D., Efremov, D. G., and Burrone, O. R. (1996). Characterisation of a second secreted IgE isoform and identification of an asymmetric pathway of IgE assembly. *Proc Natl. Acad. Sci. USA.* 93, 3399.
157. Robertson, M. W., and Liu, F. T. (1991). Heterogeneous IgE glycoforms characterized by differential recognition of an endogenous lectin (IgE-binding protein). *J. Immunol.* 147, 3024.
158. Truong, M. J., Gruart, V., Kusnierz, J. P., Papin, J. P., Loiseau, S., Capron, A., and Capron, M. (1993). Human neutrophils express immunoglobulin E (IgE) binding proteins (Mac-2/εBP) of the S-type lectin family: role in IgE dependent regulation. *J. Exp. Med.* 177, 243.

159. Wollenberg, A., Salle, H., Hanau, D., Liu, F. T., and Bieber, T. (1993). Human keratinocytes release the endogenous  $\beta$ -galactoside-binding soluble lectin immunoglobulin E (IgE-binding protein) which binds to Langerhans cells where it modulates their binding capacity for IgE glycoforms. *J. Exp. Med.* 178, 777.
160. Young, R. J., Owens, R. J., Mackay, G. A., Chan, C. M., Shi, J., Hide, M., Francis, D. M., Henry, A. J., Sutton, B. J., and Gould, H. J. (1995). Secretion of recombinant human IgE-Fc by mammalian cells and biological activity of glycosylation site mutants. *Protein Eng.* 8, 193.
161. Max E., Battey J., Ney R., Kirsch I and Leder P. (1982) Duplication and deletion in the human immunoglobulin E genes. *Cell* 29, 691.
162. Batista F. D., Efremov D. G., Tkach T. and Burrone O. R. (1995) Characterisation of the human immunoglobulin epsilon mRNAs and their polyadenylation sites. *Nucleic Acids Res.*, 23, 4805.
163. Dorai H. and Gillies S. D. (1989). The complete nucleotide sequence of a human immunoglobulin genomic C mu gene. *Nucleic Acids Res.* 17, 6412.
164. Bensmana M. and Lefranc M. P. (1990) Gene segments encoding membrane domains of the human immunoglobulin gamma 3 and alpha chains. *Immunogenetics*, 32, 321.
165. Diaz-Sanchez D., Dotson A. R., Takenaka H. and Saxon A. (1994) Diesel exhaust particles induce local IgE production in vivo and alter the pattern of IgE messenger RNA isoforms. *J. Clin. Invest.*, 94, 1417.
166. Efremov D. G., Batista F. D. and Burrone O. R. (1993). Molecular analysis of IgE H-chain transcripts expressed in vivo by peripheral blood lymphocytes from normal and atopic individuals. *J. Immunol.* 151, 2195.
167. Sitia R. (1985) Biosynthesis of membrane and secreted epsilon chains during lipopolysaccharide induced differentiation of an IgE<sup>+</sup> murine B- lymphoma. *Mol. Immunol.*, 22, 1289.
168. Struck F. and Collins J. (1994). Simple and rapid 5' and 3' extension techniques in RT-PCR. *Nucleic Acids Res.*, 22, 1923.
169. Venkitaraman, A. R., Williams, G. T., Dariavach, P., and Neuberger, M. S. (1991). The B-cell antigen receptor of the five immunoglobulin classes. *Nature*, 352, 777.
170. Campbell, K.S., Hager, E. J., and Cambier, J. C. (1991). Alpha-chains of IgM and IgD antigen receptor complexes are differentially N- glycosylated MB-1-related molecules. *J. Immunol.* 147, 1575.
171. Pogue, S.L., and Goodnow, C. C. (1994). Ig heavy chain extracellular spacer confers unique glycosylation of the Mb-1 component of the B cell antigen receptor complex. *J Immunol.*, 152, 3925.
172. van Noesel, C.J.M., Brouns, G. S., van Schijndel, G. M. W., Bende, R. J., Mason, D. Y., Borst, J., and van Lier, R. A. W. (1992). Comparison of human B cell antigen receptor complexes: Membrane-expressed forms of immunoglobulin (Ig)M, IgD, and IgG are associated with structurally related heterodimers. *J. Exp. Med.* 175, 1511.
173. Gold, M.R., Law, D. W., and DeFranco, A. L. (1990). Stimulation of protein tyrosine phosphorylation by the B-lymphocyte antigen receptor. *Nature*, 345, 810.
174. Boyd, A.W., and Schrader, J. W. (1981). The regulation of growth and differentiation of a murine B cell lymphoma. II. The inhibition of WEHI 231 by anti-immunoglobulin antibodies. *J. Immunol.*, 126, 2466.
175. Tisch, R., Roifman, C. M., and Hozumi, N. (1988). Functional differences between immunoglobulins M and D expressed on the surface of an immature B-cell line. *Proc. Natl. Acad. Sci. USA.* 85, 6914.



176. Chomczynski P., and Sacchi N. (1987). Single-step method of RNA isolation by acid guanidinium thiocyanate-phenol-chloroform extraction. *Anal. Biochem.*, 162, 156.
177. Sambrook. J., Fritsch E. F., and Maniatis T. (1989). **Molecular Cloning: A Laboratory Manual**, 2nd Edn. Cold Spring Harbor Laboratory Press, Cold Spring Harbor, NY
178. Frohman. M. A., Dush M. K., and Martin G. R. (1988). Rapid production of full length cDNAs from rare transcripts: amplification using a single gene specific oligonucleotide primer. *Proc. Natl. Acad. Sci. U.S.A.* 85, 8998.
179. Bruggemann, M., Williams, G. T., Bindon, C. I., Clark, M. C., Walker, M. R., Jefferies, R., Waldman, H., and Neuberger, M. S. (1987). Comparison of the effector functions of human immunoglobulins using a matched set of chimeric antibodies. *J. Exp. Med.* 166, 1351.
180. Dul, J., Burrone, O. R., and Argon, J. (1992). A conditional secretory mutant in an Ig L chain is caused by replacement of tyrosine/phenylalanine 87 with histidine. *J. Immunol.*, 149, 1927.
181. Kim, K.M., and Reth, M (1995). The B cell antigen receptor of class IgD induces a stronger and more prolonged protein tyrosine phosphorylation than that of class IgM. *J Exp. Med.*, 181, 1005.
182. Cambier, J.C., Pleiman, C. M., and Clark, M. R. (1994). Signal transduction by the B cell antigen receptor and its coreceptors. *Annu. Rev. Immunol.* 12, 457.
183. Flaswinkel, H., and Reth., M. (1994). Dual role of the tyrosine activation motif of the Ig-alpha protein during signal transduction via the B cell antigen receptor. *EMBO. J.* 13, 83.
184. Kim, K.M., Alber, G., Weiser, P., and Reth, M. (1993). Differential signalling through the Ig-alpha and Ig-beta components of the B cell antigen receptor. *Eur. J. Immunol.* 23, 911.
185. Matsuo, T., Nomura, J., Kuwahara, K., Igarashi, H., Inui, S., Hamaguchi, M., Kimoto, M., and Sakaguchi, N. (1993). Cross-linking of B cell receptor-related MB-1 molecule induces protein tyrosine phosphorylation in early B lineage cells. *J. Immunol.* 150, 3766.
186. Clark, M.R., Campbell, K. S., Kazlauskas, A., Johnson, S. A., Hertz, M., Potter, T. A., Pleiman, C., and Cambier, J. C. (1992). The B cell antigen receptor complex: association of Ig-alpha and Ig-beta with distinct cytoplasmic effectors. *Science*, 258, 123.
187. Clark, M.R., Johnson, S. A., and Cambier, J. C. (1994). Analysis of Ig-alpha-tyrosine kinase interaction reveals two levels of binding specificity and tyrosine phosphorylated Ig-alpha stimulation of Fyn activity. *EMBO. J.* 13, 1911.
188. Dymecki, S.M., Zwollo, P., Zeller, K., Kuhajda, F. P., and Desiderio, S. V. (1992). Structure and developmental regulation of the B-lymphoid tyrosine kinase gene blk. *J. Biol. Chem.* 267, 4815.
189. Rudd, C.E., Janssen, O., Prasad, K. V., Raab, M., da Silva, A., Telfer, J. C., and Yamamoto, M. (1993). src-related protein tyrosine kinases and their surface receptors. *Biochem Biophys. Acta.* 1155, 239.
190. Yamanashi, Y., Kakiuchi, T., Mizuguchi, J., Yamamoto, T., and Toyoshima, K. (1991). Association of B cell antigen receptor with protein tyrosine kinase Lyn. *Science* 251, 192.
191. Gold, M.R., Matsuuchi, L., Kelly, R. B., and DeFranco, A. L. (1991). Tyrosine phosphorylation of components of the B-cell antigen receptors following receptor crosslinking. *Proc. Natl. Acad. Sci. USA.*, 88, 3436.
192. Rogers, J., Early, P., Carter, C., Calame, K., Bond, M., Hood, L., and Wall, R. (1980). Two mRNAs with different 3' ends encode membrane-bound and secreted forms of immunoglobulin mu chain. *Cell*, 20, 303.

193. Brown, S. L., and Morrison, S. L. (1989). Developmental regulation of membrane and secretory Ig gamma 2b mRNA. *J. Immunol.*, 142, 2072.
194. Diaz-Sanchez, D., Zhang, K., Nutman, T. B., and Saxon, A. (1995). Differential regulation of alternative 3' splicing of  $\epsilon$  messenger RNA variants. *J. Immunol.*, 155, 1930.
195. Sheets, M. D., Ogg, S. C., and Wickens, M. P. (1990). Point mutations in AAUAAA and the poly (A) addition site: effects on accuracy and efficiency of cleavage and polyadenylation in vitro. *Nucl. Acids Res.* 18, 5799.
196. Chen, F., MacDonald, C. C., and Wilusz, J. (1995). Cleavage size determinants in the mammalian polyadenylation signal. *Nucl. Acids Res.* 23, 4805.
197. Aveskogh, M., and Hellman, L. (1995). A single major transcript encodes the membrane bound form of rat IgE. *Scand. J. Immunol.* 42, 535.
198. Yuan, D. (1984). Regulation of IgM and IgD synthesis of murine immunoglobulin D: heterogeneity of glycosylation. *J. Immunol.* 132, 1566.
199. Terashima, M., Kim, K. M., Adachi, T., Nielsen, P. J., Reth, M., Kohler, G., and Lamers, M. C. (1994). The IgM antigen receptor of B lymphocytes is associated with prohibitin and a prohibitin-related protein. *EMBO. J.* 13, 3782.
200. Kim, K.M., Adachi, T., Nielsen, P. J., Terashima, M., Lamers, M. C., Kohler, G., and Reth, M. (1994). Two new proteins preferentially associated with membrane immunoglobulin D. *EMBO. J.* 13, 3793.
201. MacKenzie, T., and Dosch, H. M. (1989). Clonal and molecular characteristics of the human IgE committed B cell subset. *J. Exp. Med.* 169, 407.
202. Chan, M.A., Benedict, S. H., Dosch, H. M., Hui, M. F., and Stein, L. D. (1990). Expression of IgE from a nonrearranged  $\epsilon$  locus in cloned B lymphoblastoid cells that also express IgM. *J. Immunol.* 136, 3563.
203. Annaert, W. G., Becker, B., Kistner, U., Reth, M., and Jahn, R. (1997). Export of cellubrevin from the endoplasmic reticulum is controlled by BAP31. *J. Cell Biol.* 139, 1397.
204. Aluvihare, V. R., Khamlichi, A. A., Williams, G. T., Adorini, L., and Neuberger, M. S. (1997). Acceleration of intracellular targeting of antigen by the B-cell antigen receptor: importance depends on the nature of the antigen-antibody interaction. *EMBO. J.* 12, 3553.
205. Sefton, B. M., and Campbell, M. A. (1991). The role of tyrosine protein phosphorylation in lymphocyte activation. *Annu. Rev. Cell. Biol.* 7, 257.
206. Reth, M., and Wienands, J. (1997). Initiation and processing of signals from the B cell antigen receptor. *Annu. Rev. Immunol.* 15, 453.
207. Lorenzi, R., and Burrone, O. R. (1998). Sequence-specific antibodies against human IgE isoforms induced by an epitope display system. *Immunotechniques* (in press).